



Regulation of cellular surface exposure of soluble MMPs in primary human macrophages

Dissertation

zur Erlangung des Doktorgrades

**an der Fakultät für
Mathematik, Informatik und Naturwissenschaften
Fachbereich Biologie
der Universität Hamburg**

vorgelegt von
Artur Ratt
geboren am 12.05.1992
in Zelinograd (Kasachstan)

Hamburg, Juni 2023

Die vorliegende Arbeit wurde in der Zeit von Juli 2018 bis Dezember 2022 unter der Leitung von Prof. Dr. Stefan Linder am Institut für Medizinische Mikrobiologie, Virologie und Hygiene des Universitätsklinikums Hamburg-Eppendorf angefertigt.

Erstgutachter: Prof. Dr. Stefan Linder

Zweitgutachter: PD Dr. Andreas Pommerening-Röser

Eidesstattliche Versicherung

Hiermit erkläre ich an Eides statt, dass ich die vorliegende Dissertationsschrift selbst verfasst und keine anderen als die angegebenen Quellen und Hilfsmittel benutzt habe. Ebenfalls erkläre ich an Eides statt, dass alle dem Prüfungsamt und den Gutachtern vorliegenden Exemplare dieser Dissertationsschrift identisch sind.

Hamburg, den 07.06.2023

A handwritten signature in black ink, appearing to read 'Artur Ratt', with a long horizontal stroke extending to the right.

(Artur Ratt)

INDEX

Eidesstattliche Versicherung.....	3
Summary.....	7
Zusammenfassung.....	9
1 Introduction.....	11
1.1 Macrophages.....	11
1.1.1 The role of macrophages.....	11
1.1.2 The origin of macrophages.....	11
1.1.3 The migration of macrophages.....	12
1.1.4 Macrophages and podosomes.....	14
1.1.5 The polarization of macrophages in pathogenesis.....	15
1.2 Matrix metalloproteases.....	16
1.2.1 The classification of MMPs.....	16
1.2.2 MMP substrates.....	18
1.2.3 MMPs and the polarization of macrophages.....	19
1.2.4 MMP-trafficking.....	20
1.2.5 MMPs and diseases.....	22
1.3 ARF6 and the regulation of endocytosis.....	23
1.3.1 ARF6 and MMPs.....	23
1.3.2 The role of ARF6 in diseases.....	25
1.4 Aims of the dissertation.....	27
2 Materials.....	27
Table 2.1: Chemicals.....	27
Table 2.2: Chemicals for cell culture.....	28
Table 2.3: Buffers.....	28
Table 2.4: Antibodies for IF and WB stainings.....	29
Table 2.5: siRNA and sequences for knockdowns.....	30
Table 2.6: Oligonucleotides for cloning.....	30
Table 2.7: Purchased plasmids.....	30
Table 2.8: Kits.....	30
Table 2.9: Consumables.....	30
Table 2.10: Inventory.....	31
Table 2.11: Microscopes.....	32
Table 2.12: Software.....	32
3 Methods.....	33
3.1 Transfection with siRNA for knockdowns.....	33
3.2 Transfection with plasmids for live-cell imaging.....	33
3.3 Matrix Degradation Assay.....	34
3.4 Fixation of cells and immunofluorescence staining.....	34
3.5 Precipitation of supernatant proteins from cell culture.....	35
3.6 Surface biotinylation assay.....	35
3.7 Polyacrylamide gel.....	35
3.8 Western Blot.....	36
3.9 Mild Stripping of nitrocellulose membranes.....	36

3.10 Zymography assay.....	37
3.11 Polymerase chain reaction.....	37
3.12 Quick-change mutagenesis.....	38
3.13 Restriction digestion.....	38
3.14 Agarose gel electrophoresis.....	38
3.15 Plasmid ligation.....	39
3.16 Transformation.....	39
3.17 Maxiprep.....	39
3.18 Sequencing of plasmids with SeqLab.....	40
4 Results.....	41
4.1 Expression of soluble MMPs over time.....	42
4.1.1 Expression of soluble MMPs during macrophage differentiation.....	42
4.1.2 Correlations between protein expressions of MMPs.....	44
4.2 Intracellular localization of MMPs.....	45
4.2.1 Distinct vesicle populations of soluble MMPs.....	46
4.2.2 Colocalization of MMPs with endocytotic regulators.....	49
4.3 Degradation of extracellular matrix components by MMPs.....	53
4.3.1 Enzymatic activity in the zymography-assay.....	53
4.3.2 Matrix degradation by MMPs.....	56
4.4 MMPs and podosomes.....	60
4.4.1 Podosomes in relation to MT1-MMP-islets.....	60
4.4.2 Podosomes in relation to vesicles of soluble MMPs.....	62
4.5 Intra- and extracellular levels of soluble MMPs.....	64
4.5.1 Protein levels of soluble MMPs at ARF6 overexpression.....	64
4.5.1.1 Intracellular protein levels at overexpression of ARF6.....	65
4.5.1.2 Surface protein levels at overexpression of ARF6.....	66
4.5.2 Protein levels of soluble MMPs at knockdown conditions.....	68
4.5.2.1 Intracellular protein levels at knockdown conditions.....	68
4.5.2.2 Surface protein levels at knockdown conditions.....	70
4.5.2.3 Soluble MMPs in the culture medium at knockdown conditions.....	71
5 Conclusion.....	74
6 Discussion.....	76
6.1 Expression profiles of MMPs.....	76
6.2 Intracellular vesicle populations of MMPs.....	77
6.3 Degradation of ECM-components by soluble MMPs.....	79
6.4 MMPs and podosomes.....	81
6.5 Regulation of intra- and extracellular MMP protein levels.....	81
6.6 ARF6 and MMPs in previous publications.....	84
6.7 Model of soluble MMP regulation.....	88
References.....	91
Abbreviations.....	96
List of Figures.....	98
List of Tables.....	99
Publications and Conferences.....	100
Danksagung.....	101

SUMMARY

Matrix Metalloproteases (MMPs) are zinc-dependent endopeptidases, which degrade mainly components of the extracellular matrix (ECM) such as collagens, fibronectins and laminins, but also proteins responsible for adhesion such as integrins or even other MMPs and are thus a crucial factor for the capability of primary macrophages to detach and migrate through various tissues. MMPs especially produced by primary macrophages, which are part of the innate immune system, are also involved in the regulation of pro- and anti-inflammatory processes by releasing cytokines and chemokines through their enzymatic activity in both homeostatic or pathogenic circumstances.

Since The MMP-family contains 28 members, subgrouped in Membrane-type-MMPs (MT-MMPs) or collagenases, stromelysins, gelatinases and matrilysins and others, which show different structural properties, they have only a few domains in common. All MMPs contain a catalytic domain, endowed with a zinc-ion, which is responsible for its enzymatic activity, a propeptide, which must be cleaved off for activation and a signal sequence, which is important for the respective intracellular trafficking. Except for matrilysins or type II-MT-MMPs, most subgroups share a hemopexin-domain, which is required for a more specific substrate recognition. MT-MMPs are additionally endowed with either a transmembrane-domain (TM-domain) to be covalently anchored at the plasma membrane or a GPI-anchor domain for non-covalent binding. MMPs, which lack of a TM-domain, are called soluble MMPs, which are mainly secreted into the extracellular space, but are occasionally also surface-associated at the plasma membrane.

The goal of this dissertation was to elucidate the regulation and trafficking of soluble MMPs in primary human macrophages and their role for the degradative capability of them. It is shown that MMP7, -9 and -12 change their protein expression profile in monocytes, differentiating into macrophages, also in a polarization-dependent manner and localize in distinct intracellular vesicle populations distinguishable from MT1-MMP and each other. In contrast to MT1-MMP, these soluble MMPs are not associated with podosomes, the main adhesive- and degradative structures of macrophages. The surface-exposure of MMP7 as *pars pro toto* for soluble MMPs is important for the degradative capability of macrophages and is regulated by ADP-ribosylation factor 6 (ARF6), which is an important endocytosis regulator. Summarized, soluble MMPs are an inhomogenous group, which contributes to the degradative capability of macrophages. Soluble MMPs show distinct intracellular localization and are thus selectively transported and regulated. Some show a correlation with the polarization state of macrophages. Soluble MMPs can be surface-associated without a transmembrane-domain. The surface-associated population of MMP7 is regulated by the endocytosis regulator ARF6. However, the mechanistic connection between MMP7 and ARF6 (a putative receptor) has not been identified, yet and needs further investigation. Some potential candidates are heparan-

Summary

sulfate-proteoglycans (HSPGs) or low density lipoprotein receptor-related proteins (LRPs), but also tissue inhibitor of metalloproteinases (TIMPs) [69]. The dependency on the pro-or anti-inflammatory polarization of their protein expressions is an important difference to MT1-MMP - a constitutively expressed MMP in macrophages - in pathogenic contexts. This offers a more specific therapeutic targeting of regulatory mechanisms in macrophages and their role in various diseases e.g. as tumour-associated macrophages (TAMs) as a future perspective.

ZUSAMMENFASSUNG

Matrix-Metalloproteasen (MMPs) sind zinkabhängige Endopeptidasen, die vor allem Bestandteile der extrazellulären Matrix (EZM) wie Kollagene, Fibronektine und Laminine, aber auch für die Adhäsion verantwortliche Proteine wie Integrine oder auch andere MMPs proteolytisch spalten und damit ein entscheidender Faktor für die Fähigkeit primärer Makrophagen sind, sich abzulösen und durch verschiedene Gewebe zu wandern. MMPs, die insbesondere von primären Makrophagen produziert werden, die Teil des angeborenen Immunsystems sind, sind auch an der Regulation von pro- und antiinflammatorischen Prozessen beteiligt, indem sie durch ihre enzymatische Aktivität sowohl unter homöostatischen als auch unter pathogenen Bedingungen Zytokine und Chemokine freisetzen.

Da die MMP-Familie 28 Mitglieder umfasst, die in Membran-Typ-MMPs (MT-MMPs) oder Kollagenasen, Stromelysinen, Gelatinasen und Matrilysinen und anderen unterteilt sind, die unterschiedliche strukturelle Eigenschaften aufweisen, haben sie nur wenige Domänen gemeinsam. Alle MMPs enthalten eine katalytische Domäne, die ein Zink-Ion bindet und für seine enzymatische Aktivität verantwortlich ist, ein Propeptid, das zur Aktivierung abgespalten werden muss, und eine Signalsequenz, die für den jeweiligen intrazellulären Transport benötigt wird. Mit Ausnahme von Matrilysinen oder Typ II-MT-MMPs teilen sich die meisten Untergruppen eine Hämpexin-Domäne, die für eine spezifischere Substraterkennung erforderlich ist. MT-MMPs sind zusätzlich entweder mit einer Transmembrandomäne (TM-Domäne) ausgestattet, die kovalent an der Plasmamembran verankert ist oder mit einer GPI-anchor Domäne, die nicht kovalent bindet. MMPs, denen eine TM-Domäne fehlt, werden als „soluble MMPs“ bezeichnet, die hauptsächlich in den extrazellulären Raum sezerniert werden, gelegentlich aber auch oberflächen-assoziiert an der Zellmembran zu finden sind.

Das Ziel dieser Dissertation war es, die Regulation und den Transport von löslichen MMPs in primären humanen Makrophagen und ihre Rolle für deren Abbaufähigkeit aufzuklären. Es wird gezeigt, dass die Proteinexpressionsprofile von MMP7, -9 und -12 in Monozyten während der Differenzierung zu Makrophagen aber auch polarisationsabhängig sich verändern und in unterschiedlichen intrazellulären Vesikelpopulationen lokalisieren, die von MT1-MMP und untereinander unterscheidbar sind. Im Gegensatz zu MT1-MMP sind diese „soluble MMPs“ nicht mit Podosomen, den wichtigsten adhäsiven und abbauenden Strukturen von Makrophagen, assoziiert. Des Weiteren wird gezeigt, dass die Oberflächenexposition von MMP7 ein relevanter Faktor für die Abbaufähigkeit von Makrophagen ist und durch den ADP-Ribosylierungsfaktor 6 (ARF6) gesteuert wird, der ein wichtiger Endozytoseregulator ist.

Es lässt sich zusammenfassen, dass lösliche MMPs eine inhomogene Gruppe sind, die zur Abbaufähigkeit von Makrophagen beitragen. Lösliche MMPs zeigen eine eigene intrazelluläre

Lokalisation und werden daher selektiv transportiert und reguliert. Einige zeigen eine Korrelation mit dem Polarisationszustand von Makrophagen. Lösliche MMPs können ohne Transmembrandomäne oberflächen-assoziiert sein. Die oberflächen-assoziierte Population von MMP7 wird durch den Endozytoseregulator ARF6 gesteuert. Die mechanistische Verbindung zwischen MMP7 und ARF6 (einem mutmaßlichen Rezeptor) ist jedoch noch nicht identifiziert und muss weiter untersucht werden. Einige potenzielle Kandidaten sind Heparansulfat-Proteoglykane (HPSGs) oder „Low-Density-Lipoprotein-Rezeptor-related Proteins“ (LRPs), aber auch „Tissue-inhibitors of Metalloproteinases“ (TIMPs) [69]. Die Abhängigkeit der Protein Expression von „soluble MMPs“ von der pro- oder antiinflammatorischen Polarisation ist ein wichtiger Aspekt in Krankheiten, in dem sich diese von MT1-MMP - einem konstitutiv exprimierten MMP in Makrophagen - unterscheiden. Dies ermöglicht eine spezifischeres therapeutisches Targeting auf Regulationsmechanismen in Makrophagen und deren Rolle in verschiedenen Krankheiten, z.B. als tumorassoziierte Makrophagen (TAMs) für künftige Arbeiten.

1 INTRODUCTION:

1.1 Macrophages

1.1.1 The role of macrophages

Macrophages are immune cells, which are present in animals in the metazoan phylogeny. Especially in mammals, macrophages are localized in every tissue and show a high functional and transcriptional diversity under normal physiological or pathological conditions. These cells are part of the innate immune system and are involved in the interplay between the adaptive and the innate immune system [1]. Tissue resident macrophages (TRMs) are found in various organs. For almost all of these macrophages, the major lineage regulator is the colony stimulating factor 1 receptor (CSF1R), which is expressed on mononuclear phagocytic cells and activated by CSF1 [2].

They are phagocytic mononuclear cells, which were once subsumed together with endothelial-, dendritic- and reticular cells to the “mononuclear phagocyte system” due to their functional and morphological properties. The phagocytic cells were subdivided into 2 groups: the polymorphonuclear phagocytes (granulocytes) and the mononuclear phagocytes. Circulating monocytes, promonocytes and their respective precursor cells in the bone marrow as well as tissue macrophages were classified as mononuclear phagocytes [3]. When classically activated, macrophages move to inflammation hot spots such as tumour cells or local infections and are attracted by their hypoxic conditions. But also monocytes are attracted by tumour cells by CSF-1, CCL2, CCL3, CCL4, CCL5 and CCL8, macrophage inflammatory protein-1 (MIP-1), macrophage migration inhibition factor (MIF) and the vascular endothelial growth factor (VEGF) [4].

1.1.2 The origin of macrophages

The traditionally postulated origin of macrophages are circulating blood monocytes. But there are also prenatally established populations identified, which reside at different tissues, persist through adulthood and show self-renewing properties. These earliest macrophage populations are derived from precursors from the extra-embryonic yolk sac (YS) during embryogenesis. The mentioned precursor cells are hematopoietic stem cells (HSCs), which colonize the fetal liver (FL) and differentiate into tissue-resident macrophages (TRMs) such as Kupffer cells, the brain and develop into microglia cells and the bone marrow [5]. The origin of blood-derived macrophages are circulating monocytes. Both are part of the innate immune system and derived from myeloid progenitor cells. These cells differentiate into promonocytes, the progenitor cells of monocytes [4]. Mononuclear phagocytes were subdivided into circulating mononuclear phagocytes and tissue macrophages, which reside in the spleen, the liver, lymph nodes and the lung. Bone marrow promonocytes were identified as the origin of circulating monocytes by isotope labeling and

subsequent x-irradiation of organs in mouse model experiments. This allowed to identify these circulating monocytes as the origin of inflammatory macrophages [6].

Macrophage Lineages Redefined

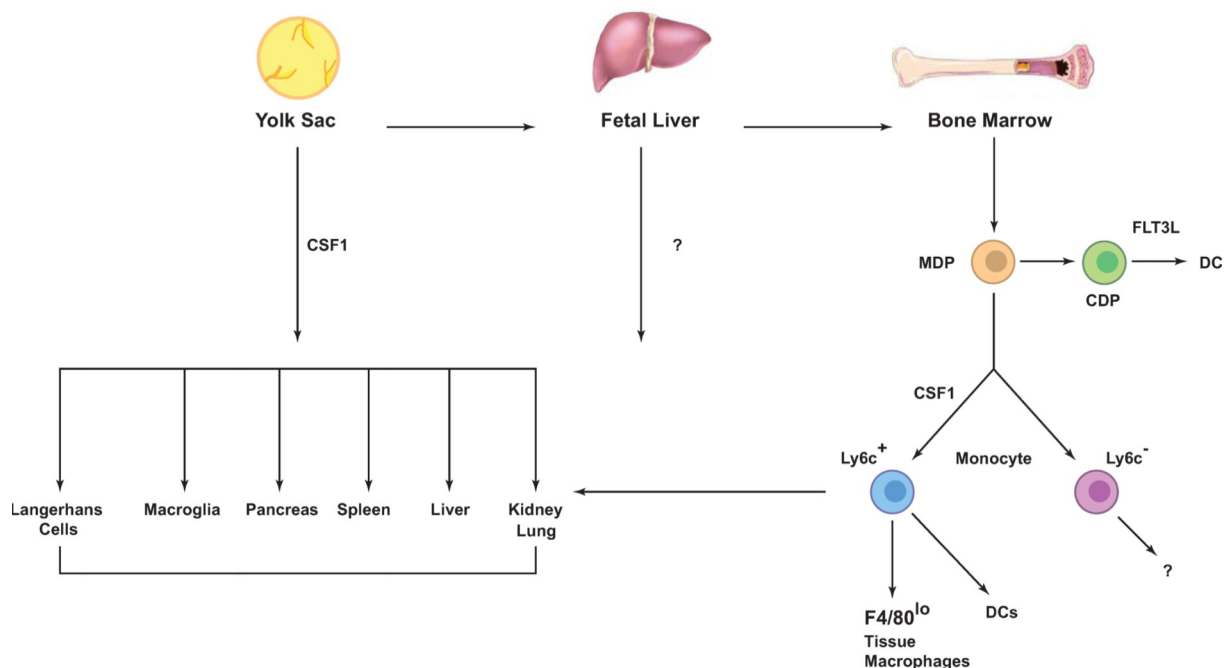


Figure 1.1.2: Macrophage lineages redefined in mice. 3 major origins of adult macrophages are the yolk sac (YS), the fetal liver (FL) and the bone marrow (BM). The YS is the source for both the tissue resident macrophages, promoted by CSF1 and probably the less well defined source: fetal liver (FL). The progenitor cells in the FL originate form in the third source, the bone marrow (BM), which is generating the progenitor cells for circulating monocytes and macrophage cells. Modified from Wynn et al., 2013.

1.1.3 The migration of macrophages

To infiltrate tissue, macrophages can enter the amoeboid or the mesenchymal mode of migration. The capability of macrophages to infiltrate the tissue is an important aspect to execute their properties in innate immune response, but is also important for (chronic) inflammation in a pathological context [7].

The migration through most of the tissues is one of the key abilities of macrophages and necessary to target the local inflammation. Macrophages are capable of amoeboid, mesenchymal and the pseudopodial amoeboid migration through the tissue. Amoeboid migration neither depends on (integrin-mediated) adhesion to the extracellular matrix nor degradation of it [8].

In contrast to that, the mesenchymal migration requires integrin-mediated adhesion to the extracellular matrix (ECM)-surface. In the pseudopodial amoeboid mode, macrophages pass narrow areas without degrading the surrounding ECM by forming a pseudopodial leading edge [8]. Both migration modes require a cytoskeletal deformability.

Both amoeboid-, and the pseudopodial amoeboid migration modes are Rho kinase (ROCK)-dependent and integrin-independent, in contrast to the mesenchymal migration mode, which is

ROCK-independent and integrin and Src-kinase dependent. The migration mode is dependent on the ECM composition, its stiffness and architecture. For the majority of connective tissue, which is composed of cross-linked fibrillar collagen I, the amoeboid migration mode is sufficient to pass the loose and porous structure of this ECM. To pass rather dense and highly cross-linked structures of the basement membrane, which separates endothelial and epithelial cells and is composed of perlecan, nidogen, collagen IV and laminin, the mesenchymal migration mode is entered and proteolytic degradation and adhesion of macrophages is required [7].

To describe the process of mesenchymal migration, a five-step model of cell migration was postulated: After initial attachment, the formation of a leading pseudopod can be observed (1), followed by pseudopod adhesion (2). Then, the cell body translocates to the leading edge (3) and the rear end of the cell is released (4) and retracted (5) [8] (figure 1.1.3).

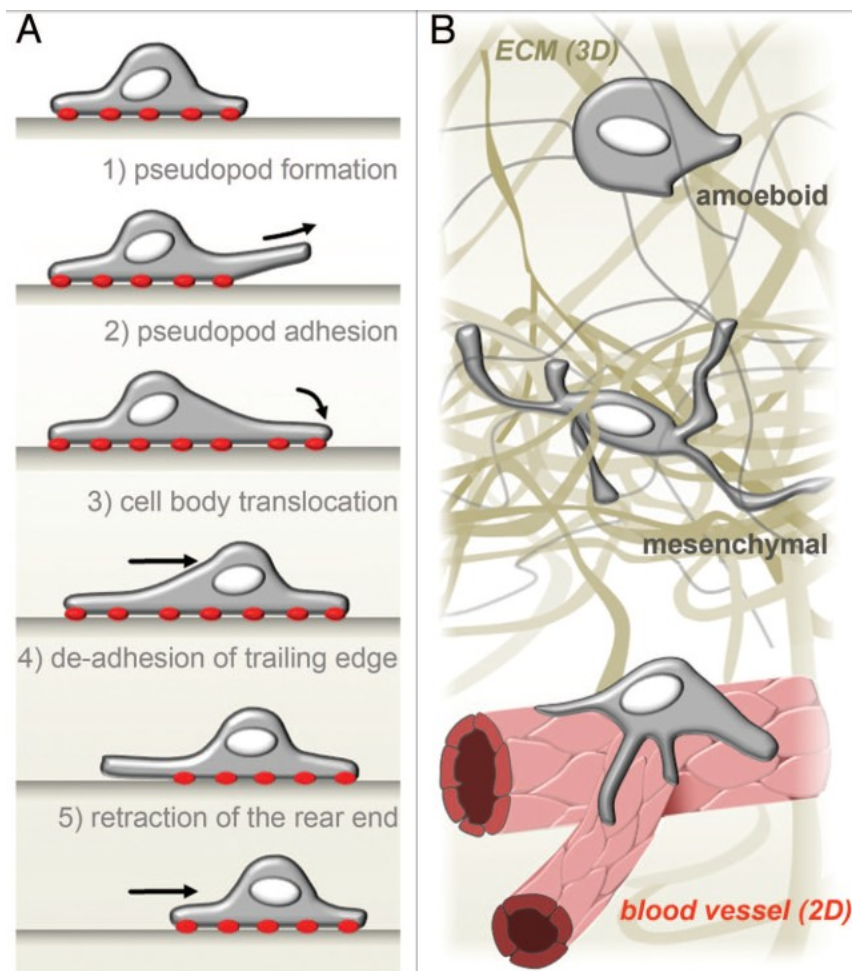


Figure 1.1.3: 2- and 3- dimensional migration modes of macrophages. (A) In vitro five-step model of the mesenchymal migration mode of macrophages with podosomes for adherence in red. **(B)** Macrophages *in vivo*, migrating through the extracellular matrix (ECM) either in amoeboid mode through highly porous tissue or in mesenchymal mode through dense ECM 3-dimensionally, or 2-dimensionally at the surface of blood vessels. From Wiesner et al., 2014.

1.1.4 Macrophages and podosomes

The adhesion of macrophages to ECM during the mesenchymal migration is dependent on their main adhesive structures, the so-called podosomes, which are observed in both 2D- and 3D culture conditions. These adhesive structures promote also the ECM-degradation by associated proteases such as matrix-metalloproteinases (MMPs) and a disintegrin and metalloproteases (ADAMs). Podosomes are also constitutively formed by other monocytic-derived cells such as dendritic cells and osteoclasts and can be induced in smooth muscle and endothelial cells. The podosomal structure can be divided into 3 parts, endowed with some typical components: 1. A core, which is composed of highly dense F-actin filaments, the Arp2/3 complex, cortactin and gelsolin. 2. a core-surrounding ring structure, which is composed of the adhesion plaque proteins vinculin and talin. 3. a cap-structure, which is located at the top of the core and consists of formin INF2 and the myosin-binding protein supervillin. Macrophages form super structures of many podosomes at the adhesive site, the so-called podosome-rosette [8] (figure 1.1.6), but also podosome-rings, -belts and -clusters. Podosomes need Filamin A (FLNa) for stabilization by cross-linking and polymerization of actin filaments and rosette formation. FLNa is the most abundant of 3 other filamin isoforms and localizes at podosomes in a ring-form together with paxillin and vinculin and is responsible for mechanosensing, a process to sense the resistance of the contacted extracellular matrix [9].

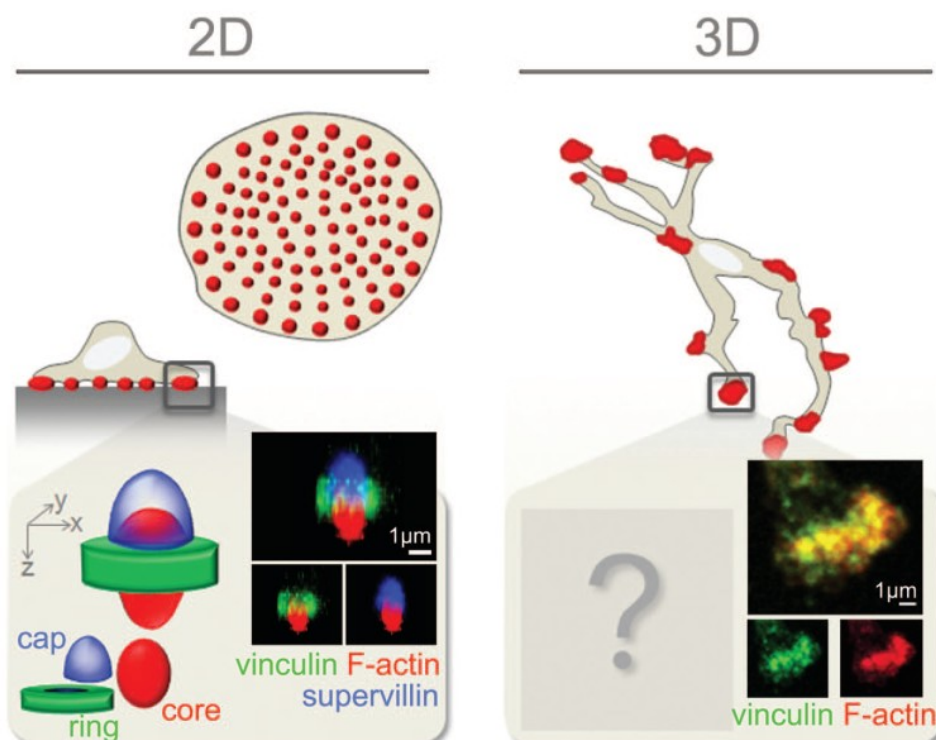


Figure 1.1.4: General podosome structure of macrophages in 2D and 3D. Podosomes displayed as red dots on macrophages and their general structures, evaluated in 2D-cultivation with a core structure composed of F-actin (red), a surrounding ring composed of vinculin (green) and the cap structure composed of supervillin (blue) and podosomes without resolved substructures in 3D cultivation. Modified from Wiesner et al., 2014.

Podosomes are usually examined in 2D-culture models, but they can also be observed in 3D culture conditions, mainly formed on the cell-surface of macrophages. By that, macrophages perform the proteolytic mesenchymal migration mode [9].

1.1.5 The polarization of macrophages in pathogenesis

Macrophages are involved in both physiological and pathological processes, e.g. as so-called tumour-associated macrophages (TAMs). Once monocytes and macrophages are recruited by tumour cells, macrophages become differently activated into an anti-inflammatory polarization state as TAMs. After that, TAMs provide an immune-evasive environment for tumour cells, also promoting angiogenesis. The presence of TAMs in the tumour micro environment (TME) correlates with an increased metastasis and poor prognosis. TAMs promote the inflammation by expressing $TNF\alpha$, which is internalized by tumour cells and leads to NF- κ B activation. NF- κ B acts as a gene switch, that promotes the production of anti-apoptotic and pro-inflammatory proteins. M2-like TAMs also express cytokines as TGF- β for immunosuppression by weakening the cytotoxic T cell response [4] (figure 1.1.5).

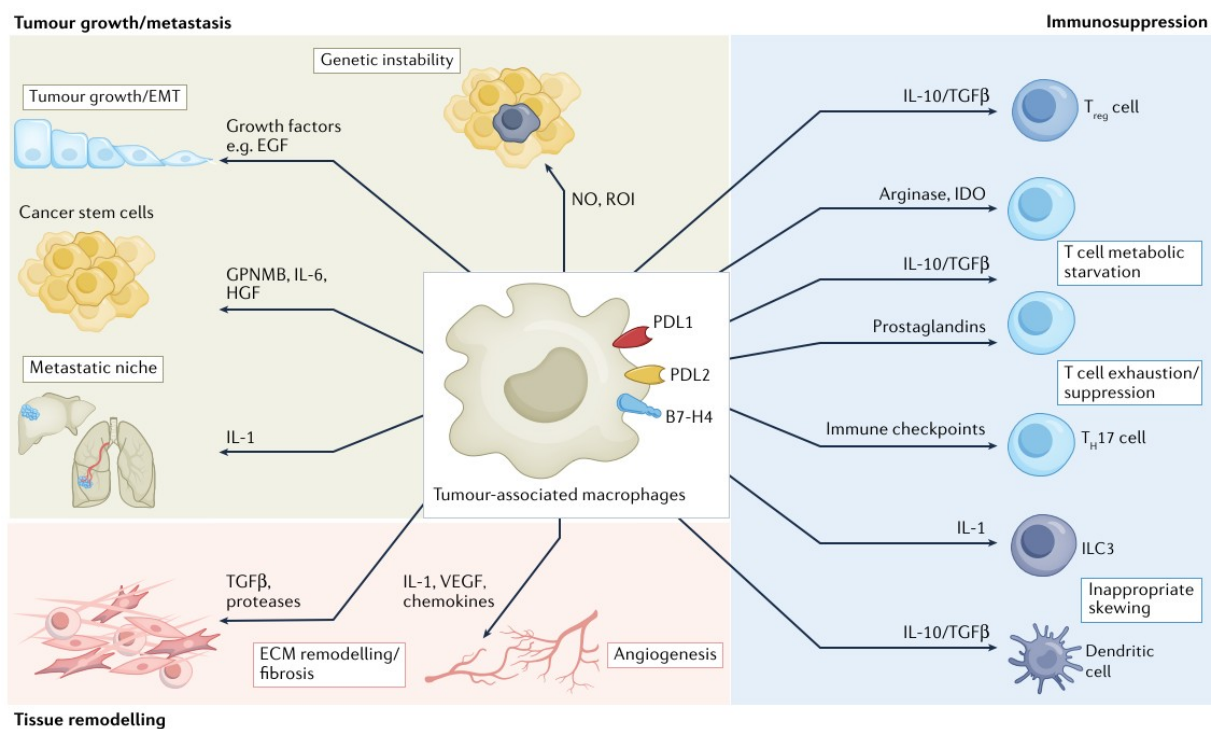


Figure 1.1.5: Tumour-associated macrophages in tumour-supporting activities. TAMs promote tumour-growth/metastasis, immunosuppression and tissue remodeling by producing pro-inflammatory cytokines and chemokines. From Mantovani et al.; 2022.

Angiogenesis is an important process to supply the tissue with nutrients and oxygen. This process promotes hereby wound repair in injuries and counteracts tissue ischemia and is provided by TRMs through stimulation of endothelial tip cells [10]. The anti-inflammatory activation of macrophages

is controlled by tumour cells, which express cytokines like IL-10 and colony-stimulating factor 1 (CSF1), and chemokines: CXCL4, CCL2, CCL17 and CCL18. The main source for TAMs are TRMs, which are directly accessible for the respective tumour cells and are known as a part of the TME [4]. These macrophages interfere with the immune response as a natural response to tumour cells, which are recognized as a local inflammation. TAMs subvert the immune response by immunosuppression, and defeat chemotherapy or checkpoint-blockade immunotherapy by expressing PDL1 and PDL2 as inhibitory receptors. By that, macrophages became a valuable therapeutic target [1]. The function of macrophages in both pathological and physiological conditions is defined by their polarization state. Classically activated macrophages (AMs) – also named M1-activated macrophages – are pro-inflammatory cells, which usually perform phagocytosis of both pathogens and tumour cells and promote antibody-dependent cytotoxic tumour killing. They combat pathogens by the production of nitric oxide (NO) or signal molecules such as interleukin 6 (IL-6), IL-12 or the tumour necrosis factor α (TNF- α) to induce apoptosis [11]. Another way of activation or polarization leads to the alternatively-activated macrophages (AAMs) or M2-activated macrophages. In homeostasis, they promote tissue-repair and resistance to pathogens such as parasites in an anti-inflammatory manner. Tumour-associated macrophages (TAMs) are a crucial factor for cancer pathology, promoting ECM-remodeling, angiogenesis, immunosuppression and even cancer progression and metastasis. This activation is induced by interleukins IL-3 and IL-14. They promote a pro-inflammatory reaction by producing IL-10, IL-1 receptor antagonist and transforming growth factor β (TGF- β) and thus supporting tumour growth and proliferation, angiogenesis and also immune evasion [11]. But since different cells with a transcriptomically dynamic phenotype are known, which show both polarization properties, this classification seems to be outdated and has rather a supporting function [1]. Resident or infiltrating macrophages usually react on tissue injuries with the production of angiogenic, fibrogenic, mitogenic and cytotoxic mediators to prevent infections, resolve inflammation and support wound healing. The balanced interplay between classically activated (M1) macrophages, which are capable of cytotoxicity, and alternatively activated subpopulations of macrophages (M2), promoting immunosuppression and wound repair, is required for a physiologically balanced response under homeostatic conditions [11], [12].

1.2 Matrix metalloproteases

1.2.1 The classification of MMPs

In the previously described physiological and pathological processes, the proteolytic degradation of the ECM is the major function of macrophages either for mesenchymal migration to defeat local inflammations or to promote metastasis for cancer cells. The proteolytical degradation of the ECM by macrophages is promoted by matrix metalloproteases (MMPs). MMPs are members of the zinc-dependent endopeptidase family and are further classified as matrixins, a subgroup of the metzincin

superfamily. This family includes 28 different enzymes in vertebrates and 23 of them are known to be expressed in human tissues [13],[14]. One way to classify MMPs, is the substrate-specificity. MMPs can be classified as Matrilysins, Collagenases, Gelatinases, Stromelysins and other MMPs, even though, the substrate-specificity overlaps, partially [14], [15]. Another way to categorize MMPs is to distinguish their structural properties, which partially overlaps with the substrate-specificity. Structural features like the transmembrane-domain, the GPI-anchor or furin-like motifs connecting the propeptide and the catalytic domain (secreted, type I and II MT-MMPs, GPI-anchored MT-MMPs) or hemopexin-like domains[16], [17].

Beside of the prominent MT1-MMP and others, endowed with a transmembrane domain, which belong to type I MT-MMPs, structural features as furin-like motifs connecting the propeptide and the catalytic domain (secreted, type I and II MT-MMPs, GPI-anchored MT-MMPs), or hemopexin-like domains (Matrilysins), but also substrate specifications were used to distinguish between MMPs (Collagenases, Gelatinases, Stromelysins and other MMPs). The soluble MMPs, lacking a transmembrane-domain or a GPI-anchor, are expressed and secreted as zymogens [14], [15].

This proteases are expressed as zymogens – inactive forms of enzymes endowed with propeptides, which need to be cleaved off [13]. The MMPs - as zymogens expressed - consist of a propeptide with a length of approx. 80 amino acids, the catalytic metalloproteinase domain (approx. 170 amino acids), a linker peptide, also called hinge region with variable length (exceptions are MMP7, 23 and 26, which do not have this linker peptide and the hemopexin domain), and a hemopexin domain (approx. 200 amino acids) [18], [19], [20], [21]. The only exceptions are MMP7, 23 and 26, which do not have the linker peptide and the hemopexin domain. MMP23 is also the only one endowed with a C-terminal cysteine-rich domain and an immunoglobulin-like domain immediately after the C-terminus of the catalytic domain. The propeptide represses the catalytic activity by interacting with the catalytic domain with its cysteine switch motif PRCGXP. The sulfhydryl group of the cysteine switch motif chelates with the active site of the zinc ion binding motif. The catalytic domain requires a Zn^{2+} ion, bound by three histidines from the conserved sequence HEXXHXXGXXH and additionally bound by a glutamate and the so-called met-turn (XBMX) for the catalytical active three-dimensional structure [22], [23], [24], [15]. By these structural features, MMPs can be distinguished (figure 1.2.1).

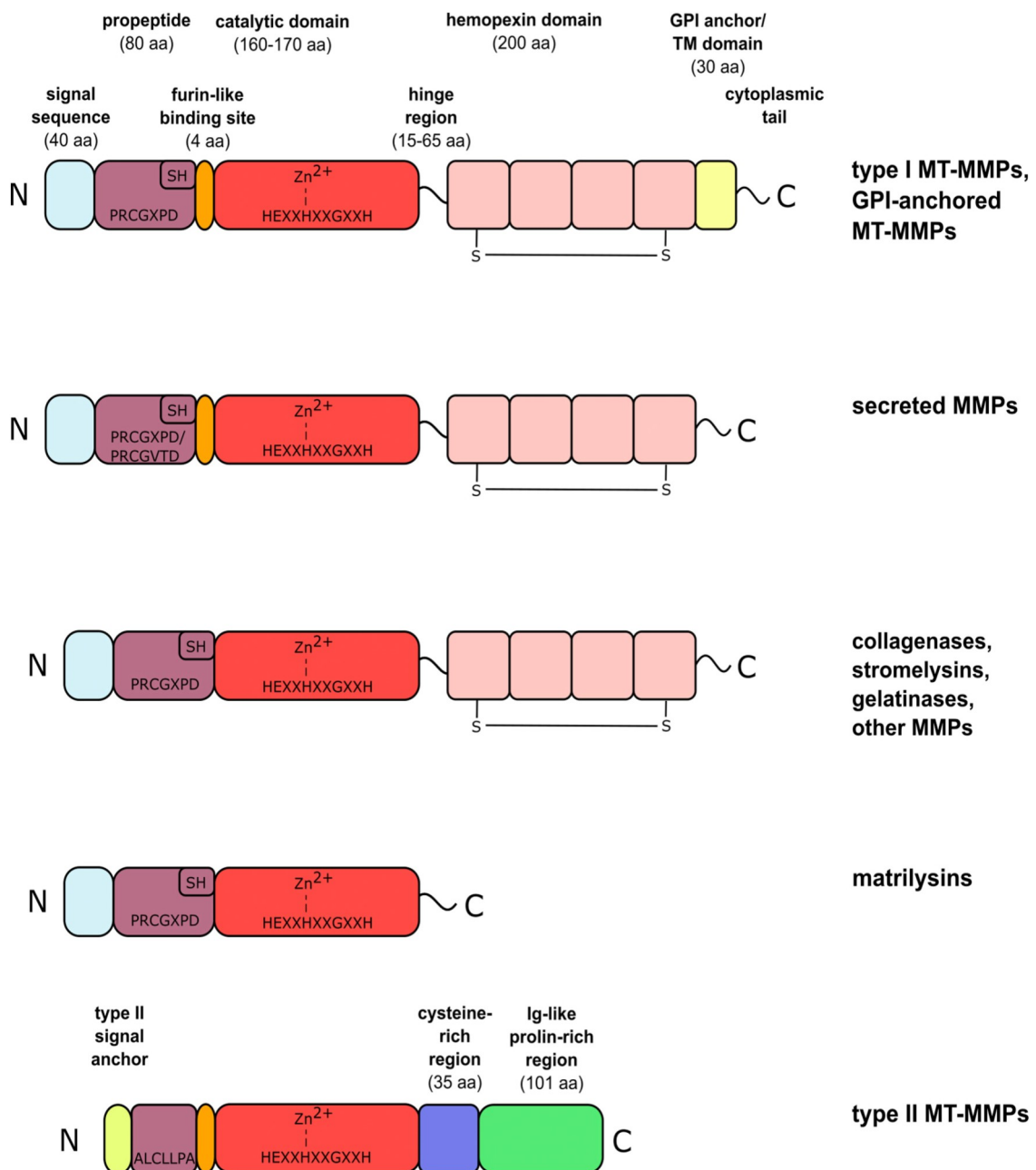


Figure 1.2.1: Overview of schematic MMP-domain structures. MMPs are expressed as zymogens, endowed with an N-terminal signal sequence (light blue and yellow) and an inhibitory propeptide (brown), followed in some types from a furin-like binding site (orange) and the catalytic domain (red) – responsible for the enzymatic cleavage of substrates. Flexible hinge regions connect the catalytic domain with the hemopexin domain (rose), which is important for substrate recognition. Type I transmembrane MT-MMPs are endowed with a transmembrane (TM) domain to anchor in the plasma membrane of the cell; Type II MT-MMPs contain also a cysteine-rich region (blue) and an Ig-like prolin-rich region (green). From Hey et al., 2021.

1.2.2 MMP substrates

As previously described, MMPs can be distinguished by their substrate specificity, which also describe their functionality. The main function of MMPs is the degradation of ECM components to provide macrophages the mesenchymal migration through dense tissue by degrading ECM components such as collagen type I, II and III and IV, fibronectin, aggrecan, fibrin, vitronectin, laminin 1 and 5 [13].

But not only ECM components are substrates. The shedding of surface proteins is also an important role of MMPs. MT1-MMP sheds surface proteins such as CD44, syndecan 1 and αv integrins 1. MT1-MMP activates also other MMPs by removing enzymatically their prodomain. It must be cleaved off by other MMPs such as MT1-MMP to provide enzymatic activity. The activity of MMPs is mainly regulated by prodomain removal or association with inhibitors such as TIMPs and to a lesser extent oligomerization with other MMPs. The prodomain is cleaved off by autoactivation, convertases such as furin or by other MMPs (e.g. proMMP-2, which is activated by MT1-MMP) [13]. TIMP-2 binds the catalytic domain, the first MT1-MMP binds the HPX-domain and the second MT1-MMP cleaves the zymogen [25]. MMP7 is also involved in the degradation of the ECM. It is associated as a known biomarker to different tumours, for example in solid cancer. MMP7 promotes metastasis and invasion by cleaving casein, gelatin I, II and IV, proteoglycans and fibronectin [26]. Also signal molecules like cytokines are substrates and thus affecting the pro- or anti-inflammatory communication between cells. IFN-gamma upregulation is known to induce inflammatory processes. This upregulation is caused by reduced MMP12 levels. MMP12 has several substrates, which are part of the ECM like elastin, fibronectin, laminin, collagen type I and IV, proteoglycan core protein, but also the cytokine IFN-alpha. It is shown in both human and mouse by enzyme kinetic analyses that the proinflammatory cytokine IFN-gamma, but not the immunosuppressive IL-4, is a substrate for MMP12. MMP12 truncates IFN-gamma at the C-terminus and thus removes the receptor binding site to the IFNGR. The posttranslational truncation by MMPs is a common regulatory mechanism for cytokines and chemokines. This prevents the proinflammatory macrophage activation via JAK/STAT1-signaling [27]. MMP12 contributes as well in an anti-inflammatory way by inhibiting corneal neovascularization through the regulation of CCL2. CCL2 and its receptor CCR2 regulate the neovascular and inflammatory responses of injuries as a part of tissue homeostasis. In this inflammatory response, neutrophils and macrophages are recruited, which infiltrate the damaged tissue and release proteases like MMP12 to prevent fibrosis. A negative correlation was observed in both expression and mRNA-levels of CCL2 and MMP12 after injury in mice corneal tissue. CCL2 is cleaved and inactivated by MMP12 [28]. Summarized, MMPs cleave a vast field of substrates, which are not only part of the ECM, but also of intercellular communication, especially in the inflammatory response, which is relevant for pathological processes.

1.2.3 MMPs and the polarization of macrophages

Macrophages can be either pro- or anti-inflammatory polarized, expressing different properties for initial response of the immune system and good resolution [29]. Therefore, macrophages need to migrate through the tissue to the hotspot of inflammation – occasionally by degradation of ECM-components. This ability is provided by MMP-expression. But also more complex processes such as signaling and adherence is maintained by MMP-activity. For instance, endoglin (also called CD105), an

important cell surface receptor of endothelial cells and macrophages, is shedded by MMP12 [29]. Endoglin is upregulated at inflammatory conditions and involved in angiogenesis as a co-receptor for TGF- β and interacts with integrins of monocytes. This process is initiated by TNF- α , leading to an upregulated MMP12-expression. There are also other (soluble) MMPs, which are known to be up- or downregulated in respective polarization states of macrophages such as MMP7, also reported to be upregulated in pro-inflammatory macrophages or MMP19, which is significantly down-regulated. MT1-MMP (also named MMP14) seems not to be affected by the polarization and is constitutively expressed in macrophages. But also some soluble MMPs are independently expressed by the polarization (MMP2, MMP9, etc.)[29] (figure 1.2.3).

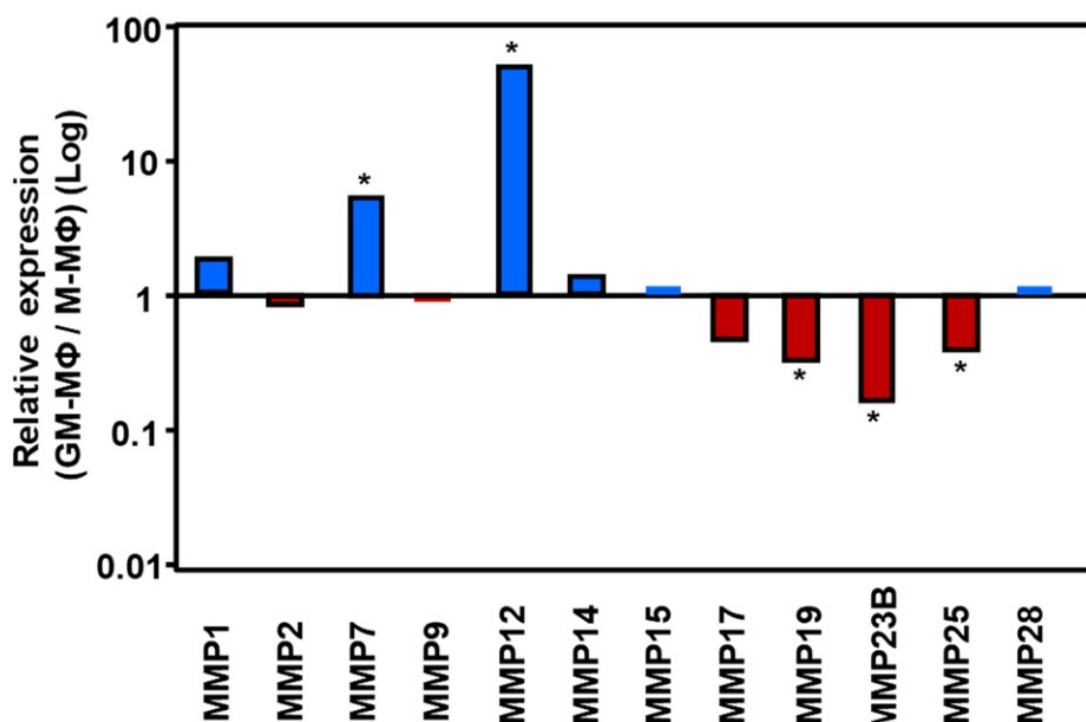


Figure 1.2.3: MMP expressions in M1- or M2-polarized macrophages. Logarithmic relative expression ratios of MMPs show increased expression of MMP1, MMP7 and MMP12 in M1- (/GM-M ϕ) polarized macrophages and a decreased expression of MMP23B, MMP25, MMP19 and MMP17 and *vice versa* for M2- (/M-M ϕ) polarized macrophages. Others such as MMP14 (also named MT1-MMP) or MMP2 and MMP9 are not affected. From Bernabeu et al., 2019.

1.2.4 MMP-trafficking

MMPs, expressed by cells such as macrophages, can not only be distinguished by their structural properties or their substrates. The initial step of discriminating MMP subgroups and their substrate-specificity, leads to the question of intracellular regulation of controlled MMP expression and secretion. Intracellular MT1-MMP-trafficking is often used as a representative example for MMP-trafficking in general. MT1-MMP is the most researched one and easily to localize at the cell surface due to its transmembrane domain. But also so-called soluble MMPs are known to be surface-associated such as pro-MMP2, which bind to TIMP-2 or MMP9 in complex with CD44 and $\alpha 4\beta 1$ integrin in malignant B-cells [30], [31]. And also heparan sulfate proteoglycans (HSPGs) are known to

bind soluble MMPs such as MMP2 or MMP7 at the cell surface and even receptor-independent surface-association is known at exposed positive charges with hydrophobic groups to the lipid bilayer [13] (figure 1.2.4).

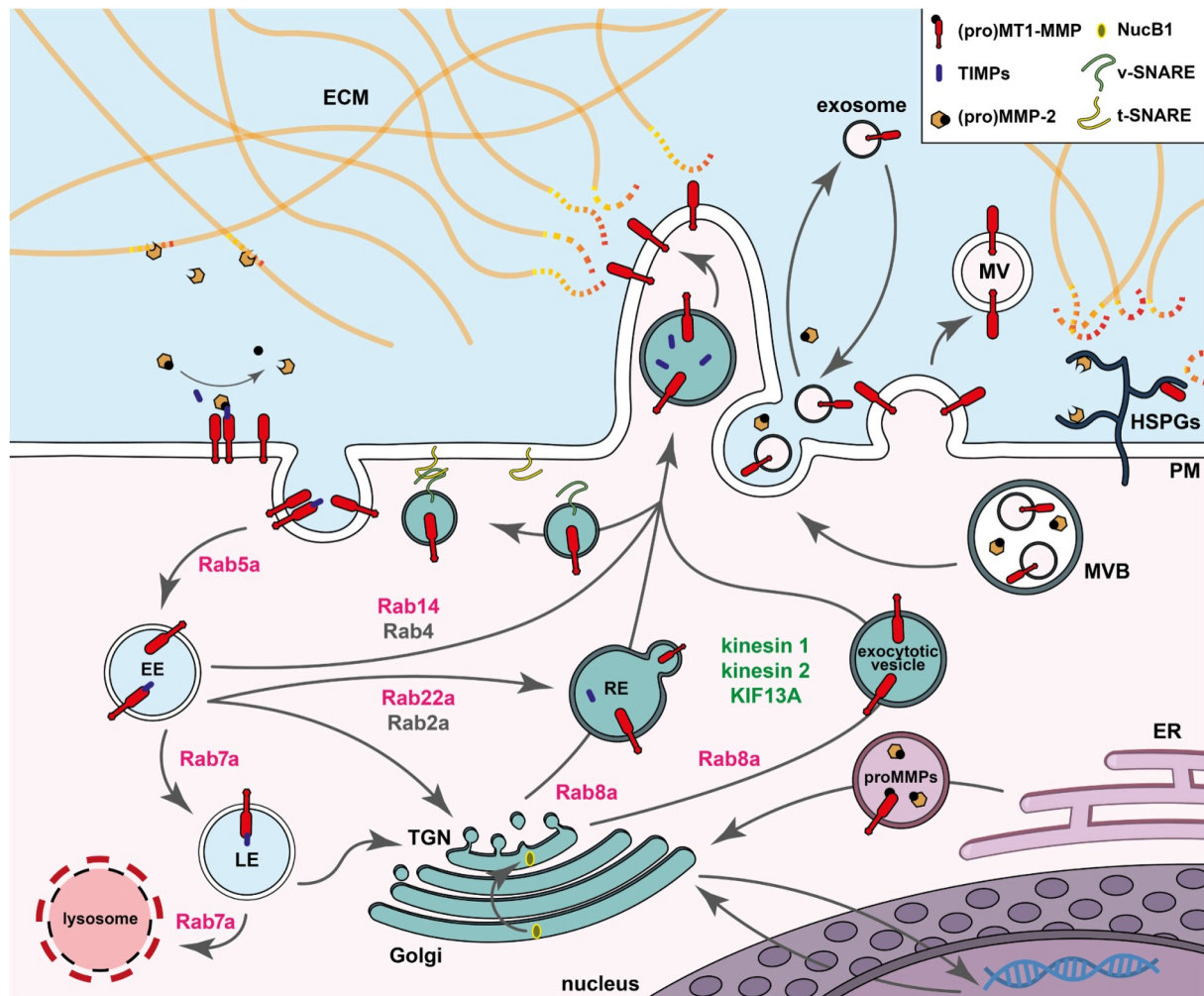


Figure 1.2.4: Trafficking pathways of MMPs. Translated immature proMMPs from the ER were transported to the Golgi apparatus and get posttranslationally modified in the trans-Golgi network (TGN), subsequently transported to the cell-surface by exocytotic vesicles (predominantly to structures such as invadosomes) and are either surface-exposed or further transported into the extracellular space by exosomes or multivesicular bodies (MVBs) to degrade the extracellular matrix (ECM). Some MMPs regulate transcription factors in the nucleus. Extracellular MMPs are endocytosed in early endosomes (EE) and either further transported in late endosomes (LE) to lysosomal degradation) or back to the TGN or recycled back in recyclin endosomes (RE). Cell-surface association occurs either through the own transmembrane-domain of proteases such as MT1-MMP or through association to heparan sulfate proteoglycans. RabGTPases regulate the physiological transport in macrophages (pink) and in tumour cells (grey) as well as microtubule-dependent kinesins (green). From Hey et al., 2021.

Vesicles with MT1-MMP-cargo are transported to the cell surface at microtubuli. For MT1-MMP, this process is promoted by the motor proteins kinesin-1 and -2 (also known as KIF5B and KIF3A/KIF3B) for exocytosis, also termed plus-ended transport at the microtubuli. But also MMP9 was observed to be associated with kinesin-1 and -2. The opposite direction is promoted by cytoplasmic motor protein dynein, called minus-ended transport after endocytosis. The c-Jun NH2-terminal kinase interacting

proteins (JIP)-3 and -4 are responsible for the regulation of these motor proteins as well as the plasma membrane-associated GTPase ARF6 or EEA1, which are responsible for endocytosis. The endocytosis itself is also an important regulative mechanism to internalize and hereby regulate the availability of (active) surface-associated proteases. This occurs mainly for MT1-MMP via clathrin- or caveolin-dependent pathways, but also by clathrin-independent carriers/GPI-anchored protein enriched compartments (CLIC/GEEC). Soluble MMPs such as MMP9 or MMP2 were reported to be endocytosed by the surface-receptor LRP-1 in HT1080 fibrosarcoma cells [13]. Once internalized, the fate of MT1-MMP in human macrophages is decided by the small RabGTPases Rab5 for endocytosis, or Rab22 and Rab14 for slow and fast recycling, respectively, and Rab7 for lysosomal degradation [32]. One recycling pathway is mediated by the so-called retromer-complex, which is composed of VPS (vacuolar protein sorting) proteins, VPS26, VPS29 and VPS35, which associate with sorting nexin SNX27 [13].

1.2.5 MMPs and diseases

Although different MMPs are important for physiological processes [33], they are also well-known biomarker for diseases like acute lymphoblastic leukemia (ALL) [26], glioma and glioblastoma [34], NSCLC [35], breast cancer [36], melanoma [37], prostate cancer [17], hepatocellular carcinoma [38], colorectal cancer [39], rheumatoid arthritis [27], [40], and cardiovascular diseases [28], [41], [42]. Even insensitivity to chemotherapy is affected by MMPs [43] as well as antitumour-effects [44]. Tumour cell invasion and migration is affected by many factors such as the capability to degrade the extracellular matrix (ECM) by MMPs, located at the vicinity of degradative structures as invadopodia and podosomes on macrophages [45], [46]. MT1-MMP, one of the major ECM-degrading proteases, is transported from endosomal compartments to invadopodia via microtubules to promote this process. The formation of invadopodia needs dynamic F-actin- and cortactin-rich assemblies, which accumulate MT1-MMP. This assembly is managed the multi-domain scaffold protein cortactin, which binds actin and Arp2/3 complex-dependent branched actin filament networks[47].

RabGTPases are key components of MMP-exocytosis and recycling regulation in this intracellular vesicles, which influence the invasive and degradative capability of cancer cells and tumour-associated macrophages (TAMs). One regulatory mechanism is the recycling of MT1-MMP and thus the surface exposure in proximity to invadopodia and podosomes. The master switches of recycling are RAB4 in cancer cells and RAB14 in macrophages. The endocytic uptake of MT1-MMP is regulated by the RABGTPase RAB5a, acting as a negative regulator in primary human macrophages [13], [30], [32]. The downregulation of its activity showed increased invasive capacity and degradation capability. Surprisingly, the effect in cancer cells such as MDA-MB-231 breast cancer cells, is an opposite one. RAB5a is also known to be overexpressed in breast cancers and lymph node metastases and correlates positively with poor prognosis. It is necessary for invadopodia formation and turnover

in this cells, but not in podosomes of macrophages [45].

The metastasis and invasion of tumour cells is caused by invadopodia endowed with MMPs such as MT1-MMP [45], [46]. The localization of MT1-MMP at invadopodia is regulated by intracellular trafficking factors like v-SNARE TI-VAMP/VAMP7. SNAREs are important for membrane fusion and VAMP7 is known to localize on lysosomal structures and the TGN. MT1-MMP localizes mainly in late endosome, acting as putative intracellular storage pool [48]. Another facet of the regulatory mechanism of MT1-MMP trafficking to invadosomes is the recycling by the SNX27/retromer assembly, also investigated in MDA-MB-231 cells. MT1-MMP is overexpressed in various cancer cells and localizes in endosomal storage pools. SNX27 interacts directly with MT1-MMP as a cargo adaptor to assist the retromer in recycling processes of proteases, mediating endocytosis by transmembrane recycling and sorting. The depletion of SNX27 affected selectively the MT1-MMP population at the cell surface in close proximity to invadopodia [49].

MMPs can offer novel alternative targets to established diagnostic methods [50], [51]. E.g. MMP19 is known as a biomarker for cancer diseases like glioma [52] or colorectal cancer (CRC) [39]. In patients with rheumatoid arthritis (RA), MMP19 is found in increased levels, but not involved in the synovial destruction during RA, although it is capable of ECM degradation, cartilage destruction [40].

In different publications, not only the correlation of increased or decreased MMP levels with putative signaling pathways in respective diseases are described, but also approaches for future treatments, targeting MMPs or their upstream and downstream signaling pathways. The inhibition of the beta-catenin/MMP7 signaling pathway by DKK-1 in breast cancer inhibited migration and invasion of the respective tumour cells. DKK-1 is known as a tumour suppressor in renal cell carcinoma and colorectal cancer, but has an opposite effect in hepatocellular carcinoma and myeloma. Increased MMP7 expression is a marker for poor prognosis in brain, breast, pancreas and colon cancer. The downregulation of MMP7 via DKK-1 inhibited migration and invasion of the cancer cells, suggesting MMP7 as a therapeutic target [36]. The importance of MMP12 for hepatocellular carcinoma (HCC) was also investigated. The development of HCC is promoted by upregulation of PD-L1, which showed a correlating expression to MMP12 and poor prognosis in different solid tumours and poor cell differentiation.

1.3 ARF6 and the regulation of endocytosis

1.3.1 ARF6 and MMPs

The correlation between ARF6-activity and the degradative capability of cells became a causal relation, when MT1-MMP was discovered to be an effector of the endocytosis regulator ADP-ribosylation factor 6 (ARF6) [53]. The Endocytosis of MMPs is crucial to provide the degradative capability of macrophages. The ADP-ribosylation factor 6 (ARF6), a Ras-related GTPase, is an important regulator of membrane trafficking and actin cytoskeleton formation. In primary murine

dendritic cells, ARF6 regulates both clathrin-dependent and clathrin-independent endocytosis (CDE and CIE) [54]. ARF-proteins are regulated by GTP exchange factors (GEFs), which activate ARF6 via exchanging GDP to GTP, and GTPase activating proteins (GAPs), which facilitate the hydrolysis of GTP to GDP, inactivating ARF6. The constitutively activated mutant ARF6-Q67L binds continuously GTP, being resistant to GAPs. In contrast to that, the constitutively inactivated mutant ARF6-T44N binds only GDP [54]. Both mutants are known to reduce the migrating activity of dendritic cells by impairing F-actin-rich podosome formation of immature dendritic cells, which shows that only the cycling between inactive and active form of ARF6 enables its proper function. Besides, the ARF6-Q67L-mutant causes an accumulation of surface proteins such as integrin 1β , E-cadherin or MHC I in endocytotic vesicles, but is also leading to an inhibited endocytosis via classical clathrin-pathway and an accumulation of surface proteins such as CD71, a marker for clathrin-dependent endocytosis [54]. ARF6 is an effector of clathrin-mediated endocytosis in human pulmonary artery endothelial cells [45]. In these cells, ARF6 regulates the endocytosis of bone morphogenetic protein receptor II (BMPRII). BMPRII induces the NF- κ B-dependent activation of hypoxia induced factors (HIF), which leads to NF- κ B activated inflammation [45]. After endocytosis, the surface protein is either directed to lysosomal degradation or redirected to the cell surface. Clathrin-mediated endocytosis requires gyrating clathrin (g-clathrin) for the endosomal, clathrin-dependent internalization. The activity of g-clathrin is regulated by chloride extracellular channel 4 (CLIC4) via ARF6, which is responsible for vesicular trafficking and lysosomal function of these cells. CLIC4 localizes in endosomal vesicles and interacts with the GTPase activating proteins (GAPs) GIT1 and GIT2, which facilitate the GTP hydrolysis, leading to an inactivation of ARF6. This impairs clathrin-mediated endocytosis, but not clathrin-independent endocytosis in human pulmonary artery endothelial cells. The pathological phenotype of overexpressed ARF6 is called pulmonary arterial hypertension (PAH) with remodeled small intrapulmonary arteries and increased vasoconstriction [45].

Clathrin-mediated endocytosis of plasma-membrane proteins requires a clathrin internalization sequence (containing tyrosine or dileucine motifs), which is recognized by the adaptor protein 2 (AP2) complex [55]. But there are various proteins, chemicals and pathogens, which are internalized as well without a clathrin internalization sequence via pinocytosis, macropinocytosis and phagocytosis. Two different clathrin-, dynamin and lipid raft-independent early endosome populations are known, with do not require such a sequence: ARF6-associated tubular recycling endosomes and other clathrin-independent endosomes, which are EEA1-associated [55]. These early endosome populations fuse with each other to Rab7-regulated late endosomes, supposed to degrade the cargo proteins of both clathrin-dependent and clathrin-independent endocytosed proteins. In the ARF6-Q67L mutant-condition, the fusion of these endosomes together with clathrin-endocytosed endosomes is impaired, leading to a selective degradation of only clathrin-cargo proteins.

Another important regulator of ARF6 is the Platelet-Derived Growth Factor (PDGF), which leads to the activation of PAK by the MAPK/ERK1/2 and PI3K/AKT pathways [53]. PDGF is known to show an increased activity in atherosclerosis and restenosis. In this pathology, the ECM-components in the tunica intima of vessels are structurally remodeled. PDGF PAK is necessary for the invasive capability of HASMCs and induces MT1-MMP expression. MT1-MMP cleaves inactive secreted MMP2 and enables its degradative activity of the ECM. The PDGF- and AngII-induced invasion of human aortic smooth muscle cells (HASMCs) could be reduced by ARF6-knockdown. It is reported, that in this model with ARF6-knockdown condition, MT1-MMP regulated MMP2 activity was reduced [53]. The ability of cells to invade and migrate is dependent on the degradation of extracellular matrix components by matrix-metalloproteases (MMPs) Especially in cancer cells, the epithelial-to-mesenchymal transition (EMT) is important for this process. MMP7 regulates this process by shedding E-cadherin - an important EMT-marker - and thus prevents its paracrine activity [56]. The production of MMP7 is mediated by the MAPK kinase pathway, which is regulated by ARF6, an important prognostic tumor marker in upper tract urothelial carcinoma (UTUC) cells [56]. Hence, ARF6 is not only important for endocytosis of different surface proteins or the formation of podosomes affecting the migration, but also directly to the degradative capability of tumour cells.

1.3.2 The role of ARF6 in diseases

Macrophages and their expressed MMPs play an important role in different pathological processes. ARF6 is reported to be involved in various processes affecting the activity of mainly MT1-MMP and by that, it is a key regulator in various processes of cancer-cell activities such as invasion, proliferation and metastasis [57]. In head and neck squamous cell carcinomas (HNSCCs), clear cell renal cell carcinomas (ccRCCs) and lung adenocarcinoma, ARF6 internalizes E-cadherin, which is important for cell adhesion and induces also the recycling of β 1-integrin and thereby promotes the epithelial to mesenchymal transition (EMT) [57]. The activation of the epidermal-growth factor receptor (EGFR) by AMAP1 leads to the activation of the GEF GEP100, GEP100 activates for its part ARF6. This process describes the process of epithelial, adherent cells, which become mesenchymal, migrating cells [57]. The EGFR-ARF6 signaling pathway is also responsible for actin cytoskeleton remodeling, which is important for ameboid, but also mesenchymal migration of cells. This promotes the invadopodia edge extension in breast cancer cells. The hepatocyte growth factor (HGF) also induces ARF6 activity and thus the recycling of β 1-integrin, which important for angiogenesis [57]. The proliferation of cancer cells is promoted by ARF6 through the activation of phospholipase D (PLD). This starts the PLD-mTORC1-S6K1/4E-BP1 signaling pathway, which initiates the mitosis of tumour cells [57].

In invasive and so far therapy-lacking high grade triple-negative breast cancer cells (TNBCs), ARF6, kinesin-1 and MT1-MMP are upregulated [58]. In these cells, MT1-MMP is rapidly surface-exposed on the plasma membrane, and subsequently internalized into endosomal compartments, followed by a subsequent transport to invadopodia via microtubules. Silencing of ARF6 led in MDA-MB-231-cells as a model for breast cancer cells to reduced exocytosis of MT1-MMP and a reduced invasiveness and degradative capabilities [58]. This is caused by the impaired interaction of ARF6 with c-Jun NH2-terminal kinase–interacting protein 3 and 4 (JIP3 and JIP4), which are important exocytotic regulators. JIPs are responsible for recruiting dynein-dynactin and kinesin-1 on MT1-MMP endosomes, which are exocytosed again by the interaction with ARF6. This was concluded as the cause of an impaired surface exposure of MT1-MMP [58]. As other cancer cells mentioned before, Esophageal Adenocarcinoma (EAC) and Barrett's esophagus (BE) cells have a tissue-invasive capability [59]. The purinic/aprimidinic endonuclease (APE1/REF-1) is overexpressed in these cells. It possesses a redox-function on critical cysteine residues of transcription factors such as STAT, p53 and NF- κ B and is also responsible for DNA-repair in the DNA base excision repair (BER) pathway [59]. By this, APE1 promotes the survival of tumour cells. The redox-specific inhibitor E3330 of APE-1 reduced cell invasion without impairing its DNA-repairing activity. MT1-MMP is known to be overexpressed in various cancer cells and a correlation between MT1-MMP- and APE1-expression in esophageal cell lines suggested a potential interdependence. APE1-silencing and defective mutant expression was reported to reduce the MT1-MMP cell surface levels. MT1-MMP is known to activate MMP2, which showed a reduced activity in zymography assays in APE1-knockdown conditions. Hence, it was postulated that ARF6 regulated APE1 activity and thereby the activity of MT1-MMP and MMP2 [59].

1.4 Aims of the dissertation

For the present dissertation, 3 objectives were pursued to characterize the regulation of soluble MMPs: The first aim was to analyze the protein expression of soluble MMPs over time during the differentiation of monocytes into macrophages and in correlation with their polarization *in vitro* to characterize their importance for the degradative ability.

The second aim was to investigate the intracellular distribution of soluble MMPs in relation to MT1-MMP and podosomes to identify distinctly regulated vesicle populations.

The third aim was to investigate the role of soluble MMPs at the cell surface and their importance for the degradative capability of macrophages and hereby the identification of their endocytosis regulation.

2 MATERIALS:

Table 2.1: Chemicals

Name:	Company:
Agar-agar	Roth, Karlsruhe (D)
β -mercaptoethanol	Sigma-Aldrich, St. Louis (USA)
CD14-beads	Miltenyi Biotec, Bergisch Gladbach (D)
Dimethyl sulfoxide (DMSO)	Roth, Karlsruhe (D)
Disodium hydrogen phosphate	Merck, Darmstadt (D)
DPBS (sterile)	Thermo Scientific, Waltham (USA)
ECL-substrate (Pico)	Thermo Scientific, Waltham (USA)
ECL-substrate (Femto)	Thermo Scientific, Waltham (USA)
Acetic acid (100%)	Roth, Karlsruhe (D)
Ethyldiamin-tetra-acetat (EDTA)	Roth, Karlsruhe (D)
Ethanol (96%)	Roth, Karlsruhe (D)
Glycerin	Roth, Karlsruhe (D)
Glycin	Sigma-Aldrich, St. Louis (USA)
Isopropanol	Merck, Darmstadt (D)
Potassium dihydrogen phosphate	Merck, Darmstadt (D)
Methanol	Roth, Karlsruhe (D)
Milk powder	Roth, Karlsruhe (D)
Mowiol	Roth, Karlsruhe (D)
NaCl	Roth, Karlsruhe (D)
NaOH 32%	Roth, Karlsruhe (D)
Normal goat serum (NGS)	Jackson ImmunoResearch Laboratories
NHS-Rhodamine	Thermo Scientific, Waltham (USA)
Hydrochloric acid	Roth, Karlsruhe (D)
SDS	Roth, Karlsruhe (D)
Sucrose	Roth, Karlsruhe (D)
SybrSafe	Thermo Scientific, Waltham (USA)
Triethyl amine	Sigma-Aldrich, St. Louis (USA)
Tris-Base	Sigma-Aldrich, St. Louis (USA)
Tris-HCl	Sigma-Aldrich, St. Louis (USA)
Triton-X	Sigma-Aldrich, St. Louis (USA)
Tween-20	Sigma-Aldrich, St. Louis (USA)

Table 2.2: Chemicals for cell culture

Name:	Company:
Human Serum	Transfusion medicine, UKE Hamburg (D)
L-Glutamin-Penicillin-Streptomycin (100x)	Sigma-Aldrich, St. Louis (USA)
Lymphocyte-Separation-Medium-1077	PAA Laboratories, Pasching (A)
OptiMEM	Thermo Scientific, Waltham (USA)
Accutase	eBioscience, San Diego (USA)
RPMI1640	Sigma-Aldrich, St. Louis (USA)

Table 2.3: Buffers

Name:	Recipe:
Blocking solution (IF)	PBS with 3% (v/v) normal goat serum
Blocking solution (WB)	TBS-T with 5% (v/v) milk powder
Staining buffer (IF)	PBS with 1,5% (v/v) normal goat serum
Primary antibody solution (WB)	TBS-T with 5% (v/v) milk powder
Secondary antibody solution (WB)	TBS-T with 5% (v/v) milk powder
Gelatin solution	50 mM sodium borat solution with 0,36% (w/v) NaCl and 0,2% (w/v) gelatin
Permeabilization buffer	PBS with 0,1% (v/v) Triton-X
Laemmli buffer	H ₂ O with 125 mM Tris-HCl, 4% (w/v) SDS, 10% (v/v) Glycerin, 10% (v/v) β-Mercaptoethanol and 0,02% (w/v) Bromopphenol blue
LB-Agar	H ₂ O with 1 % (w/v) Trypton, 0,5% yeast extract, 5% NaCl and 1,6% Agar-Agar; pH 7,2
LB-Medium	H ₂ O with 1 % (w/v) Trypton, 0,5% yeast extract and 5% NaCl; pH 7,2
Lysis buffer	H ₂ O with 50 mM Tris-HCl, 150 mM NaCl and 1% (v/v) Triton-X-100
Mild stripping buffer	H ₂ O with 1,5% (w/v) Glycin; 0,1% (w/v) SDS and 1% (v/v) Tween-20; pH 2,2
Monocyte buffer	PBS with 2 mM EDTA and 0,5% (w/v) humanem Serumalbumin; pH 7,4
Monomedium	RPMI with 20% (w/v) human serum and 1:1000 Pencillin/Streptomycin
Mowiol	H ₂ O with 100 mM Tris-HCl, 10% (w/v) Mowiol, 25% (v/v) Glycerin and 2,5% (w/v) Triethylamin
PBS (10x)	H ₂ O with 8% (w/v) NaCl, 1,4% (w/v) Na ₂ HPO ₄ , 0,2% KH ₂ PO ₄ and 0,2% (w/v); pH 7,3
SDS running buffer (10x)	H ₂ O with 25 mM Tris-HCl, 192 mM Glycin and 0,1% (w/v) SDS

TAE buffer (10x)	H ₂ O with 40 mM Tris-HCl, 20 mM acetic acid and 1 mM EDTA, pH 8,4
TBS-T (1x)	H ₂ O with 20 mM Tris-HCl, 150 mM NaCl and 5% Tween-20; pH 7,4
PBS-T (1x)	PBS (dil. 1:10 in H ₂ O) and 5% Tween-20; pH 7,4

Table 2.4: Antibodies for IF and WB stainings

Name:	Host species:	Dilution for WB:	Dilution for IF:	Company:	Catalogue number:
Anti-GAPDH	rabbit	1:40.000 in TBST, 5% milk	-	Proteintech, Planegg (D)	10494-1-AP
Phalloidin-AF-488	amanita	-	1:100	Thermo Scientific, Waltham (USA)	A12379
Phalloidin-AF-647	amanita	-	1:100	Thermo Scientific, Waltham (USA)	A22287
Anti-MT1-MMP	Mouse	1:1.000 in TBS-T, 5% milk	1:200	Merc-Millipore	MAB3328
Anti-MMP7	Mouse	1:1.000 in PBS-T, 5% milk	1:200	Arcis/OriGene Europe	AF8210
Anti-MMP9	Rabbit	1:1.000 in PBS-T, 5% milk	1:200	GeneTex	GTX100458
Anti-MMP12	Rabbit	1:1.000 in PBS-T, 5% milk	1:200	Proteintech	22989-1-AP
Anti-ARF6	Rabbit	1:1.000 in TBS-T, 5% milk	1:200	Invitrogen	PA1-093
Anti-EEA1	Mouse	-	1:200	Cell Signaling Technology	48453
Anti-CD163	Mouse	1:1.000 in TBS-T, 5% milk	-	Biorad	MCA1853
Anti-mouse IgG HRP-linked	Horse	1:10.000 in TBS-T/ PBS-T, 5% milk*	-	Cell Signaling Technology	7076P2
Anti-rabbit IgG HRP-linked	Goat	1:10.000 in TBS-T/ PBS-T, 5% milk*	-	Cell Signaling Technology	7074S

*The dilution buffer of secondary antibodies was the same as from the primary antibodies, respectively.

Table 2.5: siRNA and sequences for knockdowns

Target:	Sequence (5' → 3'):
MMP7	GUUAAACUCCCCGCGUCAUA
MT1-MMP	AACAGGCAAAGCUGAUGCAGA
ARF6	GUGGCAAUAAUGAGUAAU
SNX1	GAACAAGACCAAGAGCCAC
KIF5B	AAACCGAGUCCCUAUGUAAA
Luciferase (control siRNA)	AGGUAGUGUAACCGCCUUGUU

Table 2.6: Oligonucleotides for cloning

Name:	Sequence (5' → 3'):
QC-Arf6wt-FW	CGTATGGGATGTGGGCGGCCAGGACAAGATCCGGCCGCTC
QC-Arf6wt-RV	GAGCGGCCGGATCTTGTCTGGCCGCCACATCCCATACG

Table 2.7: Purchased plasmids

Name:	Company:	Catalogue number:
Arf6Q67L-EGFP	Addgene	#49883

Table 2.8: Kits

Name:	Company:
FastDigest Restriction Enzyme Kit	Thermo Scientific, Waltham (USA)
iBlot 2 NC miniStack-Kit	Thermo Scientific, Waltham (USA)
Miniprep Classic Kit	Zymo Research, Freiburg (D)
Neon Transfection Kit	Thermo Scientific, Waltham (USA)
Phusion High Fidelity Kit	Thermo Scientific, Waltham (USA)
QIAquick Gel Extraction Kit	Qiagen, Hilden (D)
μMacs ProteinA/G-Isolation Kit	Miltenyi Biotec, Bergisch Gladbach (D)
μMacs GFP-Isolation Kit	Miltenyi Biotec, Bergisch Gladbach (D)

Table 2.9: Consumables

Name:	Company:
Dialysis cassettes	Life Technologies, Carlsbad (USA)
glass coverslips (Ø 12/18 mm)	Karl Hecht GmbH, Söndheim v. d. Rhön (D)
Cultivation plates (6-/12-wells)	Sarstedt, Nümbrecht (D)

glass slides	Karl Hecht GmbH, Söndheim v. d. Rhön (D)
Petri dishes	Nerbe plus GmbH, Winsen (Luhe) (D)
Pipette tips (10/100/1000 µL)	Sarstedt, Nümbrecht (D)
Reaction tubes (0,5/1,5/2 mL)	Sarstedt, Nümbrecht (D)
Falcon tubes (15/50 mL)	Sarstedt, Nümbrecht (D)
Serological pipettes (5/15/25 mL)	Sarstedt, Nümbrecht (D)
Scalpel	B.Braun, Melsungen (D)
Stericup Vakuum Filter 0,2 mm Pore	Millipore, Billerica (USA)
Sterile filter, Filtopur S, 0,2 µm Pore	Sarstedt, Nümbrecht (D)

Table 2.10: Inventory

Name:	Company:
Neon transfection system (electroporator)	Thermo Scientific, Waltham (USA)
Gel chamber (Agarose)	Peqlab, Erlangen (D)
Gel chamber (SDS PAGE)	Bio-Rad, Hercules (USA)
Incubator Heracell 150i	Thermo Scientific, Waltham (USA)
Refrigerator (4°C)	Liebherr Premium, Bulle (CH)
Magnetic stirrer IKA RH Basic 2	Thermo Scientific, Waltham (USA)
pH-meter	Five easy, Mettler Toledo, Columbus (USA)
Pipetts	Peqette, VWR International, Radnor (USA)
Biometra LT 12 (shaker)	Analytik Jena, Jena (D)
Nanodrop (spectral photometer)	Nanodrop, Thermo Scientific, Waltham (USA)
Sterile bench MSC Advantage	Thermo Scientific, Waltham (USA)
Dual-Action shaker KL2	Edmand Bühler GmbH, Bodelshausen (D)
Freezer (-20°C)	Gram bioline, Vojens (DK)
Thermomixer	Thermomix Compact, Eppendorf, Hamburg (D)
Brightfield microscope Eclipse TS100	Nikon, Chiyoda (JP)
Transilluminator TFX-20M	Bio-Rad, Hercules (USA)
Reax top (vortexer)	Heidolph Instruments, Schwabach (D)
Scale PFB-300	Kern and Sohn GmbH, Balingen (D)
Iblot dry blotting system	Life Technologies, Carlsbad (USA)
Western Blot Detektor	Cytiva, Amersham (UK)
Neubauer chamber	Neubauer, Hartenstein, Würzburg (D)

Cell culture pump	Integra Vacusafe, Integra.Bioscience, Zizers (CH)
Centrifuge 5417R	Eppendorf, Hamburg (D)
Centrifuge 5810R	Eppendorf, Hamburg (D)

Table 2.11: Microscopes

Name:	Company:	Laser lines:	Objective:	Software:
Leica TCS SP8 X	Leica-microsystems	WLL 470-670 nm; Diode 405 nm; Multi-Ar 458 nm/476 nm/488 nm/496 nm/514 nm; DPSS 561 nm; HeNe 594nm, HeNe 633 nm	63x HC PL APO Oil CS2 NA: 1.40 WD (mm): 0.14	Leica LAS X
Visitron SD-TIRF	Visitron Systems	405nm/445nm/488nm/515nm/561nm/640nm	100x CFI Plan Apo Lambda NA: 1.45 WD (mm): 0.13 Pixel size in image (µm): spinningDisk: 0.110	VisiView

Table 2.12: Software

Name:	Company:
GraphPad Prism	GraphPad Software Inc., San Diego
ImageJ/FIJI	Wayne Rasband (NIH), Bethesda
LibreOffice	The Document Foundation, 2010
Unipro UGENE Integrated Bioinformatics Tools	Fursov et al., 2008
Trackmate	Tinevez et al., 2017
GraphPad Prism	GraphPad Software Inc., San Diego
Inkscape Vector Graphics Editor	Inkscape Community, 2003
Fiji – ImageJ Macro for objected corrected colocalization analyses with automated MaxEntropy threshold	J. A. Schmid et al., 2016

3 METHODS:

3.1 Transfection with siRNA for knockdowns

The siRNA-pellets were solved with 1 mL solution buffer (200 μ L 5x manufacturer's solution buffer (Eurofins) + 800 μ L RNase free water). The solution was pipetted up and down 3-5 times, avoiding the introduction of bubbles. The tubes were gently mixed for 30 min at RT. 50 μ L aliquots (20 μ M) were prepared.

Medium from primary human macrophages (from 6 days old cells) was removed, cells were washed with 1 mL PBS and subsequently detached with 500 μ L Accutase/well and incubated for 50 min at 37°C. 2 wells per condition were used. Accutase-activity was blocked by adding 500 μ L Monomedium. Cells (approx. 1 mio.) were detached by careful flushing. Cells were centrifuged for 5 min at 1100 rpm at 20°C. Supernatant was removed, cells were 1x washed with 5 mL PBS. Cells were centrifuged for 5 min at 1100 rpm at 20°C.

5.5 μ L siRNA (20 μ M) was added to 120 μ L of 1 mio cells, dissolved in R-buffer. Mixture was taken up with a 100 μ L-stamp and placed in the cuvette with 3 mL E2-buffer in the microporator. The electroporation was performed with 2 pulses at 1000 V, 40 ms. Transfected cells were pipetted in 1.5 mL Optimem in a well and incubated at 37 °C. After 4 h, medium was changed to 1.5 mL Monomedium per well and cells were incubated at 37°C for 3 days.

3.2 Transfection with plasmids for live-cell imaging

Medium from 6 days old primary human macrophages was removed, cells were washed with 1 mL PBS and subsequently detached with 500 μ L Accutase/well and incubated for 50 min at 37°C. Accutase-activity was blocked by adding 500 μ L monomedium. Cells were detached by careful flushing.

Cells were centrifuged for 5 min at 1100 rpm at 20°C. The supernatant was removed, the cells were 1x washed with the adjusted amount of PBS (100.000 cells in 100 μ L) and centrifuged again for 5 min at 1100 rpm at 20°C. 0.8 μ g Plasmid (1 μ g/ μ L) was added to 48 μ L of 500.000 cells. The mixture was taken up with a stamp and placed in the cuvette with 3 mL E2-buffer in the microporator. The electroporation was performed with 2 pulses at 1000 V, 40 ms. Transfected cells were immediately mixed with 500 μ L RPMI-droplet on coverslips and incubated at 37 °C for 4 h 45 min.

30 min before microscopy, cells were incubated with SirActin (dil.: 1:3000 in 500 μ L RPMI for the microscopy-chamber).

3.3 Matrix Degradation Assay

180 mg NaCl and 100 mg gelatin was dissolved in 50 ml di-sodium tetraborate decahydrate ($\text{Na}_2\text{B}_4\text{O}_7 \cdot 10\text{H}_2\text{O}$; pH: 0.3) solution for 30 min at 37°C. Then, 1.8 mg NHS-Rhodamine (25 mg; Thermo Scientific; cat. no.: 46406, stored at -20°C) was added in a beaker and mixed for 2 h for labeling of the gelatin. A dialysis membrane was put into a floating device (Slide-A-Lyzer dialysis cassette, MWCO: 2.000, Thermo Fisher), placed on 3 L PBS (1x) and equilibrated for approx. 30 min. 3 mL of Rhodamine-labeled gelatin were injected into the equilibrated dialysis-membrane (Thermo Scientific Slide-A-Lyzer Dialysis, cat. no.: 663300) and dialysed at 4 °C.

For coating, 12 mm glass coverslips were covered with dialysed Rhodamine-labeled gelatin solution. Sucrose solution was heated to 37°C. 49 µL Rhodamine-labeled gelatin was mixed with heated 1 µL sucrose solution (1 g/mL in PBS; heated to 37°C to dissolve initially and then sterile filtered with Millex GP filter unit: 0.22 µm) per CS (50 µL/CS) and vortexed for 10 s. Mixture was pipetted on parafilm in the first wet chamber and coverslips were placed on the droplets. The mixture with coverslips incubated for 15 min in the dark at RT. 50 µL of chilled milipore water was pipetted on parafilm in the prechilled second wet chamber. glass coverslips in the first wet chamber were detached with PBS, carefully dried and placed on the droplets in the second wet chamber. The glass coverslips incubated for 15 min in the dark on ice and were detached with PBS, briefly dried and placed into 12-well plate wells with the coated side on the top. glass coverslips were 2x washed with PBS for 10 min, 1x with RPMI for 10 min and incubated in RPMI at 37°C overnight.

Approx. 70.000 cells in 70 µL RPMI were seeded on briefly dried glass coverslips. 4 mL RPMI was added after 4 h. Cells were fixed after 5 h in total. Cells on coated glass coverslips were transferred in pre-warmed 1 mL 4% formaldehyde (37°C, 16% formaldehyde-solution 1:4 dil. in PBS, methanol-free, Thermo Scientific) and incubated at 37°C for 15 min. Formaldehyde was removed and coverslips were 3x for 5 min washed with PBS at RT on a shaker. Coverslips were incubated with phalloidin (1:100 phalloidin 488; 0.1% Triton-X in PBS) for 1h at RT and washed afterwards 3x with PBS for 10 min at RT on a shaker. 6 µL mowiol was pipetted on the slide and the glass coverslips were placed on the droplet with cell covered side on slides, the mowiol dried overnight.

3.4 Fixation of cells and immunofluorescence staining

Medium from cells on coverslips was removed and cells were fixed with warm (37°C) 1 mL 4 % formaldehyde (methanol-free, Thermo Scientific) in PBS for 15 min at 37°C in the cell incubator. Formaldehyde was removed and coverslips were 3x for 5 min washed with PBS and permeabilized and blocked in once with 0.1% Triton-X in PBS, fresh 10% NGS for 30 min at RT and washed afterwards 3x with PBS for 5 min at RT. Then, glass coverslips incubated with 300 µL primary antibody solution (dil.: 1:200 in PBS; 10% NGS; 0,1% Triton-X) for 60 min at RT. Coverslips were 3x washed with

1 mL PBS for 5 min and incubated afterwards with 300 μ L secondary antibody solution with phalloidin (dil.: 1:2000 in PBS; 0.1% Triton-X; 1:500 phalloidin) for 30 min at RT in the dark. Coverslips were 3x washed with 1 mL PBS at RT for 10 min. 12 μ L mowiol was pipetted on the slide and glass coverslips were placed on the droplet with the cell-covered side, the mowiol dried overnight.

3.5 Precipitation of supernatant proteins from cell culture

Medium from primary human macrophages was removed 24 h before harvest and preplaced by RPMI (1 mL per 6-well). On the next day, the supernatant was removed from the cells and centrifuged for 5 min at 14000 rpm to pellet remaining cells. 400 μ L from the supernatant were mixed with 600 μ L ice-cold methanol from -20°C. 10 μ L 5 M NaCl solution was added, the mixture incubated overnight at -20°C. On the next day, the samples were centrifuged for 15 min at 14000 rpm, 4°C. The supernatant was removed and the pellet was washed with 400 μ L ice-cold acetone from -20°C and incubated for 1 h at -20°C. After incubation, samples were centrifuged, the pellets were dried for 15 min and resolved in 160 μ L RIPA-buffer (10% protease inhibitor) + 40 μ L Lämmli-buffer per sample and incubated for 15 min at 95°C.

3.6 Surface biotinylation assay

Adherent cells were 3x washed with cold CaCl₂-MgCl₂-DPBS. After washing, cells were incubated with 1 mL cold biotin solution per well for 30 min on ice. Then, cells were 1x washed again with CaCl₂-MgCl₂-DPBS for 5 min on ice. Cells were 2x incubated with ice-cold quenching solution for 10 min on ice. After this step, cells were 2x washed again with CaCl₂-MgCl₂-DPBS for 5 min on ice. Cells were lysed with 500 μ L RIPA buffer per well for 10 min on ice, scraped and rotated for 10 min at 4°C. Lysates were centrifuged for 30 min at 4°C, 14000 rpm. 100 μ L supernatant were mixed with 50 μ L 5x Lämmli-buffer for the whole cell lysate. 650 μ L streptavidin agarose beads were centrifuged at 14000 rpm for 1 min. The pellet was washed in 800 μ L milliQ H₂O and subsequently centrifuged again at 14000 rpm for 1 min. 325 μ L beads were resuspended in 325 μ L RIPA buffer. Remaining 300 μ L supernatant were mixed with 80 μ L streptavidin-agarose bead solution and rotated at 4°C overnight. On the next day, samples were centrifuged at 14000 rpm at 4°C for 30 min. The supernatant was kept as flow-through and the pellet was washed with 500 μ L RIPA-buffer, rotated at 20 min at 4°C and subsequently centrifuged at 14000 rpm, 4°C for 30 min. This supernatant was discarded. The pellet was resuspended with 100 μ L elution buffer and incubated for 15 min at 95°C.

3.7 Polyacrylamide gel

Polyacrylamide gels were casted in 2 different gradients. First, the 14.7 % layer of the gel was prepared by mixing 1.5 mL of solution A (4%) with 3 mL of solution B (20%) and 45 μ L APS solution (10%) and

subsequent vortexing for 10s. 4.5 μ L TEMED were added to the solution and vortexed again for 10s. The solution was poured into a cassette, overlaid with isopropanol for airtight conditions and polymerized for 20 min at RT. Then, isopropanol was discarded and the second layer of 4 % was created with 2 mL of solution A (4%) mixed with 20 μ L APS (10%) and vortexed. 2 μ L of TEMED were added, mixed, and vortexed. The solution was applied on the first layer, a comb was placed into the cassette and the solution polymerized for further 20 min at RT.

For the zymography assay, 10% of the volume was Rhodamine-labeled substrate (1 mg/mL) was added to each layer before polymerization.

3.8 Western Blot

20 μ L lysed samples, mixed with Lämmli-buffer, were pipetted on a polyacrylamide gel. The gel was run in SDS-running buffer at 120 V for 2 h 30 min. 5 μ L prestained Page Ruler was used as a protein ladder. Gel was carefully removed from plastic tray and placed between a wet filter-paper and a membrane on the iBlot. A program for transfer of the proteins was run (20 v for 2 min, 23 v for 5 min, 25 V for 2 min).

The nitrocellulose membrane was removed from the iBlot tray and blocked in 5% milk in PBS-T/TBS-T buffer (1 mL Tween in 1 L 1x buffer) for 30 min at 4°C. Afterwards, the membrane was 4x washed with PBS-T/TBS-T buffer for 10 min. The membrane incubated with the primary antibody (diluted in 5 % milk in PBS-T/TBS-T buffer, dil.: 1:1000) overnight at 4°C. On the next day, the membrane was 4x washed with TBS-T/PBS-T buffer for 10 min. The membrane was incubated with the secondary antibody (diluted in 5% milk in PBS-T/TBS-T buffer, dil.: 1:10000) for 1 h at 4°C. Membrane was 4x washed with TBS-T/PBS-T buffer for 10 min.

For detection of antibody-stained proteins, either the Pico-kit (SuperSignal™ West Pico PLUS Chemiluminescent Substrate; 500 mL kit; thermo scientific; cat. no.: 34580) or the Femto-kit was used (SuperSignal™ West Femto Maximum Sensitivity Substrate; 100 mL kit; thermo scientific; cat. no.: 34095). The membranes incubated for 3 min in the ECL-detection-kit solution and the chemiluminescence was documented with the cytiva gel documentation system.

3.9 Mild Stripping of nitrocellulose membranes

15 g glycine + 1 g SDS were dissolved in 10 mL Tween 20 and adjusted to pH 2.2 (volume: ad 1000 mL with ultrapure water).

The nitrocellulose-membrane was 2x washed with approx. 15 mL stripping buffer in a small pan on a shaker at RT for 10 min. Then, the nitrocellulose-membrane was 2x washed with PBS for 10 min and afterwards 2x with TBS-T for 5 min. Before the next antibody-incubation, the nitrocellulose-membrane was blocked.

3.10 Zymography assay

Zymography assay samples were prepared together with usual lysates from whole-cell lysates (WCL) and supernatants (Ü2; 1 day before harvest, monomedium was replaced by 1 mL RPMI): After lysis in 250 µL RIPA-buffer per 6-well (with protease inhibitor without EDTA: cOmplete; EDTA-free Protease inhibitor cocktail tablets; 20 pcs; cat. no.: 11873580001; Roche. 1 tablet was dissolved in 50 mL RIPA-buffer), and centrifugation, supernatants were preserved and splitted. Zymography-samples were mixed with 4x zymography-loading-buffer (from stock solution: 10 mL 0.25 M Tris, pH 6.8; 40% glycerol; 8% SDS; 0.01% bromophenol blue). Samples were immediately stored at -20°C.

20 µL lysed samples mixed with 4x zymography-loading-buffer were pipetted on a PAA gel (1/3 4% solution + 2/3 20% solution for the resolver-gel, 600 µL dialysed Rhodamine-gelatin solution (2 mg/mL) were added to 5400 µL gel solution and polymerized for 15 min. The PAA-gel was overlaid with isopropanol. Afterwards, isopropanol was discarded and prepare the stacker-gel with only 4%, let it polymerize for at least 15 min). The PAA-gel was run in SDS-running buffer at 120 V for 2h with a cooling pack. 5 µL prestained Page Ruler was used as a protein ladder.

The PAA-gel was washed 2x for 30 min at RT and smooth shaking in renaturing buffer (2.5% Triton-X in ddH₂O, stock solution: 10 mL Triton-X in 390 mL ddH₂O) and afterwards 1x with developing buffer for 30 min at RT and smooth shaking (50 mM Tris-base; 0.2 M NaCl; 5 mM CaCl₂; 0.02% g Brij 58; 10 µM ZnCl₂ in 1 L ddH₂O, pH 7.6). The PAA-gel was finally developed in the developing buffer at 37°C in the incubator overnight for gelatin and 72 h for collagen type I and IV. The degradation was observed and documented at the Cytiva documentation system (settings: Cyt3, channel 535, UV).

3.11 Polymerase chain reaction

For the Phusion-PCR-protocol (thermofisher scientific), the following components were mixed per sample: 35 µL ddH₂O + 10 µL 5x HF-rich-buffer + 1 µL 10 mM dNTP-mix + 1 µL Fw-Primer (10 µM) + 1 µL Fw-Primer (10 µM) + 1 µL template (about 0.1 – 1 µg/µL) + 1 µL Phusion polymerase. The mix was pipetted on ice. The following program was used at the thermocycler:

Step:	Temperature:	Duration:	Cycles:
1. Denaturation	98°C	3 min	-
2. Denaturation	98°C	1 min	40 x (from 2. to 4.)
3. Annealing	60°C	1 min	
4. Elongation	72°C	1 min	
5. Elongation	72°C	10 min	-
6. Stop	8°C	infinite	-

The PCR products were purified with the QIAquick PCR Purification Kit (Cat. No.: 28104) and eluted in 20 μ L ddH₂O.

3.12 Quick-change mutagenesis

The primers were designed with a point mutation in the middle of the sequence (40 nt length) and HPLC-cleaned. Primers overlapped exactly. For the quick change mutagenesis, the following mix was prepared twice per sample with the Phusion-PCR kit (thermofisher scientific):

34.5 μ L ddH₂O + 10 μ L 5x GC buffer + 1 μ L 10 mM dNTP-mix + 0.5 μ L DMSO + 1 μ L Fw-Primer (10 μ M) + 1 μ L Rv-Primer (10 μ M) + 1 μ L template (about 50 ng) + 1 μ L Phusion DNA polymerase.

The mix was pipetted on ice. The following program was used at the thermocycler:

Step:	Temperature:	Duration:	Cycles:
1. Denaturation	98°C	1 min	-
2. Denaturation	98°C	1 min	20 x (from 2. to 4.)
3. Annealing	60°C	1 min	
4. Elongation	72°C	1 min	
5. Elongation	72°C	10 min	-
6. Stop	8°C	infinite	-

The PCR product was purified with the QIAquick PCR Purification Kit (Cat. No. 28104) and eluted in 20 μ L ddH₂O. 1 μ L (1 U/ μ L) of DpnI restriction enzyme was added to the mixture to digest the parental plasmids and subsequently incubated at 37°C for 1h. The digested mix was applied on an agarose-gel to verify the PCR-product, the respective band was excised and the DNA was extracted and applied on an agarose-gel and extracted. 5 μ L of the mixture was used for transformation.

3.13 Restriction digestion

1 μ L of backbone-plasmid (1 μ g/ μ L) was digested with 1 μ L with the first restriction enzyme in 20.5 μ L H₂O and 2.5 μ L Fast-Digest-buffer. The backbone was digested and combined on the gel. 21.5 μ L of the PCR-product was also digested with the first restriction enzyme in 2.5 μ L Fast-Digest-buffer-green. The digestion was performed at 37°C for 2 h. Then, the second restriction enzymes were added and the digestion continued for 2h. The complete digestion was heat-inactivated for 20 min at 80°C.

3.14 Agarose gel electrophoresis

The digested PCR-product was mixed with 6x DNA-loading-dye (5 μ L + 25 μ L PCR-product) and applied together with 1kb-plus DNA-Ladder (10 μ L) on a 1% Agarose-gel (1 g in 100 mL 1x TAE-buffer

was dissolved in a micro-wave, 0.4 μL SYBR-green was added and the gel was casted). The gel was run with TAE-buffer (running buffer) at 120V for approx. 1 h. Then, the desired bands were excised and the Qiagen-gel extraction-kit was used. For elution, the columns were incubated with with 20 μL RNase-free water and then eluated by centrifugation. All centrifugation-steps were performed at 20 $^{\circ}\text{C}$, 13000 rpm, 1 min; the optional washing-step with the QC-buffer was performed according to the manufacturer's protocol, the PE-buffer incubated 4 min before centrifugation.

3.15 Plasmid ligation

Approx. 200 ng of the purified plasmid (2 μL) was mixed with approx. 300 ng of the purified insert (2 μL) + 2 μL of 10x T4-DNA-Ligase buffer + 4 μL of 10x ATP (Adenosine 5'-Triphosphate, Sigma, cat. no.: A-3377; 10 mM in H_2O , pH 7), and 2 μL of the T4-DNA-Ligase ad 20 μL with dd H_2O , and incubated overnight at 15 $^{\circ}\text{C}$.

3.16 Transformation

Competent bacteria thawed on ice for 20 min. LB-Agar was molten and mixed with respective antibiotics. Agar plates were casted in 10 cm dishes (15 mL per petri-dish, +15 μL of 1000x antibiotics). The ligation complex (about 200 ng, 15 μL) was mixed with competent bacteria and gently mixed. The bacteria incubated for 30 min on ice and subsequently heat-shocked with 42 $^{\circ}\text{C}$ for 40 s and incubated for 2 min on ice. After the incubation, pre-warmed 250 μL LB-medium (5 μL of 20% glucose-solution in water + 100 μL LB-medium) without antibiotics were added to the bacteria and incubated for 1h at 37 $^{\circ}\text{C}$ under continuous shaking (300 rpm). 50 μL of the bacteria were plated on the previously prepared agar plates with the respective antibiotics. The remaining volume (about 250 μL) was plated on a second plate. The plated bacteria incubated at 37 $^{\circ}\text{C}$ overnight.

3.17 Maxiprep

200 mL LB-medium containing the respective antibiotics was inoculated with bacteria and incubated under shaking at 37 $^{\circ}\text{C}$ overnight. 500 μL of the Maxiprep were mixed with 500 μL glycerol-solution and freezed at -80 $^{\circ}\text{C}$. PureLink HiPure Plasmid Filter Maxiprep Kit (Invitrogen; cat. no.: K210017) was used to extract plasmid DNA. Therefore, bacteria were transferred in four 50 mL falcon tubes and centrifuged at 4 $^{\circ}\text{C}$ for 5 min, 4000 rcf. The supernatant was discarded, the pellets resuspended in 1 mL resuspension buffer (R3) and subsequently united. The resuspension was filled up to 10 mL with R3 and mixed. Then, 10 mL lysis buffer (L7) were added, and the mixture was inverted and incubated for 5 min. During the incubation, the PureLink HiPure Midi Column with filtration cartridge was equilibrated with 30 mL equilibration buffer (EQ1). After the incubation, 10 mL precipitation buffer (N3) was added to the mixture and inverted. Once the column was equilibrated, the mixture was

applied on the column with cartridge. When the lysate passed completely the column, 10 mL wash buffer (W8) was applied on the column. Then, the cartridge was removed, and 50 mL W8 was applied. The plasmid was eluted with 15 mL elution buffer (E4) in 50 mL falcon tubes, containing 10.5 mL isopropanol for precipitation. The precipitate was inverted and centrifuged for 40 min at 4°C, 14000 rpm. The supernatant was removed and the DNA-pellet was washed with 4 mL 70% ethanol, and subsequently centrifuged for 10 min at 4°C, 14000 rpm. The supernatant was removed again and the pellet dried before resuspension in 400 µL H₂O.

3.18 Sequencing of plasmids with Seqlab

1.0 µg plasmid-DNA was mixed with 3 µL FW- and 3 µL REV-primer (10 pmol/µL) for “premixed” samples ad 15 µL with RNase-free water in 1.5 mL-Eppendorf-tubes. For “standard primer”, no primer was added, the total volume was 12 µL.

4 RESULTS:

In this dissertation, the regulation of secreted, so-called „soluble“ matrix metalloproteases, in particular MMP7, MMP12 and MMP9 in primary human macrophages was investigated with a focus on cell-surface exposure and endocytosis by ARF6. So far, the degradative capability of migrating cells in a pathogenic and non-pathogenic context, is predominantly associated with extracellular matrix degradation by the membrane-bound matrix metalloproteinase MT1-MMP. Hence, the intracellular trafficking and its regulation of MT1-MMP is the most investigated one. Although, altered expression profiles of soluble MMPs are associated with metastasis and poor survival in different cancers or other pathological phenotypes, and with different polarization states of macrophages This might be due to the fact that soluble MMPs lack a transmembrane domain, exacerbating the microscopical analysis with a well-defined spatial area of (active) enzyme at the cell surface and at spatial proximity of the main degradative structures - podosomes - compared to MT1-MMP. Nevertheless, it was reported that some soluble MMPs are cell-surface associated even in the absence of a membrane anchor such as MMP2, MMP7 and MMP12. Here, the regulation of soluble MMPs in primary human macrophages is the centre of attention.

In the first part, the protein expression of different soluble MMPs was observed over time to detect the time point of maximal expression in context of the potential polarization and differentiation state of macrophages and also to compare the expression profiles to examine potential correlations.

In the second part, the localization and discrimination of intracellular vesicles with soluble MMP-cargo in contrast to MT1-MMP vesicles and potential regulators EEA1 and ARF6 was compared to investigate potential co-regulation of the respective soluble MMPs. Therefore, the time-point of highest protein expression from soluble MMPs (evaluated in the first part) in primary human macrophages during differentiation from blood-derived monocytes *in vitro* was chosen.

Next, the enzymatic activity of soluble MMPs in a modified fluorescent zymography assay was investigated at knockdown conditions of different MMPs and ARF6, which was identified as a colocalizing potential regulator of soluble MMPs in the previous part. The degradative capability of primary human macrophages was also investigated at the timepoint of maximal soluble MMP protein expression.

Then, the degradative capability in matrix degradation assays was compared at MMP- and ARF6-knockout conditions. The relation of soluble MMPs and respective knockdowns to the main degradative structure of macrophages – podosomes – was also examined. The proximity of overexpressed fluorescent MMP-loaded vesicles to podosomes at the plasma membrane was measured in addition by macro-based evaluation using a nearest-neighbour approach.

Last, the influence of both overexpression and knockdown of ARF6 on intracellular-, surface- and extracellular soluble MMP-levels was analyzed with a surface-biotinylation assay in combination with acetone-precipitation of proteins from the cell culture medium.

4.1 Expression of soluble MMPs over time

During differentiation, many cells alter their expression profile, which also applies to monocytes differentiating to macrophages. Especially for macrophages, the expression profile can show variations, which are associated with pro- and anti-inflammatory proteins. These variations in the pro- or anti-inflammatory influence are assigned as different polarization states. Classically activated M1-macrophages possess pro-inflammatory properties and are responsible for pathogen-clearance and degradation of ECM components as a part of the innate immune system. Alternatively activated M2-macrophages are anti-inflammatory polarized cells, which promote angiogenesis and the constitution of the ECM at physiological conditions, but provide also an immune-evasive environment to tumour cells as TAMs [1], [4], [11], [12]. In an initial step, the optimal expression of the selected soluble MMPs was investigated during differentiation of blood-derived human monocytes to macrophages. Also, the protein expression profile the M2-polarization marker CD163 was investigated for possible correlations to the respective MMPs.

4.1.1 Expression of soluble MMPs during macrophage differentiation

It has been reported, that different soluble MMPs show either increased or decreased protein expression at either M1 (pro-inflammatory) or M2 (anti-inflammatory) polarization of macrophages [29]. Western blots were evaluated with the Fiji-software. The respective lanes were selected, the integrals of the distinct bands were measured and normalized with the integrals of the respective bands from GAPDH (figure 4.1.1.1).

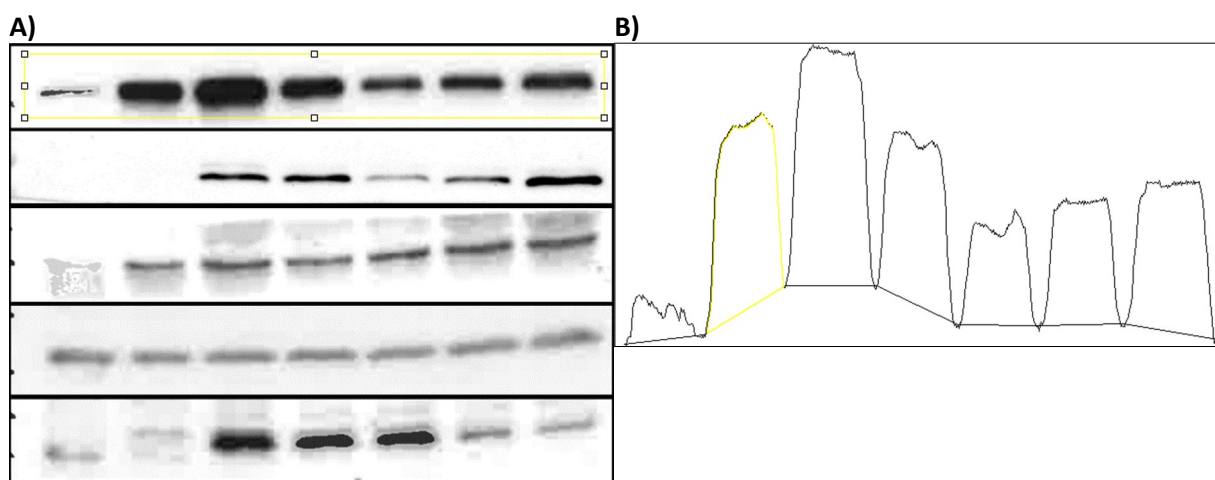


Figure 4.1.1.1: Software based analysis of Western blots. A) Western blot lanes (representative picture) were selected with a rectangle in the Fiji-software (yellow rectangle). Lanes were plotted and manually selected, integrals of the areas (yellow) were measured.

Results

To investigate the development of protein expression from soluble MMPs in correlation with each other and the polarization of the cultivated macrophages, monocytes differentiating to primary human macrophages from 3 donors were cultivated *in vitro* for 2 weeks, harvested at periodical time points every 2 days, lysed and compared with each other on western blots (figure 4.1.1.2).

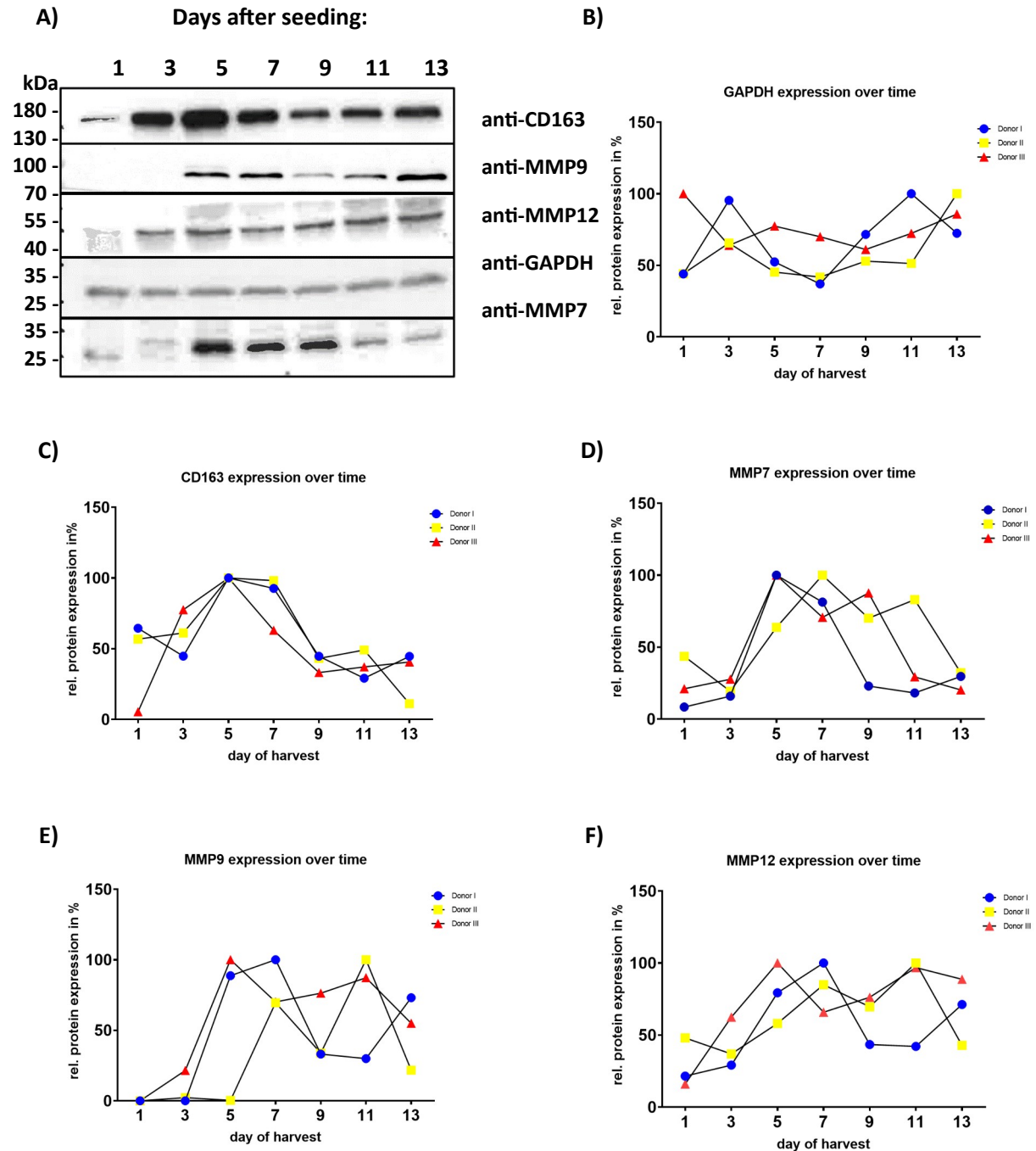


Figure 4.1.1.2: MMP expression over time in primary human macrophages. Cells were harvested on day 1, 3, 5, 7, 9, 13 after monocyte preparation during differentiation in primary human macrophages, n=3. (A) Western blots of whole-cell-lysates stained for GAPDH (house-keeping gene), CD163 as polarization marker and MMP7, MMP12 and MMP9 and the respective graphs, normalized against GAPDH. (B-F) Corresponding relative protein expression profiles of stained proteins.

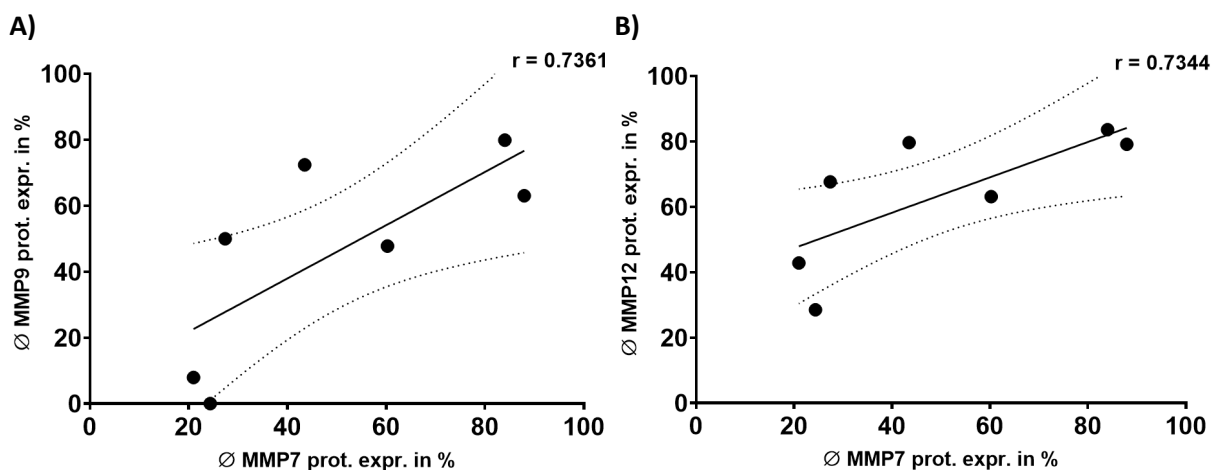
It was observed, that the expression level of MMP7 increased up to day 5-7 (1st day: 24.4% ± 17.9% to 5th day: 87.9% ± 20.9%), as well as the expression level of MMP9 (1st day: 0% ± 0% to 5th day: 79.9% ±

17.4%) and of MMP12 (1st day: 28.5% \pm 17.1% to 7th day: 83.6% \pm 17.1%)(D-F). This could also be observed for the expression level of CD163 (1st day: 42.2% \pm 32.1% to 5th day: 100% \pm 0%)(C), which is a marker for M2-polarized macrophages. The expression level of MMP7 decreased over time (13th day: 27.4% \pm 6.3%) as well as the expression level of MMP9 (13th day: 50.0% \pm 26.1%) and the expression level of MMP12 to a lesser extent (13th day: 67.6% \pm 23.1%). From day 9, the CD163 protein expression level seemed to stay on a constant low level (13th day: 32.1% \pm 18.3%).

4.1.2 Correlations between protein expressions of MMPs

To interpret the protein expression over time for a potential coherence, the correlation was calculated between the average expression levels per time point (figure 4.1.2) with Graphpad Prism. First, the correlation between the expression levels of the respective MMPs was investigated. The expression profiles of MMP9 and MMP12 showed a significant and high correlation ($r = 0.9859$) (C). MMP7 and MMP9 showed a moderate, but significant correlation ($r = 0.7361$) (A) as well as MMP7 and MMP 12 ($r = 0.7344$) (B).

It was also evaluated, whether the expression profiles of the soluble MMPs correlated with the polarization state observed by the M2 polarization marker CD163. Here, no significant correlation between the expression profile of MMP9 and CD163 could be observed ($r = 0.3250$) (E) as well as for MMP12 and CD163 ($r = 0.3889$) (F). In contrast to that, the expression profiles of MMP7 and CD163 correlated significantly ($r = 0.7580$) (D). This suggests on the one hand, that the soluble MMPs – especially MMP9 and MMP12 - might be regulated together and on the other hand, that the expression of MMP7 correlates with the polarization state of the macrophage.



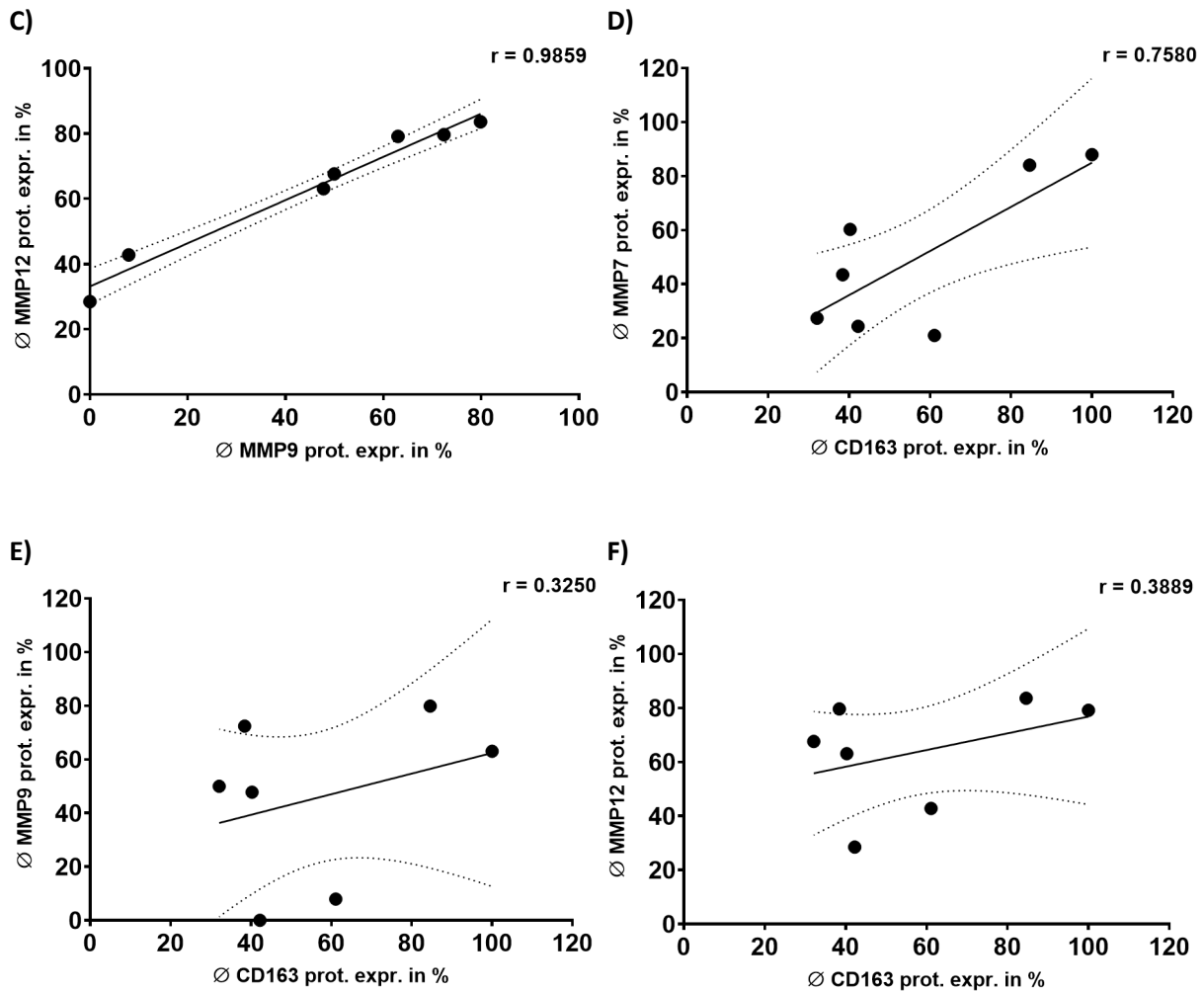


Figure 4.1.2: Correlations between average protein expressions over time. Correlation between the average protein expression of MMP7 and MMP9 (A), MMP7 and MMP12 (B), MMP9 and MMP12 (C), MMP7 and CD163 (D), MMP9 and CD163 (E) and MMP12 and CD163 (F). 90% of confidence interval, $\alpha = 0.1$.

M2 polarization is associated with anti-inflammatory characteristics of macrophages. M2-polarized macrophages are known to express an anti-inflammatory activity. Due to that, MMP7 seems to be expressed on a polarization-dependent manner as already reported. Nevertheless, further comparisons, regarding other possible correlations of soluble MMPs with other polarization markers (e.g. CD80, CD86 or TLR2, TLR4), need to be evaluated. For MT1-MMP, no dependence on the polarization state of the macrophage was reported [29], but should also be validated.

4.2 Intracellular localization of MMPs

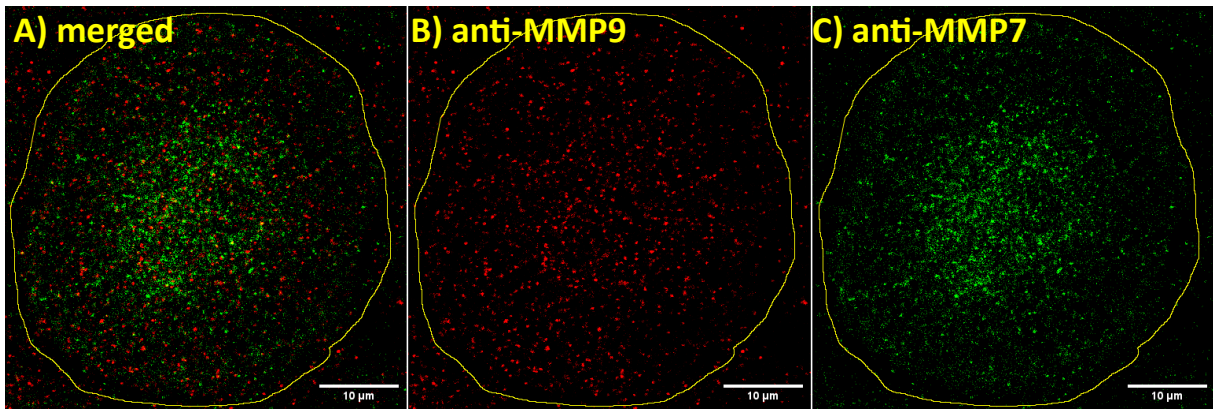
The expression profiles showed a first hint of the regulative mechanisms of soluble MMPs. The time point of maximal protein expression was evaluated as well as the correlation and thus a potential co-regulation of the respective MMPs. In a first step, the localization of vesicle populations with soluble MMP cargo was compared to MT1-MMP vesicle populations and with each other.

The regulation of soluble MMPs is investigated by their intracellular localization in distinct vesicle populations and the hypothetical colocalization with each other, potential regulators or structures such as podosomes. It has been published MT1-MMP is an activator of other MMPs (e.g. MMP2) [13] and that MT1-MMP islets are localized at podosomes [45], [46]. To observe other potential interactions in cellular structures, immunofluorescence staining of endogenous proteins with confocal microscopy to obtain a sufficient resolution is necessary. The immunofluorescence staining of endogenous proteins in fixed cells is rather reliable for the investigation of colocalization in contrast to the evaluation of the expression of fluorescent proteins after plasmid transfection, where an increasing colocalization can occur as an artefact due to a high overexpression over time. To prevent this, only endogenous proteins were stained for the colocalization analysis in fixed cells.

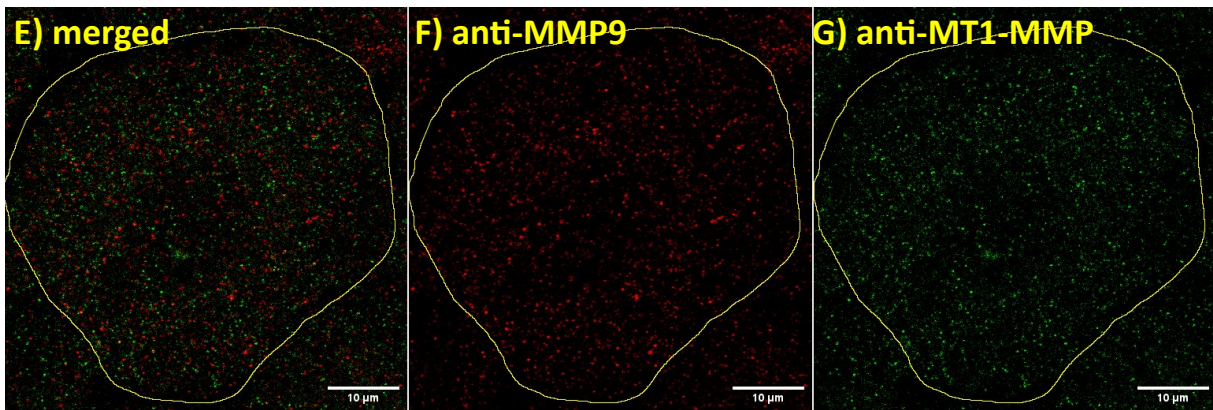
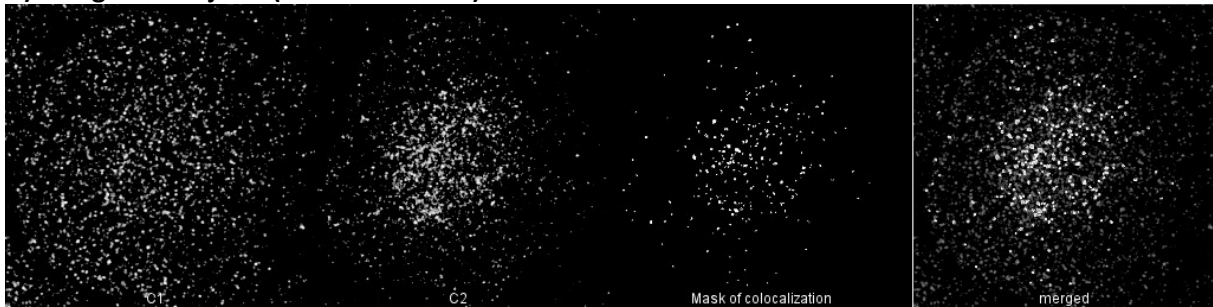
The second challenge was the evaluation of the vast amount of data with numerous vesicles and their spatial distribution. Yet, a manual evaluation of confocal microscopy pictures is a time-consuming process. To circumvent this, an automated approach with a macro analysis tool was used to characterize the colocalization of fluorescent structures. For this initial step, an object-based approach was chosen, using published macro [60] (modified for batch-analysis and with variable parameters), which is available in the open-source software FIJI, an enhanced version of ImageJ. An object-based approach means, that not the overlap of all fluorescent pixels in the respective channels is used to calculate the colocalization, but the complete or partial overlap of individual fluorescent area, counted as distinct objects, is chosen. Thus, differently sized and shaped objects, discriminated by defined parameters are selected to take structures, such as vesicles into account for the measurement of colocalization. This is more advantageous in order to exclude areas such as occasionally fluorescently oversaturated nuclei, ER or the Golgi-apparatus. Additionally a partial overlap of regulatory proteins associated at vesicles is also assigned as a full colocalization and prevents a false balancing of differently-shaped and -sized objects.

4.2.1 Distinct vesicle populations of soluble MMPs

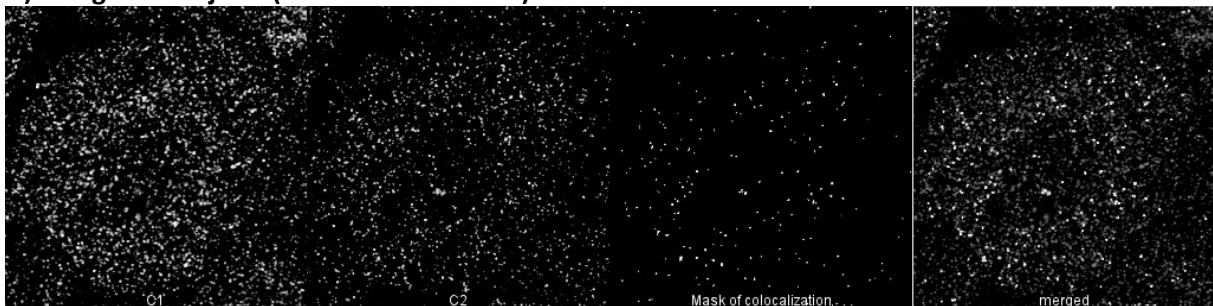
The intracellular (co-)localization of soluble MMPs is crucial for the understanding of their transport, regulation and function. Therefore, 7 days old primary human macrophages from 3 donors were fixed and stained for endogenous MMPs and documented with confocal microscopy (figure 4.2.1). The immunofluorescence stainings of endogenous MMPs showed a high colocalization between MMP7 and MMP9 of approx. 42% ($\pm 8\%$) in contrast to MT1-MMP with a colocalization to MMP9 of approx. 22% ($\pm 4\%$). MMP12 for its part was neither highly colocalized to the other soluble MMP7 with 27% ($\pm 7\%$) nor to MT1-MMP with 25% ($\pm 6\%$), suggesting either a transport, which is distributed on both populations, or an independent third vesicle population.

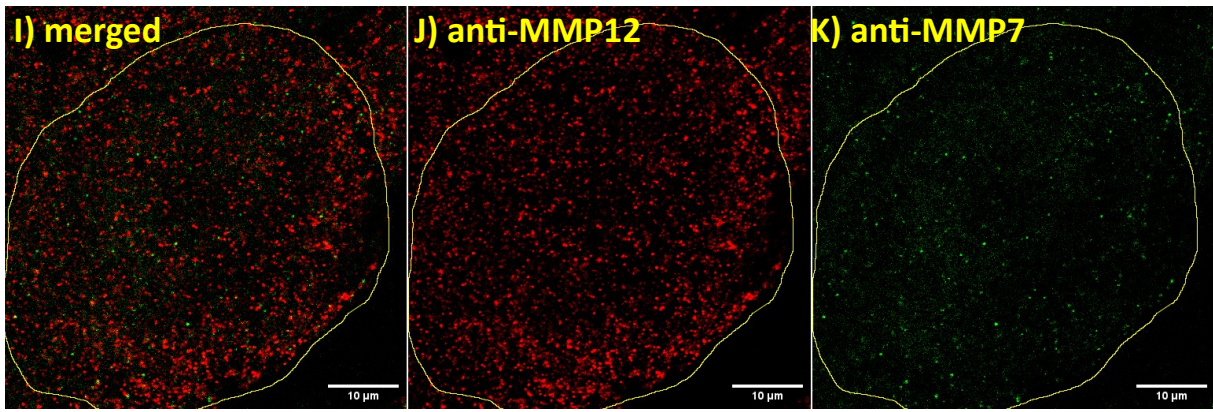


D) recognized objects (MMP7 + MMP9)

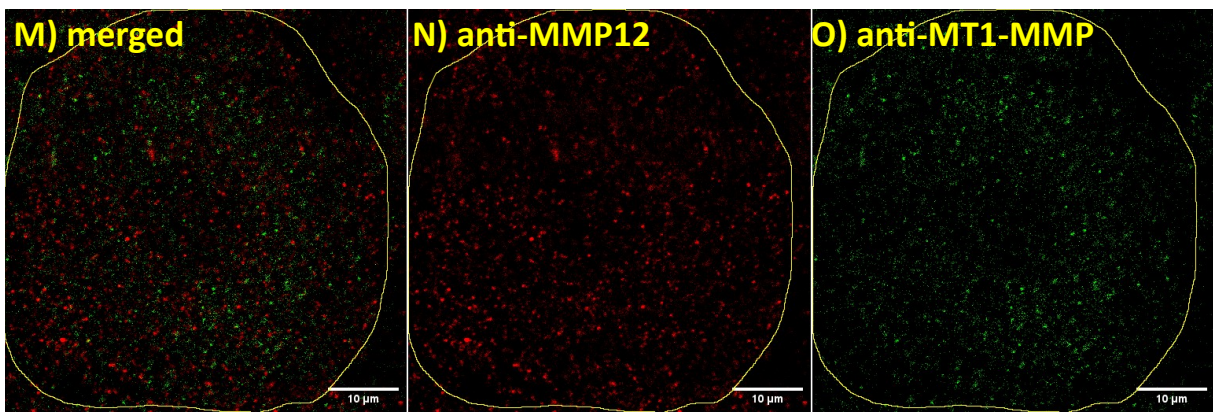
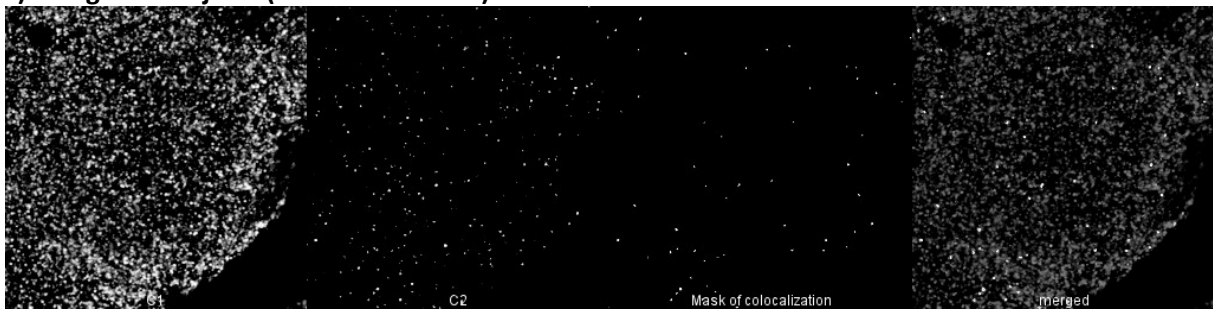


H) recognized objects (MT1-MMP + MMP9)

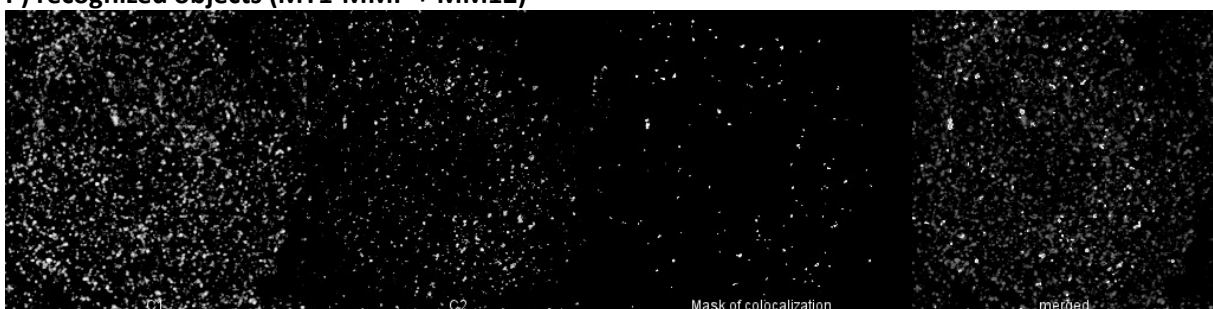




L) recognized objects (MMP7 + MMP12)



P) recognized objects (MT1-MMP + MMP12)



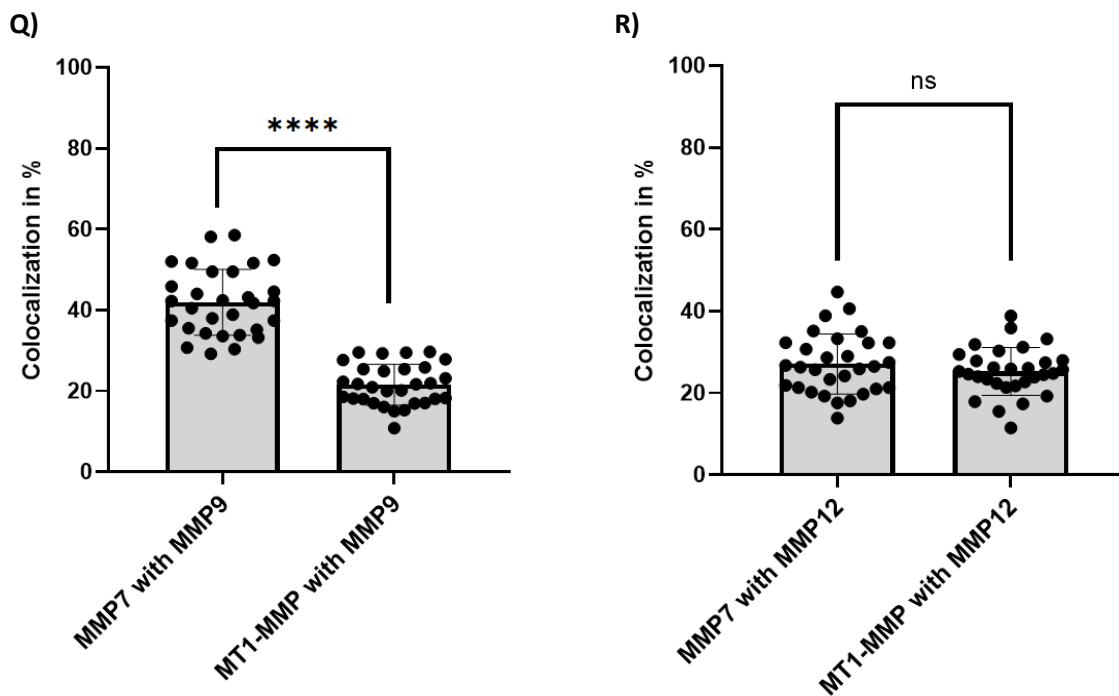


Figure 4.2.1: Intracellular IF-stainings for endogenous MMPs. Fixed primary human macrophages, $n=3 \times 10$. Immunofluorescence stainings (upper pictures) and the object-based colocalization analysis (lower pictures) (objects in channel „C1“ and in channel „C2“, mask of colocalizing objects and merged objects with channels) for endogenous MMP7 and MMP9 (A-C), MT1-MMP and MMP9 (E-G), MMP7 and MMP12 (I-K), MT1-MMP and MMP12 (M-O). Bar diagrams of object-based colocalization of MMP7 with MMP9 compared to MT1-MMP with MMP9 (Q) and MMP7 with MMP12 compared to MT1-MMP with MMP12 (R).

Considering the previously investigated correlations of protein expression profiles, these results confirm that soluble MMPs are distinctly regulated in contrast to MT1-MMP. It was reported that MT1-MMP is independently expressed of the polarization state. At least for MMP7, this is not the case. Here, it was also observed that MMP7 and MMP9 show a higher colocalization than MMP7 and MMP12. A simultaneous staining of MMP9 and MMP12 was not performed, since both antibodies were generated the same host species. It is possible that MMP9 and MMP12 would show a high colocalization, although a hypothetical co-regulation in protein expression is not evident, which could support a co-regulation in intracellular transport. Here, the relation between the intracellular transport of MMP7 and MMP9 is given. Summarized, a complex regulatory system is indicated with different regulation in expression and transport for soluble MMPs.

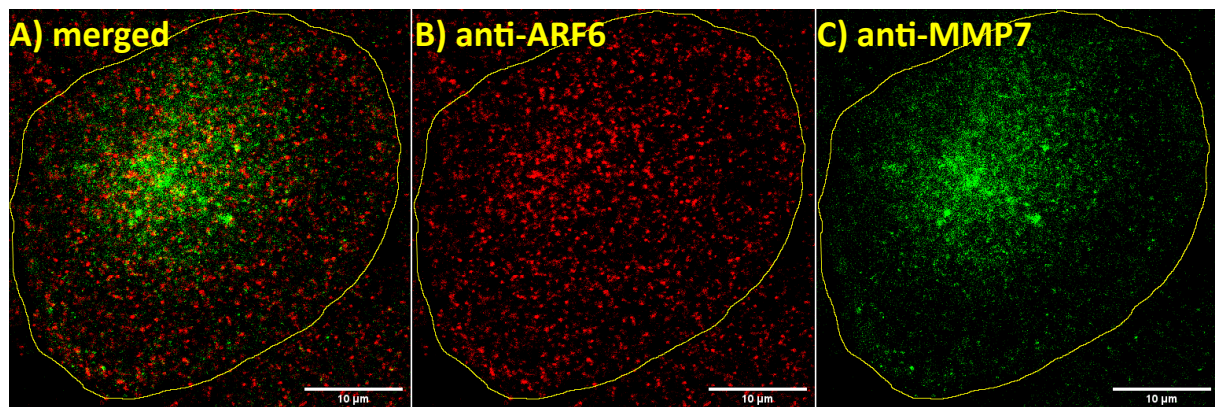
4.2.2 Colocalization of MMPs with endocytotic regulators

One aspect of regulation of proteases, is the endocytosis of surface-associated proteins. spatial proximity is associated with common regulatory mechanisms, which was further investigated with a focus on endocytosis. Endocytosis is not only a crucial mechanism of macrophages to internalize pathogens or small molecules, but also to regulate the own surface-associated, recycled or activated

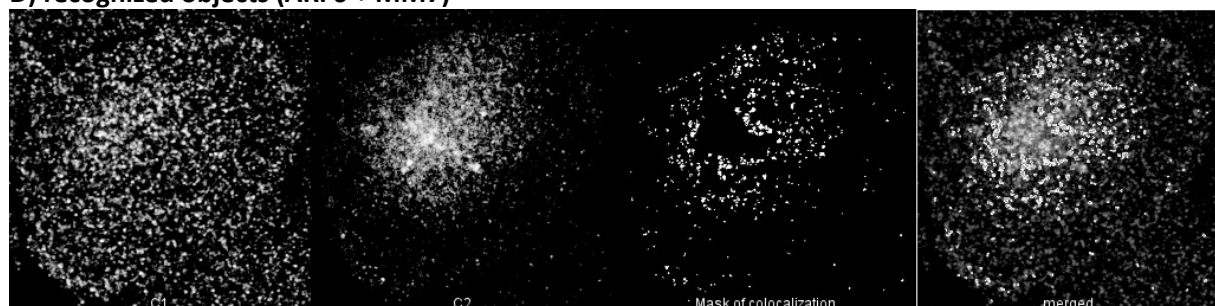
Results

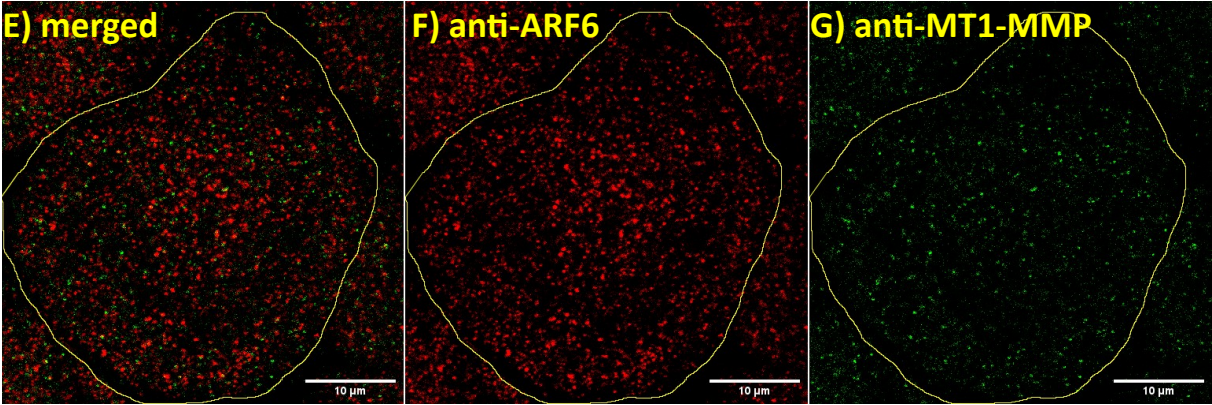
proteins, and hereby cell adherence or enzymatic activity. Usually, plasma-membrane associated proteins are known to be endocytosed via clathrin- and dynamin-dependent endocytosis and subsequently either degraded or recycled. The endocytosis of membrane-associated proteins is crucial for their surface exposure. Proteins, lacking of a clathrin-internalization sequence, are endocytosed via ARF6 or EEA1 in a clathrin-independent manner [55]. ARF6 and EEA1 are endocytic trafficking regulators responsible for different subpopulations of early endosomes. In the following experiments, the spatial association of these endocytic regulators with soluble MMPs (which lack a clathrin-internalization sequence) was investigated.

The endocytic regulation of soluble MMPs was further investigated with immunofluorescence staining of endogenous MMPs co-stained with endogenous EEA1 and ARF6 (figure 4.2.2) as previously described in 4.2.1. Therefore, 7-days old, fixed primary human macrophages, were stained for MMP7, MT1-MMP and MMP12 and co-stained for EEA1 and ARF6. A High colocalization of 59% (\pm 8%) between MMP7 and ARF6 was observed (A-C) in contrast to MT1-MMP with 36% (\pm 4%), which was previously published to be regulated by ARF6 [58], [61], [59] (E-G). Also, another alternative early endosome regulator EEA1, which regulates a distinct vesicle population of early endosomes, localized to a lesser extent to MMP7 with 21% (\pm 10%) (I-K). This suggests first a previous localization of soluble MMPs at the cell surface and second an endocytosis and regulation of at least MMP7 and colocalizing soluble MMPs via ARF6. Interestingly, MMP12 shows a high colocalization to EEA1 of 56% (\pm 9%), substantiating the hypothesis of another distinct vesicle population of MMP12 in relation to MMP7.

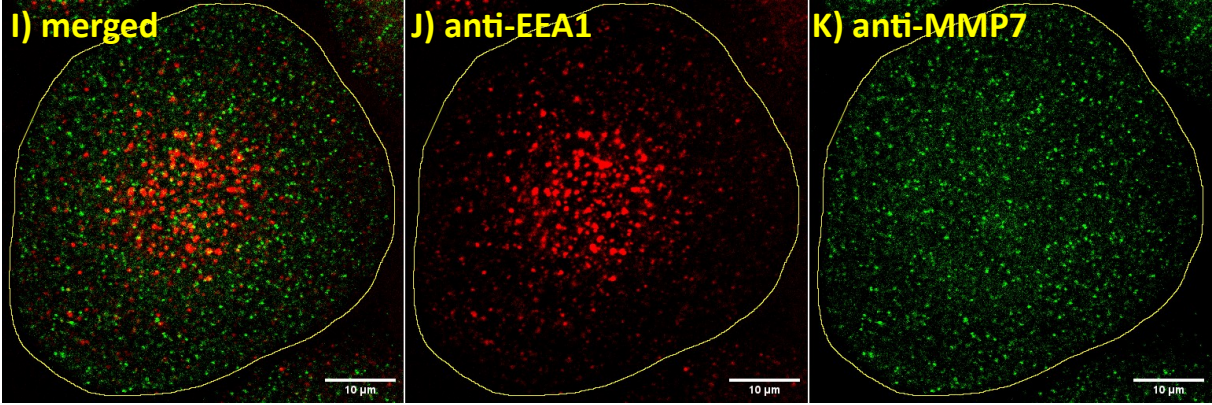


D) recognized objects (ARF6 + MM7)

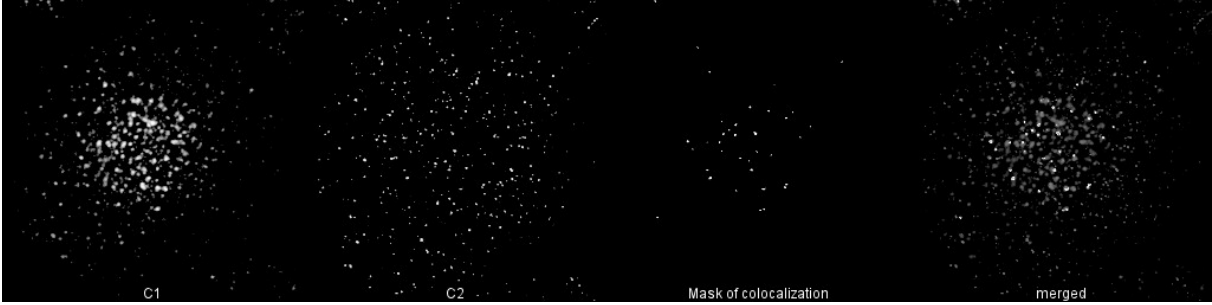


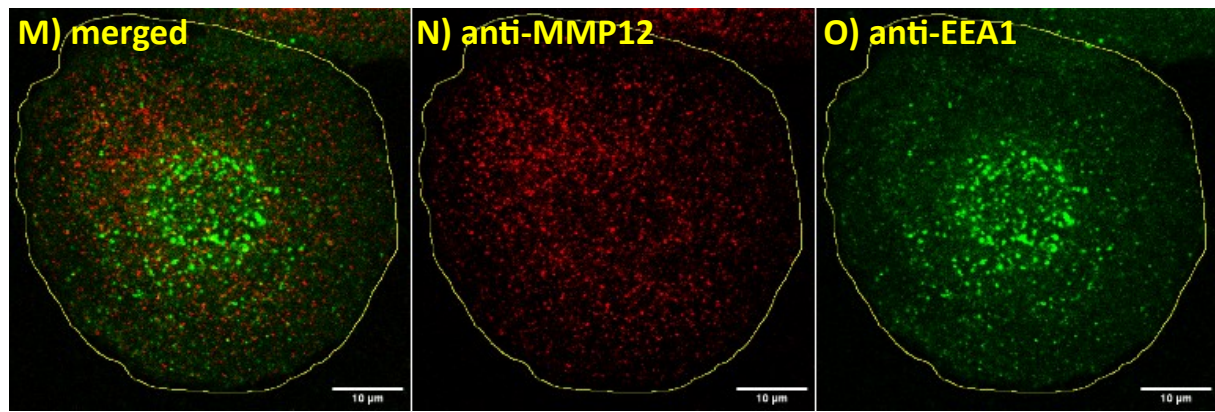


H) recognized objects (ARF6 + MT1-MMP)



L) recognized objects (EEA1 + MMP7)





P) recognized objects (EEA1 + MMP12)

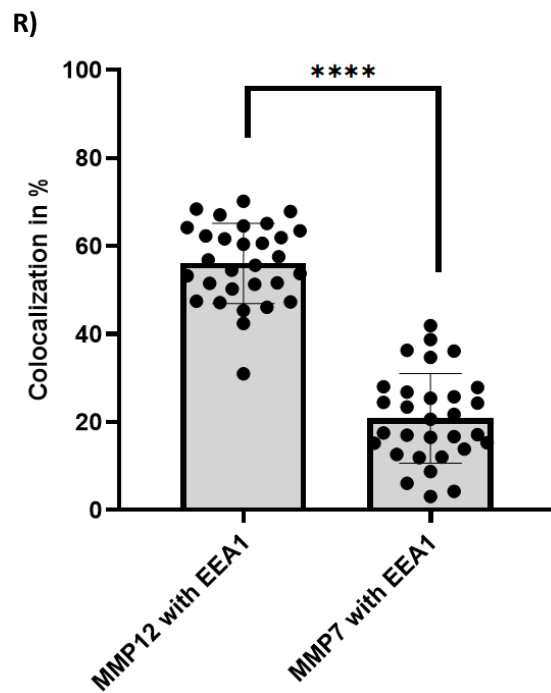
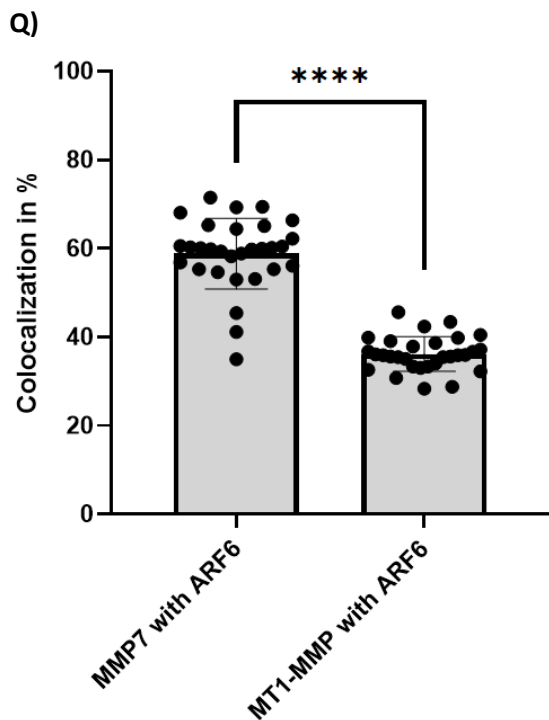
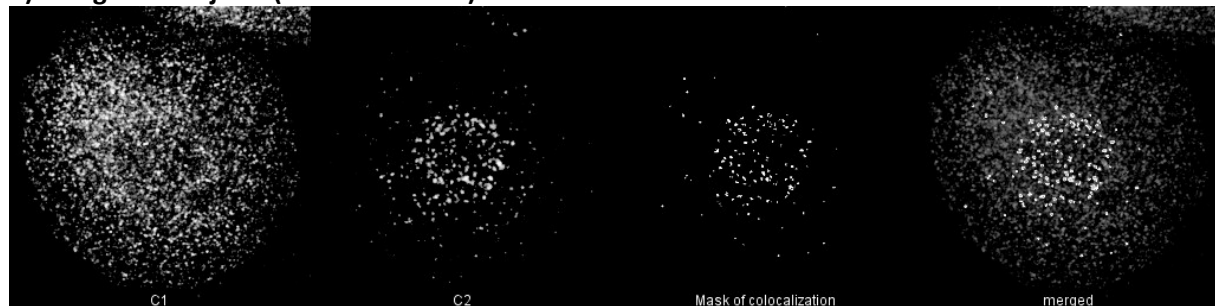


Figure 4.2.2: IF-stained endogenous MMPs, co-stained with ARF6, and EEA1. n=3x10. Immunofluorescence stainings (upper pictures) and the object-based colocalization analysis (lower pictures) (objects in channel „C1“ and in channel „C2“, mask of colocalizing objects and merged objects with channels) and their respective bar diagrams of colocalization for endogenous MMP7 and ARF6 (A-C), MT1-MMP and ARF6 (E-G), MMP7 and EEA1 (I-K). Bar diagrams of object-based colocalization of MMP7 with ARF6 compared to MMP7 with EEA1 (Q) and MMP7 with ARF6 compared to MT1-MMP with ARF6 (R).

So far, the hypothesis corroborates that soluble MMPs are differently regulated than MT1-MMP in both expression and intracellular localization and (endocytic) transport. Moreover, the respective soluble MMPs show different expression profiles, localizations and regulations of expression and transport compared to each other with overlapping localizations and correlations. A remarkable colocalization with an endocytic regulator is a first hint for a potential (prior) surface exposure, even in the absence of a membrane-anchoring domain.

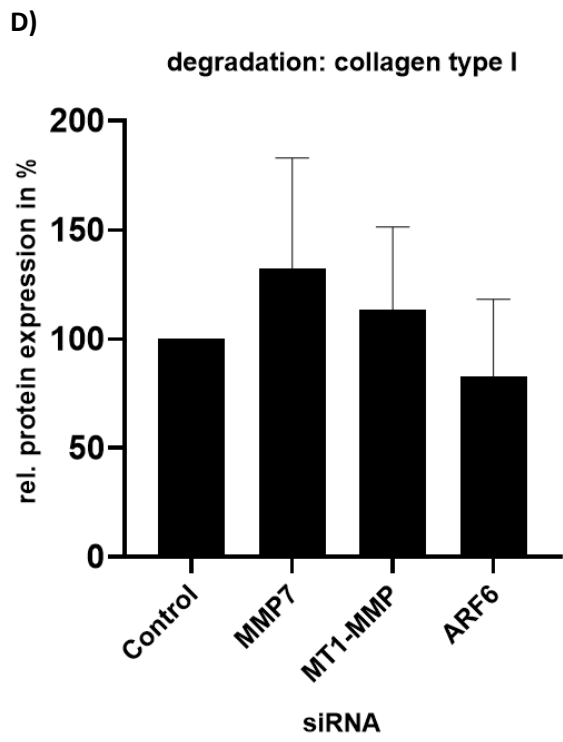
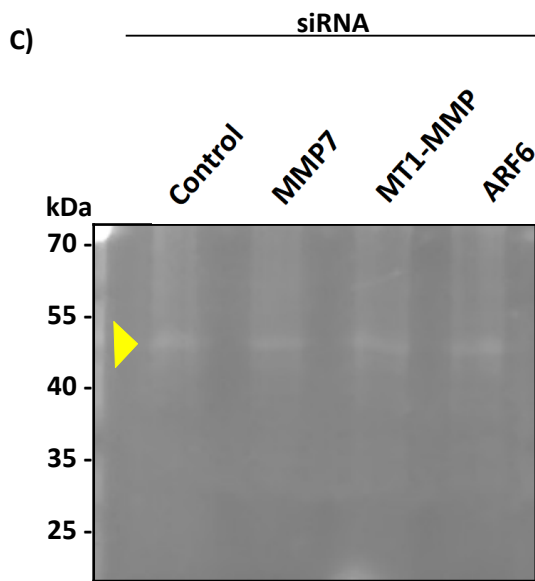
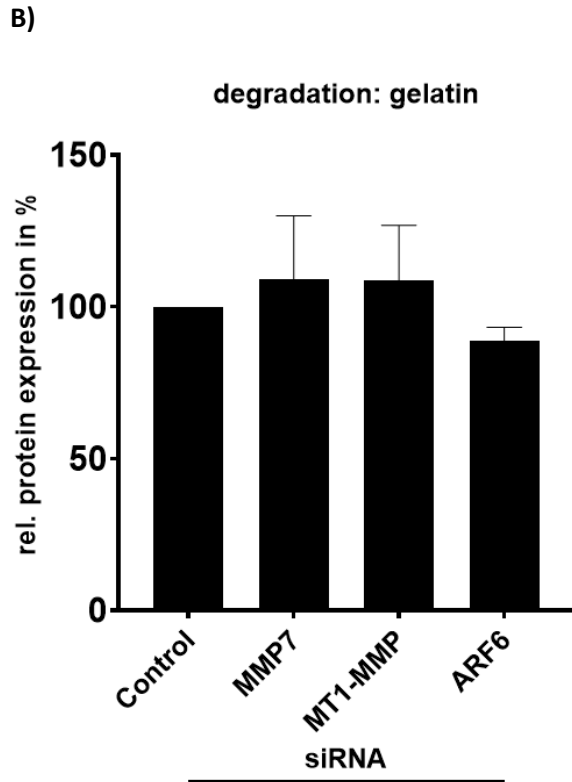
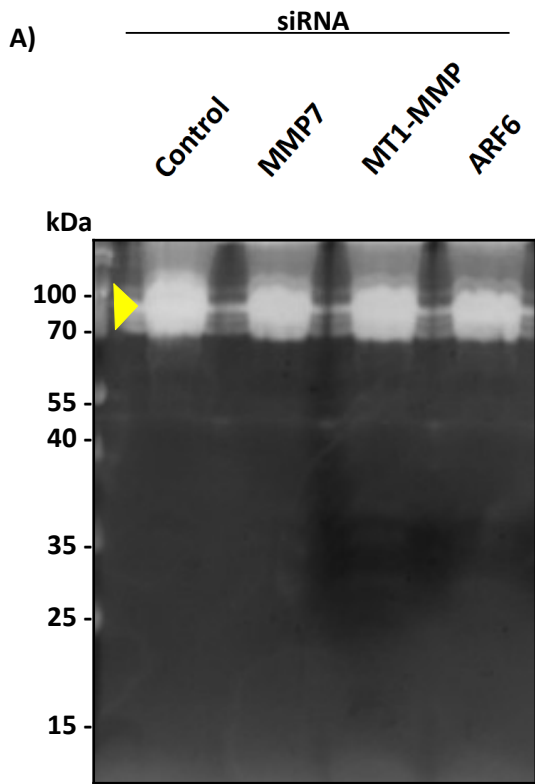
4.3 Degradation of extracellular matrix components by MMPs

Up to this point, soluble MMPs seem to be differently regulated compared to each other and to MT1-MMP. In the following experiments, the impact of knockdown conditions of MMP7 (as *pars pro toto* for soluble MMPs) was compared with MT1-MMP, and the endocytic regulator ARF6, regarding their enzymatic activity. The enzymatic activity of lysed macrophages at knockdown-conditions was compared with zymography assays and the degradative capability was compared with the matrix degradation assay.

4.3.1 Enzymatic activity in the zymography-assay

For the evaluation of enzymatic activity, whole-cell lysates from 7 days old primary human macrophages were compared at knockdown conditions. The degradation of 3 different substrates (gelatin, collagen I and IV) in the zymography assay was measured with the Fiji-software at the areas with the most prominent degradation. The standard functions of Fiji were used to select a lane with different bands, plot the intensity of this lane and measure the integral of the plots of distinct bands. The values were normalized with the lane of control siRNA and the GAPDH-values, measured the same way. The ratios were calculated and displayed in percental values.

If soluble MMPs, which are important for the degradative capability of primary human macrophages as well as the well-known MT1-MMP, are regulated via ARF6 [58], [59], [61], a reduction of degradation should be observed in ARF6-knockdown conditions. Therefore, 6 days old macrophages from 3 donors were transfected with siRNA for the respective knockdown conditions, lysed 3 days later and applied on a PAA-gel containing rhodamine-labeled substrates for zymography (figure 4.3.1): gelatin- (A), collagen type I- (C) and collagen type IV (E). This variant with fluorescently-labeled substrates allows a continuous screening of degradation without inhibition by Coomassie staining, so the optimal time-point of degradation can be evaluated and the required time for degradation can be expanded. The degradation was normalized against GAPDH-staining in western blot-stainings of the respective lysates, as described before. By that, differences caused by an increased overall-protein concentration, were taken into consideration.



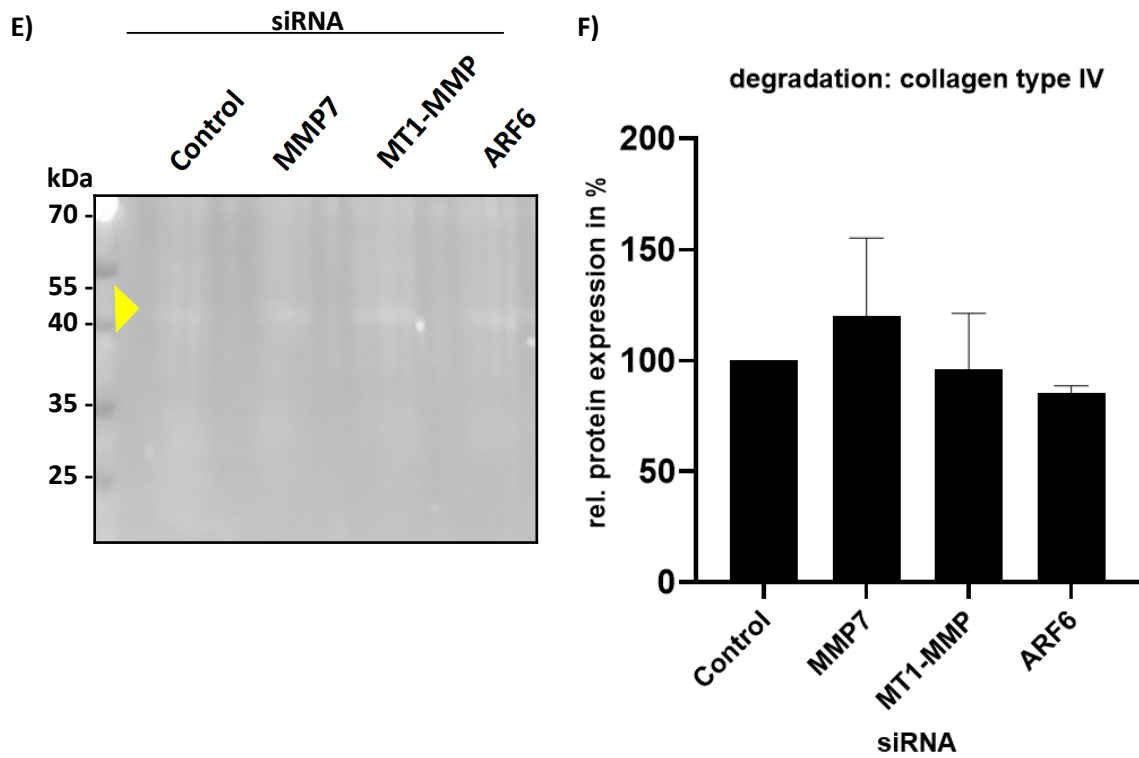


Figure 4.3.1: Zymography-assays at knockdown-conditions (left). Respective bar diagrams for degradations (right) (normalized against GAPDH), $n = 3$. Rhodamine-labeled gelatin zymography assay of whole-cell lysates from primary human macrophages, incubation time: 24 h (A,B). Rhodamine-labeled collagen type I zymography assay, incubation time: 72 h (C,D). Rhodamine-labeled collagen type IV zymography assay, incubation time: 72 h (E,F). Evaluated bands were assigned with yellow arrows.

The ARF6-knockdown showed a small, but consistent reduction in degradation in only one substrate. The rhodamine-labeled gelatin zymography assay was degrading for 24 h, and the most prominent area for this substrate between 70 and 100 kDa was measured for degradation. This area is associated with MMP9, which has a size of approx. 92 and 82 kDa. Here, only a difference in degradation could be observed between the control siRNA knockdown (set on 100%) and ARF6-knockdown with 88.8% ($\pm 4.5\%$) (A,B). Both knockdowns of MT1-MMP and MMP7 were not affecting the degradative capability at this area with 108.9% ($\pm 18\%$) for MT1-MMP-knockdown and 109% ($\pm 21\%$) for MMP7-knockdown. Although both MMPs are known to degrade gelatin as well, only a weak degradation could be observed at approx. 55 kDa (the area of MT1-MMP but also of e.g. MMP12 and MMP19) and none at about 28 kDa (the expected area of MMP7 degraded substrate). So far, this only confirms that MMP9 enzymatic activity is not affected by MT1-MMP, MMP7 or significantly by ARF6. Nevertheless, it must be mentioned that it is not possible to distinguish in the zymography assay between activated and pro-forms of MMPs. At this point, it was unclear whether ARF6-knockdown could alter the transition of inactive to active form of MMPs. This experiment showed that the overall protein expression of MMPs was not affected by ARF6-knockdown, which is an important additional information, since it was conceivable that ARF6 could have an influence on the transcription of MMPs.

For rhodamine-collagen type I zymography assay, a comparable result could be observed (C,D) with the most prominent degradation at approx. 55 kDa after a prolonged degradation timespan of 72 h. The ARF6-knockdown showed a weakly decreased enzymatic activity to 82.9 % (\pm 35.2%) compared to the control siRNA-knockdown with a remarkably high standard deviation. The MT1-MMP-knockdown showed even an increased substrate degradation of 113.3% but also with a too vast standard deviation of \pm 37.9%. The values at MMP7-knockdown conditions were not included in the evaluation, as with 132.3% (\pm 50.6%). A possible explanation could be that the optimal time-point had passed where the most significant difference could be observed. It must be mentioned, that the standard deviations of 35% to more than 50% are caused by different results of the donors. This experiment needs to be repeated with further donors. Also, the rhodamine-collagen type IV zymography assay with prolonged degradation timespan of 72% showed weak differences between the ARF6-knockdown with 85.4 % and the control siRNA knockdown but was at least consistent within the 3 donors and showed only a weak standard deviation of 3.1% (E,F) at the most prominent degraded area at approx 40 kDa. The knockdown conditions for MT1-MMP and MMP7 were poorly evaluable with too different results between different donors and need to be repeated.

In total, the zymography assay results show a remarkable variation between the different donors, but only a weak difference between the respective conditions. The most prominent impact of ARF6 knockdown with collagen type IV as substrate, since it was visible in all 3 donors. A degradative activity at the area of MMP7 of approx. 28 kDa, which showed a high colocalization to ARF6, could not be detected in all conditions, possibly due to the low concentration or a decreased substrate-concentration at the lower part of the gel. Since MMPs show an overlapping substrate affinity, it is not possible to selectively assign the observed effects to a specific MMP. Three possible candidates are MT1-MMP, MMP2, which is regulated by MT1-MMP, and MMP12 for this size. Nevertheless, the conditions of these assays need to be optimized for further conclusions.

4.3.2 Matrix degradation by MMPs

To investigate the degraded area in the matrix degradation assay, the fluorescence intensity in the degraded areas at the macrophage positions was measured and compared with the remaining area. An object-based approach as used previously for the evaluation of colocalization between fluorescent vesicles, applied on this assay, would assess differently degraded areas only in a binary way (degraded? Yes or no). The gradual degradation can be evaluated by the fluorescence intensity differences in degraded areas under the cell area. This was done with two self-written macros for the Fiji-software. These macros create regions of interests, where the fluorescence intensity is measured in standard applications of Fiji. Therefore, the fluorescence channel of stained cells was oversaturated and reduced to a binary picture. The binary picture was used to select the complete area "inside" of

the cells and “outside” of the cells. Both areas were measured in the fluorescence channel of the fluorescent gel and compared by a ratio of the fluorescence “inside” and “outside” of the cell area and finally compared in the different knockdown-conditions (figure 4.3.2.1).

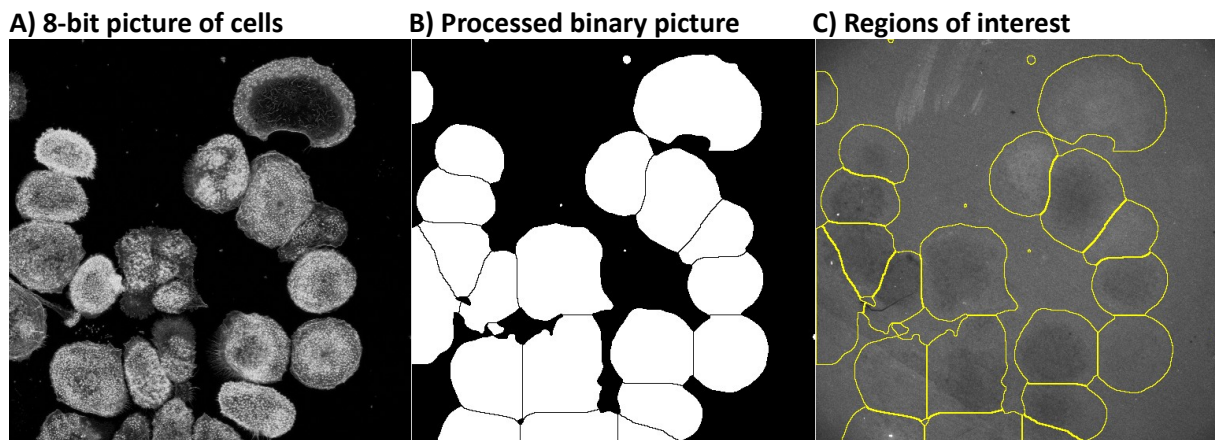
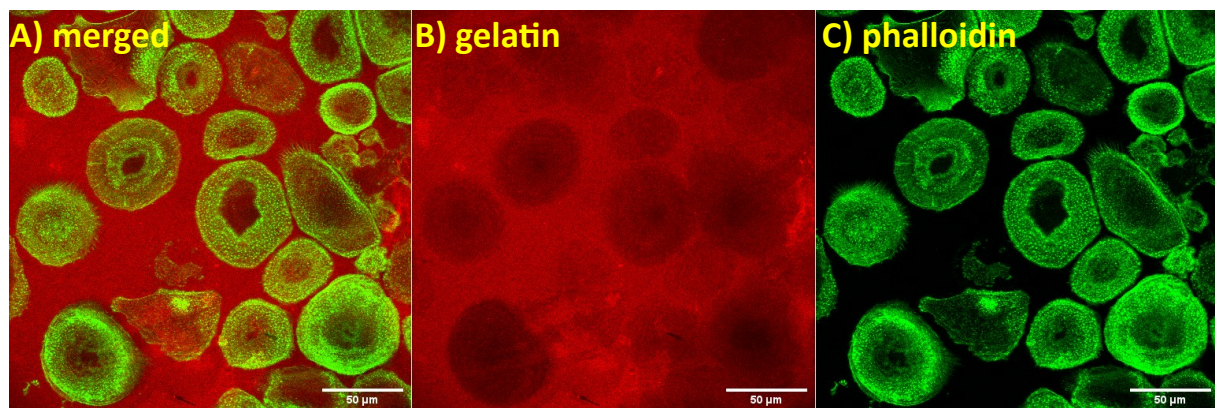


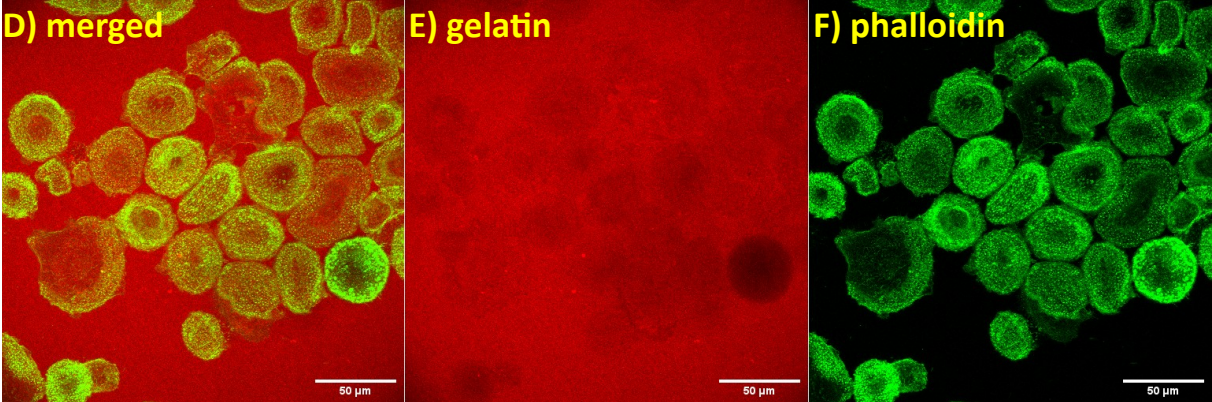
Figure 4.3.2.1: Evaluation method of the degradation assay. 8-bit picture of primary human macrophages, stained with phalloidin (A), binary processed picture, based on the phalloidin-stained cells (B). Yellow regions of interests (ROIs) based on the binary processed picture in the rhodamine-gelatin channel (C). The fluorescence intensity was measured inside of the ROIs and outside of the ROIs in comparison. The mean of individual ROIs of the cells was compared with the average intensity outside of the ROIs.

In contrast to zymography assays, the matrix degradation assay offers the opportunity to investigate directly the degradative capability of macrophages - not only the enzymatic activity of lysates parallel to possible morphological changes or an altered podosome number caused by the respective treatment. Therefore, 4 different knockdowns (ARF6, MMP7, MT1-MMP and a negative control siRNA) were performed with 6 days old macrophages and harvested after further 3 days. Cells were seeded on rhodamine-gelatin labeled coverslips, cultivated for 5 h and 30 min and subsequently fixed and stained with phalloidin (figure 4.3.2.2).

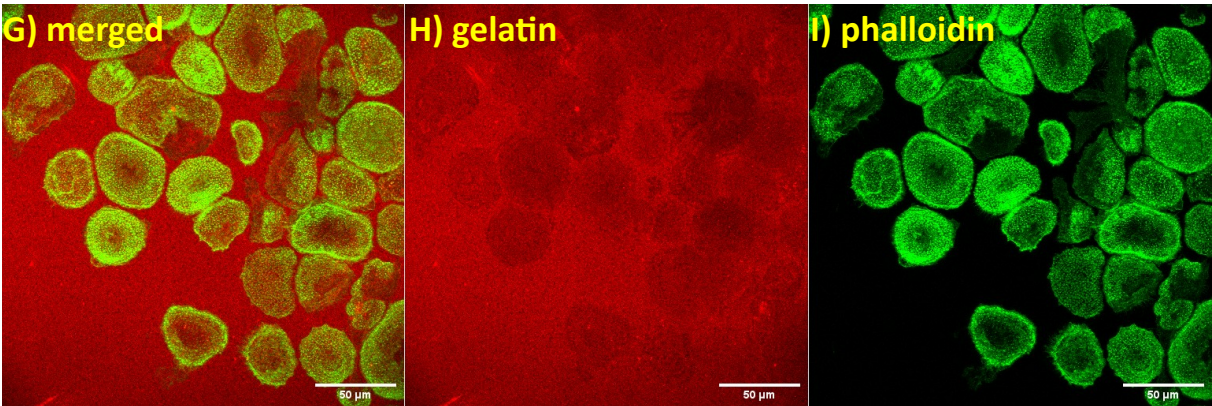
Control-siRNA:



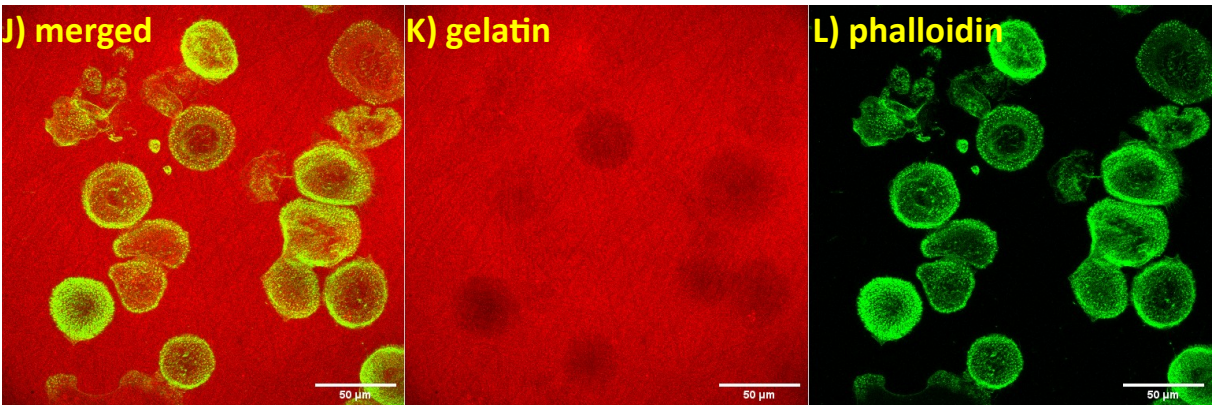
ARF6-siRNA:



MMP7-siRNA:



MT1-MMP-siRNA:



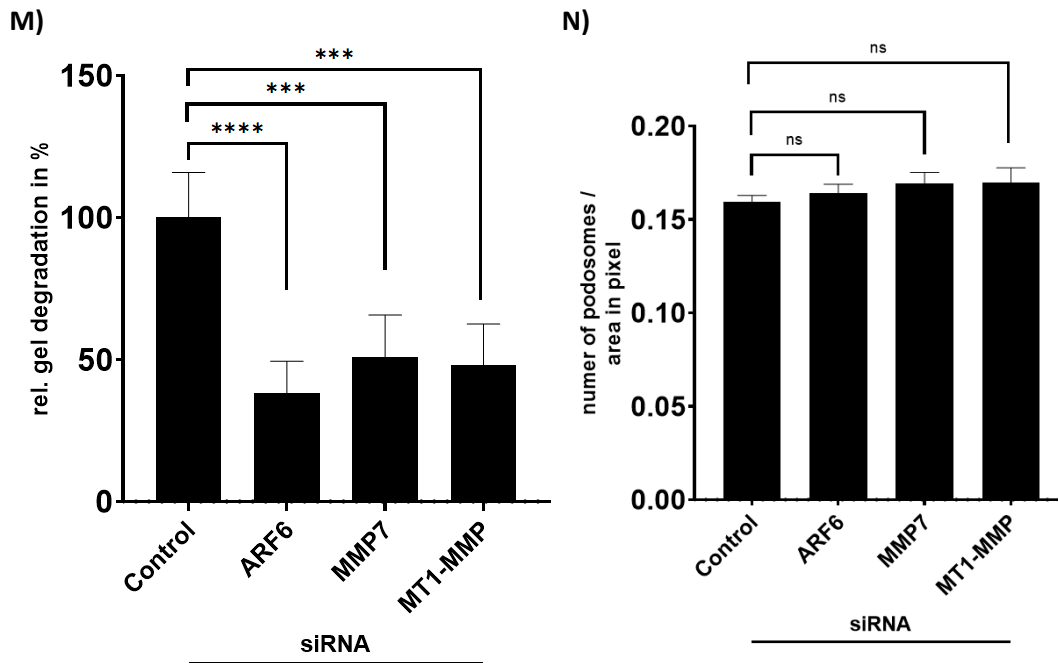


Figure 4.3.2.2: Matrix degradation assay with primary human macrophages. 9 days old primary human macrophages were transfected 3 days with respective siRNA and applied on a matrix degradation assay with rhodamine-labeled gelatin as substrate, degraded for approx. 6 h, $n=3 \times 10$ and fixed. Knockdown-conditions of negative control siRNA (A-C), ARF6 (D-F), MMP7 (G-I) and MT1-MMP (J-L) and the summarizing bar diagrams of relative gel degradation (M) and the number of podosomes per area (N).

The matrix degradation assay showed a gradually reduced degradation of the substrate at the cell areas in knockdown conditions. Hereby, the ARF6-knockdown showed a slightly higher reduction of degradation with 38% ($\pm 10\%$) (D-F) than MMP7 with 51% ($\pm 38\%$) (G-I) - or MT1-MMP-knockdowns with 48% ($\pm 31\%$) (J-L), suggesting a combined effect of the ARF6-knockdown on more than only one MMP.

Besides, the podosome density (podosome number per area) was not affected by different knockdowns. By that, an altered mechanical extrusion of gelatin by podosomes, was excluded. This confirms additionally an impairment of the degradative capability of macrophages by a reduced MMP activity. At this point, it was unclear, whether the degradation is impaired by the ARF6-knockdown due to an influence on the reduced surface exposure of MT1-MMP, as previously reported or by the influence on other, soluble MMPs. Both, MT1-MMP knockdown and MMP7 knockdown showed a reduced matrix degradation at a comparable level, confirming the importance of both MMPs for the degradative capability of macrophages.

Although both assays show different aspects, the different results between the zymography and the degradation assays are remarkable and allow further conclusions: First, the impact of ARF6 on the degradative capability is not due to a transcriptional influence on MMPs, since no significant alteration could be observed in the zymography assay. Second, the impaired degradative capability of macrophages must be caused by ARF6-knockdown due to an altered surface exposure of MMPs, since

no significant change of enzymatic activity could be observed in the whole-cell lysates with different zymography assays. Even though no change of podosome number per area could be observed, it was unclear at this point, if podosomes, as the main matrix degrading structures of macrophages, are not involved in the degradative activity of soluble, probably surface-exposed MMPs.

4.4 MMPs and podosomes

4.4.1 Podosomes in relation to MT1-MMP-islets

The podosome density was not impaired in the ARF6-knockdown conditions. Yet, it is unclear, whether the regulation of soluble MMPs in macrophages is due to a podosome-associated regulation, and thus a reduced exocytosis at podosomes, or directly caused by endocytosis and surface exposure of MMPs, as reported for MT1-MMP [58], [59], [61].

Therefore, a spatial proximity between podosomes and soluble MMPs at the plasma membrane during exocytosis would be necessary. To investigate this, the area at the plasma membrane was analyzed via total internal reflection fluorescence microscopy (TIRFM). With this technique, an area of about 120 nm is excited and becomes fluorescent. Although, no colocalization is given in the microscopy pictures between podosomes and MMP vesicles, a structural dependence cannot be excluded. Accumulation of vesicles at exocytosis might not be detected by the object-based approach to measure colocalization. Here, the distinct positions of vesicles with MMP-cargo, or MT1-MMP islets (local accumulations at the cell surface [62]) and podosomes were tracked with the Trackmate-plugin of Fiji. In a second step, the tracked positions were used to calculate vectors between the referring coordinates and their length in an automatized process with a macro. The lengths were sorted and the average values of the smallest distances was calculated for each reference position of either podosomes to podosomes or MMP-vesicle/islet to podosomes. To evaluate this data, the nearest neighbour-approach was chosen to compare the distances between the fluorescent exocytosis foci of MMPs compared to actin-stained podosomes to investigate if a non-random proximity could be observed without a biased pre-defined area around podosomes. For this purpose, the objects podosomes and vesicles at close proximity to the cell surface were tracked by the plugin Trackmate of Fiji and their vector length between the different coordinates were compared as a distance between them. The minimum distance for each object was measured to detect the closest object to the respective one in the other channel. The used macro compares the smallest distances between the coordinates of closest podosomes as the reference distance and the distance between the coordinates of MT1-MMP islets and podosomes without a pre-defined area of interest (figure 4.4.1).

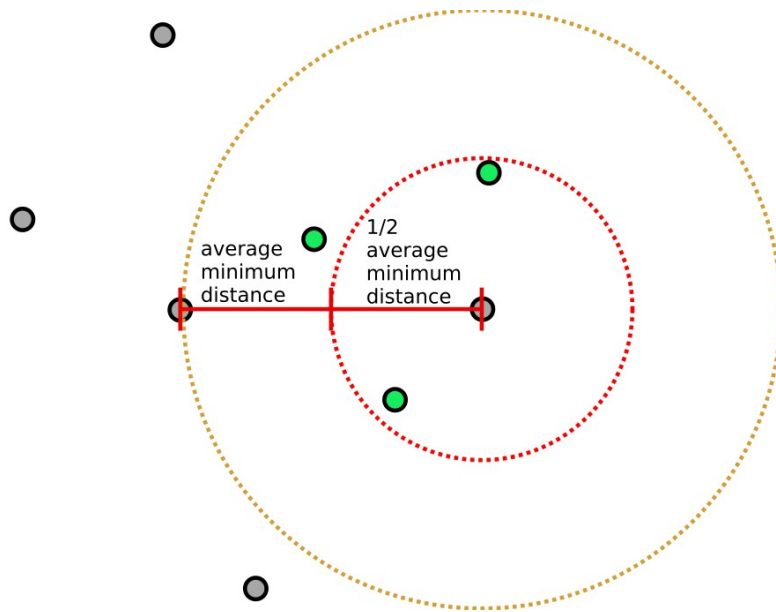
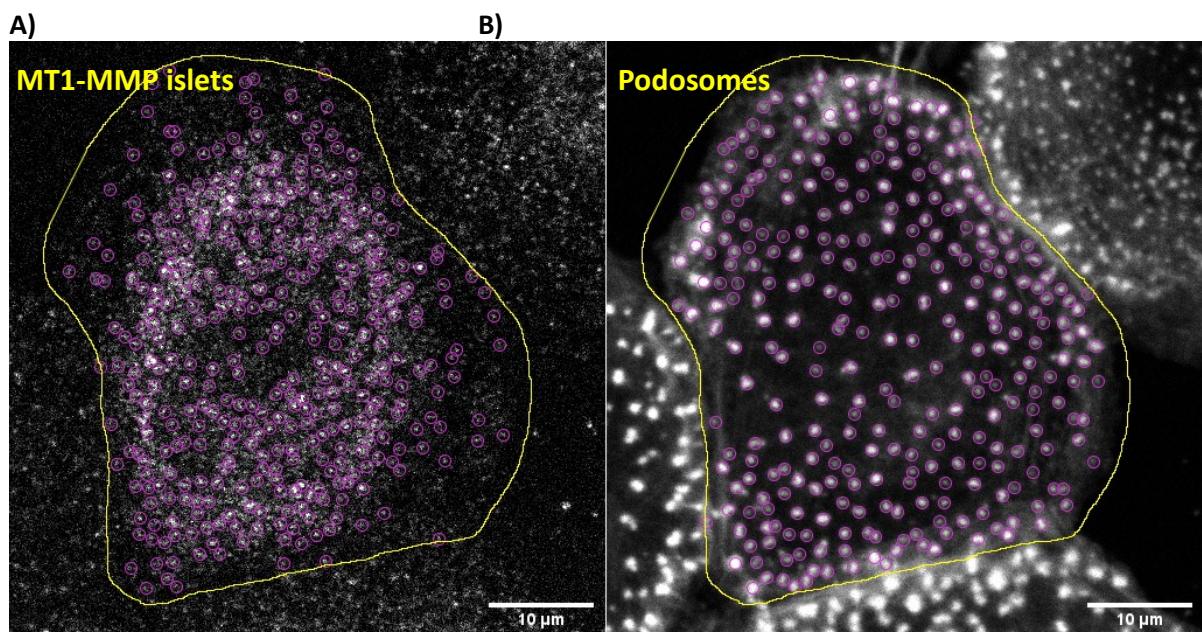


Figure 4.4.1: Schematic picture of the nearest neighbour approach. The minimum distance (red line) from one object to another (gray dots) is measured and the average is defined as reference. No other object between reference objects is closer (dashed orange cycle). If another object (green dots) is within half of the minimum distance (red dashed cycle) the distance is not randomly distributed and defined as close proximity.

In case of non-random distribution and close proximity to podosomes, the MMP-islets or release foci would show an average minimum distance of less than half of the distance between the closest podosomes. This allows an unbiased approach to define proximity and potential structural and functional dependence. To test this method, 7 days old macrophages were fixed and fluorescence-stained for MT1-MMP and podosomes (figure 4.4.2). It was reported before, that MT1-MMP islets and podosomes show a close proximity [62].



c)

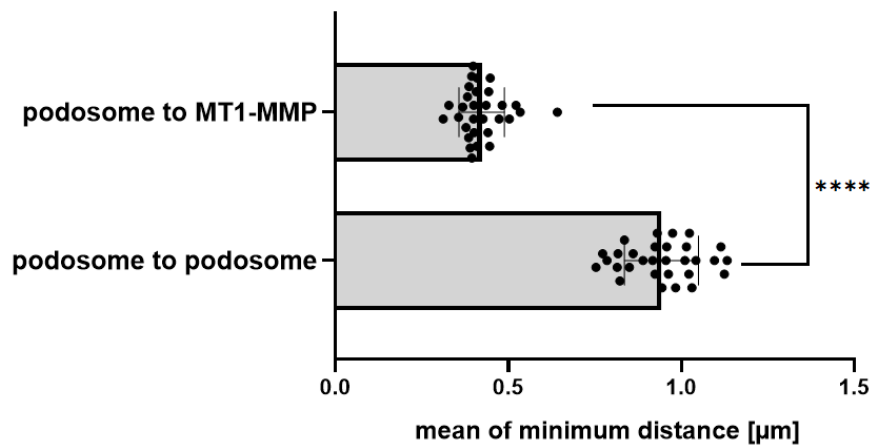


Figure 4.4.2: Trackmate-based analysis of podosomes and MT1-MMP islets. (encircled with a yellow region of interest), stained for endogenous MT1-MMP, $n=3 \times 10$. Podosome- and MT1-MMP islet-positions were tracked with TrackMate from FIJI-software (purple circles) from selected area. Macrophages were fluorescence-stained for MT1-MMP with a specific antibody (A) and for F-actin cores of podosomes (B) with phalloidin. The bar diagram compares the mean of minimum distances between podosome to podosome (reference) in comparison to podosomes to MT1-MMP islets (C).

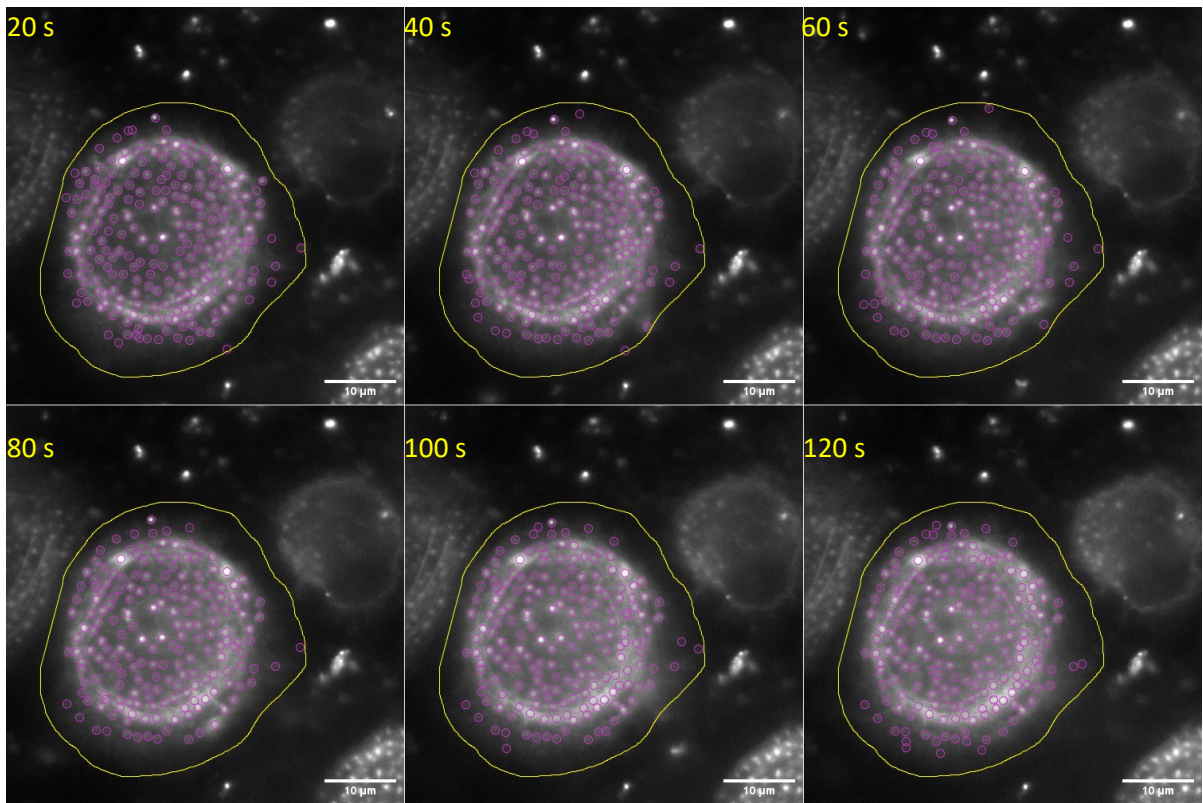
It was reported before, that MT1-MMP islets and podosomes show a close proximity [62]. And indeed, this analysis method confirms this observation by showing a very low mean minimum distance between MT1-MMP islets and podosomes of $0.42 \mu\text{m}$ ($\pm 0.06 \mu\text{m}$), which is lower than the half of the average minimum distances between the closest podosomes with a distance of $0.94 \mu\text{m}$ ($\pm 0.4 \mu\text{m}$).

4.4.2 Podosomes in relation to vesicles of soluble MMPs

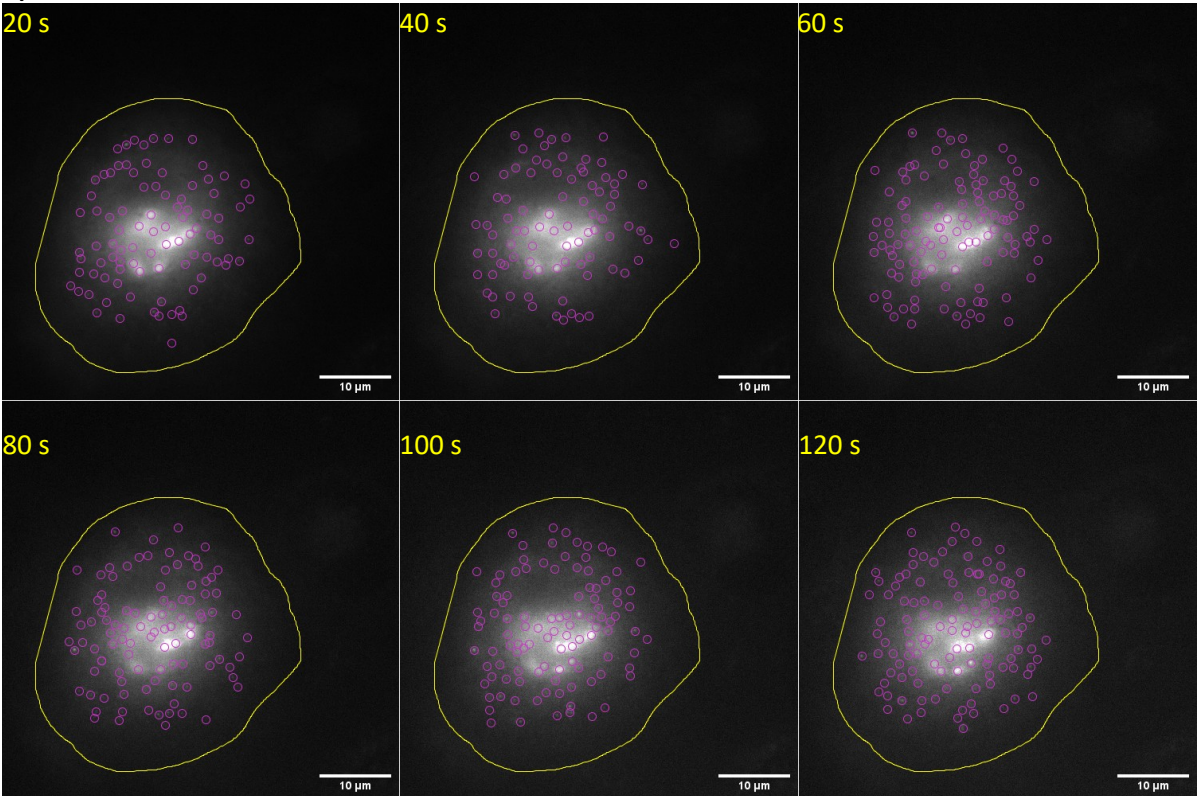
Next, the nearest-neighbour method was applied to live-cell imaging videos of macrophages overexpressing MMP7-mCherry as *pars pro toto* for soluble MMPs to detect the exocytosis events or vesicles at the plasma membrane in relation to podosomes. To observe the area at-, and closely under the cell surface of macrophages, total-internal reflection microscopy (TIRFM) was used. With this method, only a defined area at the surface of the cell is excited and fluorescent to observe only fluorescent proteins on or at the plasma membrane such as surface proteins or vesicles accumulating at the membrane for exocytosis or endocytosis.

For live-cell imaging, 7-8 days old macrophages were transfected with the MMP7-mCherry plasmid, seeded on a TIRFM-suitable glass-bottom dish and overexpressed for 5 h. Then, cells were stained with SiR-actin and incubated for further 30 min. Live-cell imaging videos were acquired with the Visitron-system in TIRFM mode (figure 4.4.3).

A) Channel 647:



B) Channel 561:



c)

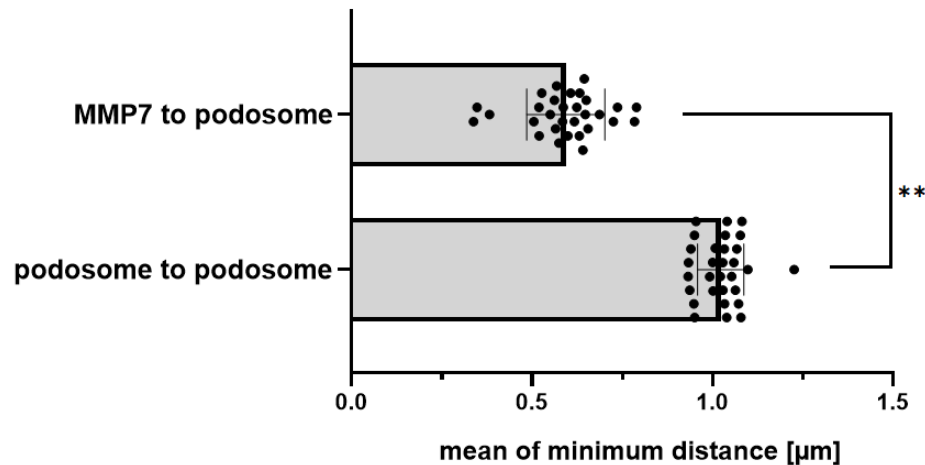


Figure 4.4.3: Trackmate-based analysis of MMP7 and podosome positions. Representative live-cell imaging TIRFM-pictures of primary human macrophages, overexpressing MMP7-mCherry and stained with SiRactin at different time points (20 s, 40 s, 60 s, 80 s, 100 s, 120 s), $n=3 \times 10$. Podosome- (A) and vesicle-positions (B) were tracked with TrackMate from FIJI-software (purple circles) from selected area (encircled in a yellow region of interest). Bar diagram shows the comparison of mean of minimum distances between podosome to podosome (reference) in comparison to the mean of minimum distances between MMP7 vesicle and podosome (C).

In contrast to the close proximity of MT1-MMP islets and podosomes, MMP7 vesicles at the plasma membrane did not show this proximity and the mean minimum distance of $0.59 \mu\text{m}$ ($\pm 0.11 \mu\text{m}$) was lower than the half of the reference distance between podosomes with $1.02 \mu\text{m}$ ($\pm 0.06 \mu\text{m}$), suggesting a rather random release or at least a podosome-independent one. The small but remarkable difference between the reference distances from podosome to podosome with $1.02 \mu\text{m}$ and $0.94 \mu\text{m}$ in the previous experiment might be due to a fixation artefact or other differences in treatment, but does not affect the function as an internal reference. With this experiment, the previous observation in the degradation assay of no impaired podosome number is added to the observation, that vesicles of soluble MMPs are not in close proximity of podosomes. This suggests a podosome-independent regulation of soluble MMPs.

4.5 Intra- and extracellular levels of soluble MMPs

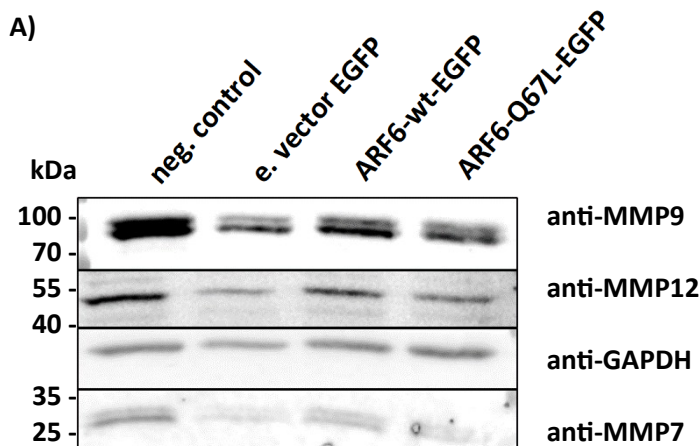
4.5.1 Protein levels of soluble MMPs at ARF6 overexpression

So far, the time point of maximal protein expression of soluble MMPs during differentiation of monocytes to primary macrophages was determined at about 1 week after harvest from buffy coats from human blood. A correlation in the expression pattern especially between MMP9 and MMP12 could also be observed as well as a correlation with MMP7 and the polarization marker CD163, associated with M2-macrophages, confirming previously reported observations [29], where some soluble MMPs are strictly dependent on the polarization state of the macrophage in contrast to the continuously expressed MT1-MMP. A colocalization of soluble MMPs with each other and ARF6 could be observed – independently of MT1-MMP. Soluble MMPs seem also not to colocalize or show close

proximity to podosomes, deviating from MT1-MMP as well. This suggests a structural independence of this main degradative structure. A dependence of the actin-forming influence of ARF6 on soluble MMPs could not be confirmed as well. Besides, an impact on the degradative capability by ARF6-knockout was proven in the matrix degradation assay, but not in the zymography assay. This suggest a specific influence of ARF6 on the surface exposure of soluble MMPs. Hence, the intracellular and surface-protein levels needed to be investigated in a comparative way. Therefore, a surface-protein biotinylation assay was performed on macrophages with different overexpression conditions. The surface biotinylation assay offers the opportunity to investigate the amount of surface-associated proteins. Especially for the challenging task of evaluating the protein levels of proteases without a membrane-anchoring domain, this method is indispensable and is more advantageous to methods like flow cytometry or surface immunofluorescence stainings with too rough conditions of washing and staining with antibodies. The relative protein expression of the respectively stained proteins in western blots was performed analogously as described before in the zymography assay with the Fiji software, normalized with GAPDH-values and calculated into a relative percental value.

4.5.1.1 Intracellular protein levels at overexpression of ARF6

To further investigate the effect of ARF6 on intracellular protein levels of MMP7, representing soluble MMPs, 6 days old macrophages were transfected with the ARF6-Q67L-EGFP plasmid encoding for a defective constitutively active mutant (ARF6-Q67L) in comparison with wild type ARF6-EGFP and empty EGFP vector and a surface-biotinylation assay was performed after 5 h 30 min of overexpression. Two different fractions were compared with each other: first, the whole-cell lysates (figure 4.5.1.1) and the surface-biotinylated proteins (figure 4.5.1.2) from the respective conditions. The western blot of whole-cell lysates was stained for MMP7, MMP9, MMP12 and GAPDH (A).



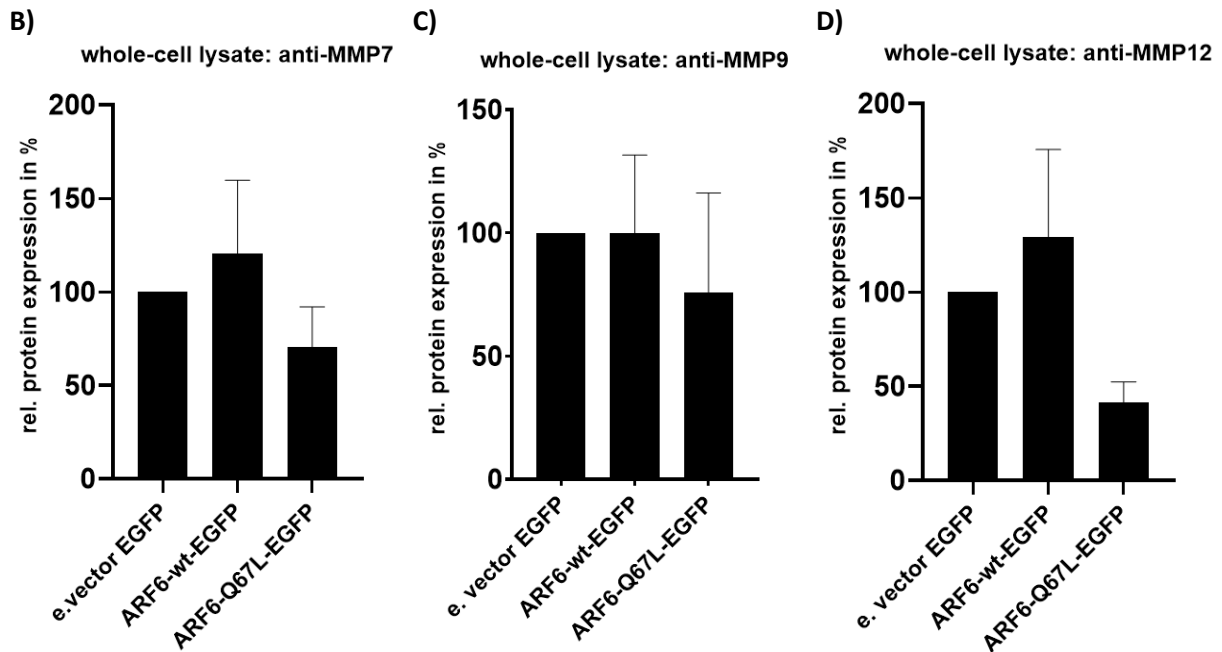


Figure 4.5.1.1: Intracellular MMP protein levels. Western blots from whole-cell lysates of 6-days old macrophages overexpressing ARF6-Q67L-EGFP, ARF6-wt-EGFP or empty vector EGFP after a surface-biotinylation assay (5 h 30 min after transfection with plasmids), n=3. Western blots of whole-cell-lysates stained for GAPDH (house-keeping gene), and MMP7, MMP12 and MMP9 (A) and the respective graphs for relative protein expression (B-D), normalized against GAPDH.

Cells overexpressing AR6-wt-EGFP showed increased intracellular protein levels of MMP7 at about 120% (B) and also of MMP12 with 129% (D). In contrast to this, cells overexpressing the ARF6-Q67L-EGFP mutant compared to the ARF6-wt-EGFP showed reduced intracellular levels of MMP7 with 70% and of MMP12 with 42%. The intracellular levels of MMP9 were not consistently reduced in all 3 donors and showed a mean value of 76%. This suggests on the one hand, that overexpressed ARF6, which is able to switch between active and inactive forms, increases the amount of intracellular soluble MMPs by enhanced endocytosis, and on the other hand, that an impaired mutant reduces the intracellular protein level by impaired endocytosis. Hence, ARF6 regulates the intracellular protein level of soluble MMPs by endocytosis. The wildtype ARF6 is required for proper endocytosis of MMP7 and MMP12 and the defective mutant compromises it in a remarkable way.

4.5.1.2 Surface protein levels at overexpression of ARF6

The biotinylated surface-protein levels were also compared with each other (figure 4.5.1.2), with the same stainings of the western blot, but MMP12 could not be detected (data not shown).

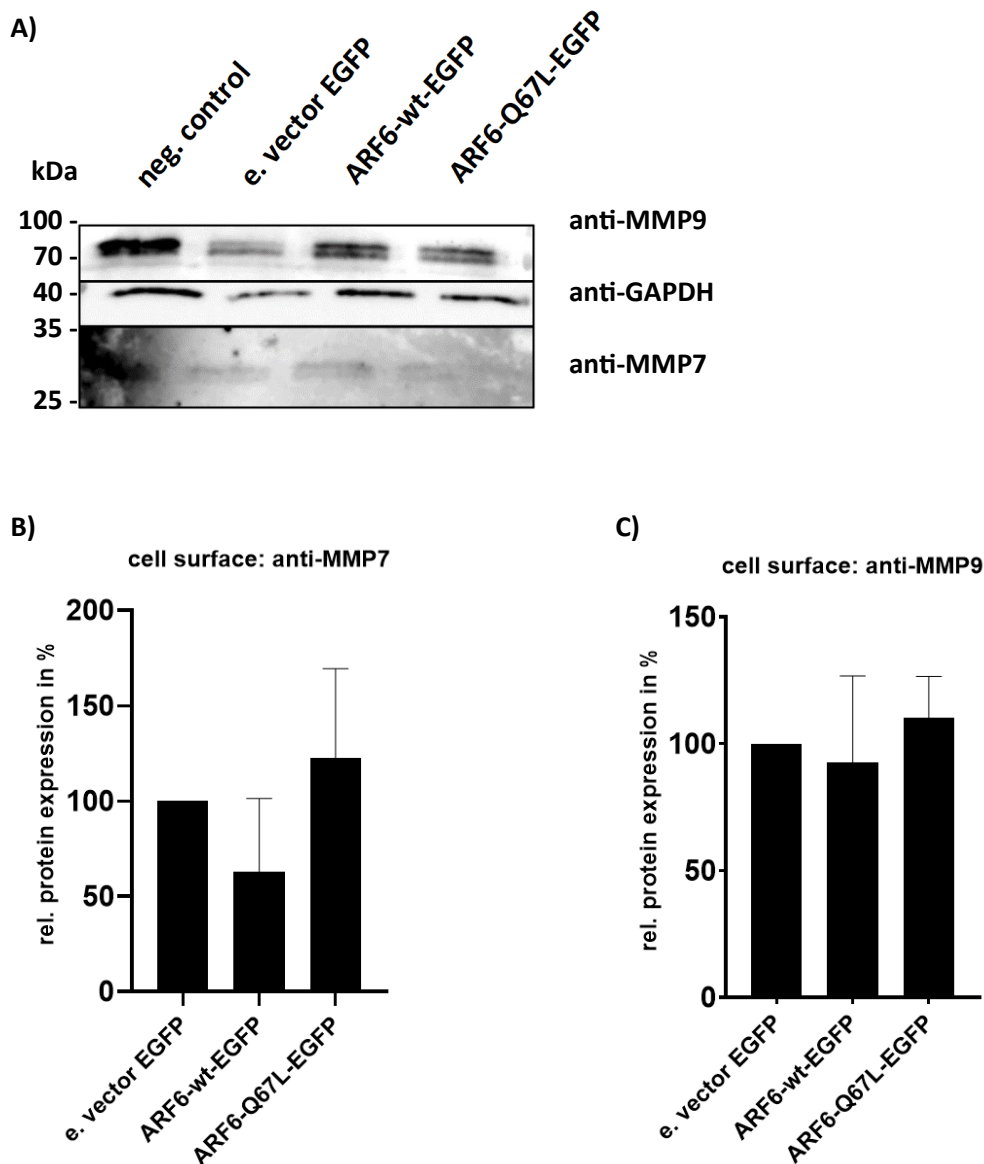


Figure 4.5.1.2: Surface MMP protein levels. Western blots from biotinylated fraction of 6-days old macrophages overexpressing ARF6-Q67L-EGFP, ARF6-wt-EGFP and empty vector EGFP after a surface-biotinylation assay (5 h 30 min after transfection with plasmids), n=3. Western blots of biotinylated fractions stained for GAPDH (house-keeping gene), and MMP7, and MMP9 and the respective graphs for relative protein expression of MMP7 (left) and MMP9 (right) - normalized against GAPDH.

As a consequence of reduced endocytosis of MMP7- and MMP9-surface proteins by the Q67L-mutant, an increased level is observed of non-internalized MMP7 protein with 123% – and to a lesser extent MMP9 surface protein levels with 110%. The overexpression of wildtype-ARF6 increased the endocytosis of MMP7 and reduced the surface protein levels to 63% and the protein level of MMP9 to 93%. Yet, the detection of MMP7 was weak and the GAPDH levels show a high variation between the donors, which aggravates the evaluation. Further replicates might be necessary to substantiate these observations. It must also be mentioned that the transfection efficiency of plasmids with the applied electroporation method was only at about 30%. This means that only one third of the cells was affected by the respective overexpressions and was not selectively analyzed or sorted with flow

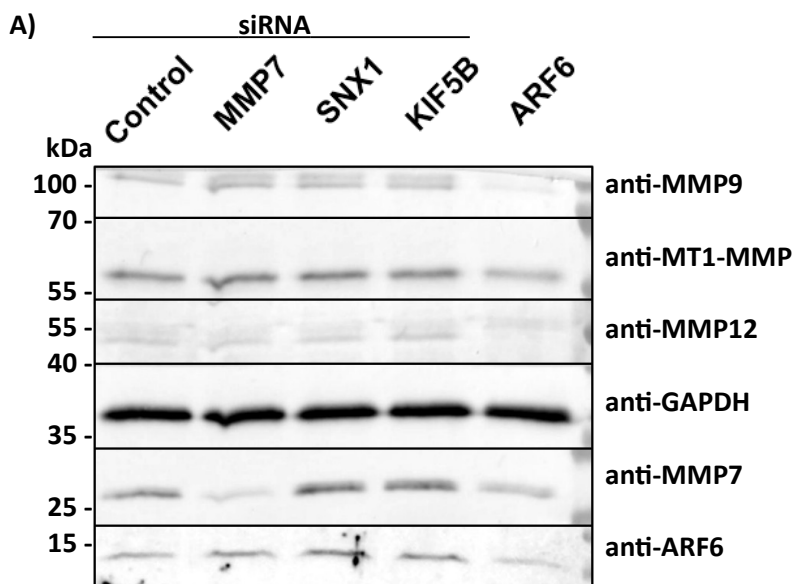
cytometry. A comparison with the far more efficient transfection of siRNA would be necessary also to observe the alteration of endogenous protein levels of ARF6 on soluble MMPs.

4.5.2 Protein levels of soluble MMPs at knockdown conditions

The overexpression of both ARF6 and its defective mutant altered the intracellular and surface-associated surface-levels on different ways. The overexpression of the wild-type ARF6 increased intracellular protein level of surface-associated MMPs, hereby reducing the surface-protein levels of at least MMP7. Overexpressing the defective Q67L-mutant caused the opposite effect. Again, MMP7 was the most affected soluble MMP under the respective conditions. MMP12 was not surface-associated in primary human macrophages.

4.5.2.1 Intracellular protein levels at knockdown conditions

To investigate a less artificial and more efficient treatment, endogenous ARF6-knockdown, SNX1 knockdown and KIF5B-knockdown on 6-days old macrophages were performed and compared. SNX1 is an adaptor protein to the retromer complex for the recycling process after endocytosis. KIF5B is known to be an exocytosis regulator for MT1-MMP [13], transporting vesicles in plus-ended direction at microtubules. SNX1 was selected to investigate the role of putative recycling of MMPs back to the cell surface as reported for MT1-MMP by the retromer complex [13]. KIF5B was selected to compare the impact of an exocytosis regulator on soluble MMP protein levels, which was already published as a regulator for MT1-MMP exocytosis. 6 days old macrophages were transfected with the respective siRNAs to perform knockdowns in 3 different donors and the surface-biotinylation assay was performed on day 3 post transfection. The harvested whole-cell lysates were stained in a western blot for MT1-MMP, MMP7, MMP9, MMP12 and GAPDH as the house-keeping gene (figure 4.5.2.1).



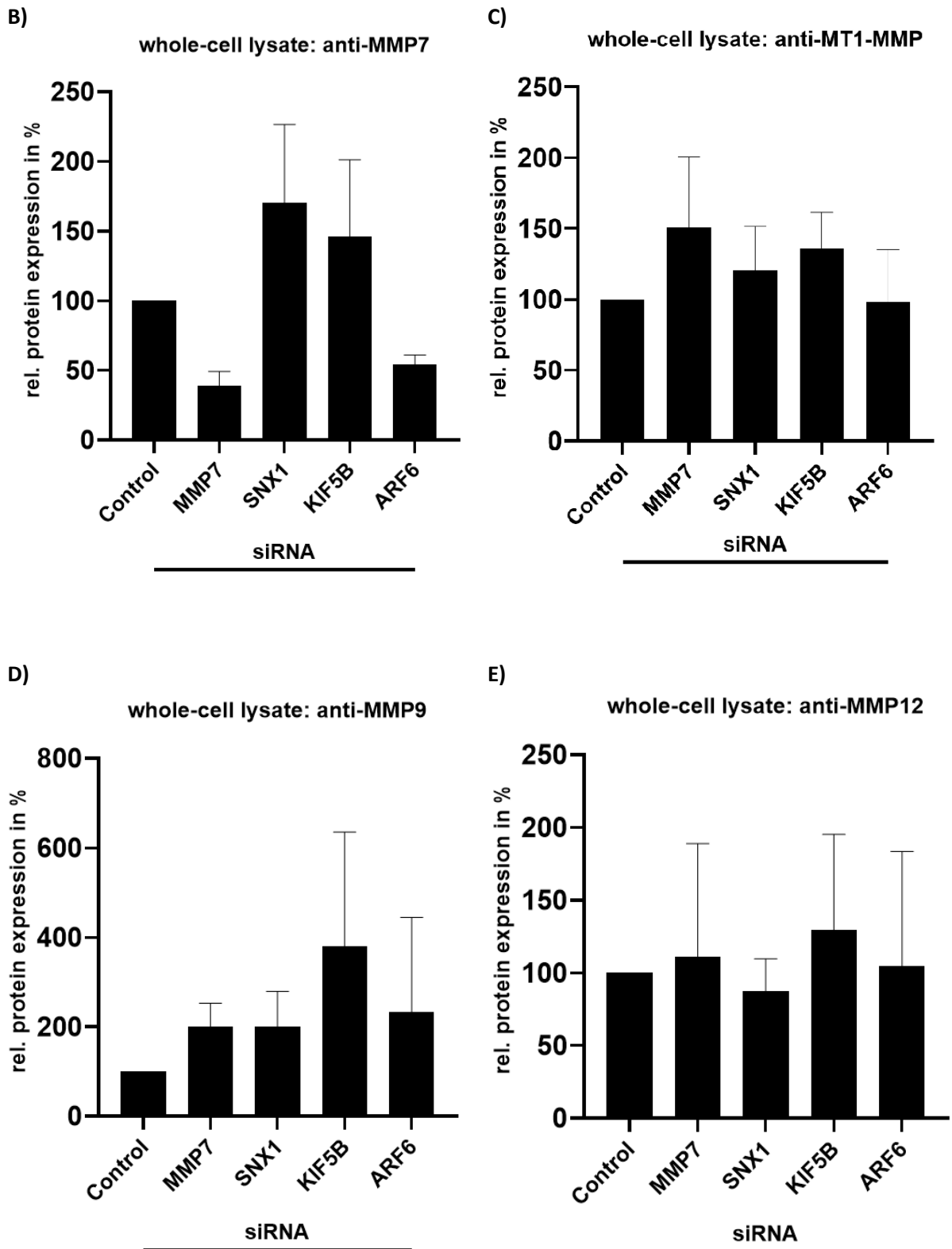


Figure 4.5.2.1: Intracellular MMP protein levels at knockdown conditions. Western blot from whole-cell lysates of 9-days old macrophages at knockdown-conditions (control-siRNA, MMP7-, SNX1-, KIF5B- and ARF6-targeted siRNA, transfected at day 6 with siRNA) after a surface-biotinylation assay (72 h after transfection with siRNA), n=3. (A) Western blot of whole-cell-lysates at the respective conditions stained for GAPDH (house-keeping gene), MT1-MMP, MMP7, MMP12, MMP9 and ARF6 and the corresponding graphs for relative protein expression of MMP7 (B), MT1-MMP (C), MMP9 (D), MMP12 (E) - normalized against GAPDH.

The results confirmed the previous observations in the overexpression experiment with impaired ARF6-regulated endocytosis for MMP7. The intracellular protein level of MMP7 was reduced to 55% in ARF6-knockdown cells as well as in the MMP7 knockdown with 39%, caused by an impaired endocytosis, which leads to increased intracellular levels (B). For MMP9 protein levels (D) at ARF6 knockdown conditions, no consistent effect could be observed: 2 donors showed an increased intracellular protein level and one was reduced. MMP12 protein levels (C) were not consistent at ARF6-conditions as well with reduced levels in 2 donors and on increased in the third. The intracellular protein level of MT1-MMP was also not consistently affected: It was two times reduced and once increased with a mean level of 98%, indicating a rather subordinate importance for this pathway compared to MMP7.

The other regulators showed an opposite effect to the ARF6 knockdown with increased levels of MMP7 to 170% at the SNX1-knockdown and an increase to 146% at KIF5B-knockdown, which seems to be counter-intuitive at first sight. Similar effects could be observed on the protein levels of MMP9 and MMP12 for SNX1- and KIF5B-knockdowns. For MMP9, the knockdown of especially KIF5B caused an increase of intracellular protein of 256%, underlining the importance of this regulator for probably exocytosis of MMP9. The SNX1-knockdown doubled the intracellular protein level of MMP9 to 201%. It is also remarkable, that the MMP7-knockdown caused the same consistent increase in intracellular protein level of MMP9 in all 3 donors. It is possible, that MMP7 acts as an activator of pro-MMP9 as well as MT1-MMP for other MMPs such as pro-MMP2. The impaired activation by MMP7 might lead to an increased endocytosis of pro-MMP9. No consistence could be observed in the intracellular protein levels of MMP12 between 3 donors at MMP7-knockdown conditions, which were once increased and two times decreased.

4.5.2.2 Surface protein levels at knockdown conditions

The surface proteins from the biotinylated fraction showed similar results with a focus on the comparison between MMP7 and MT1-MMP (figure 4.5.2.2):



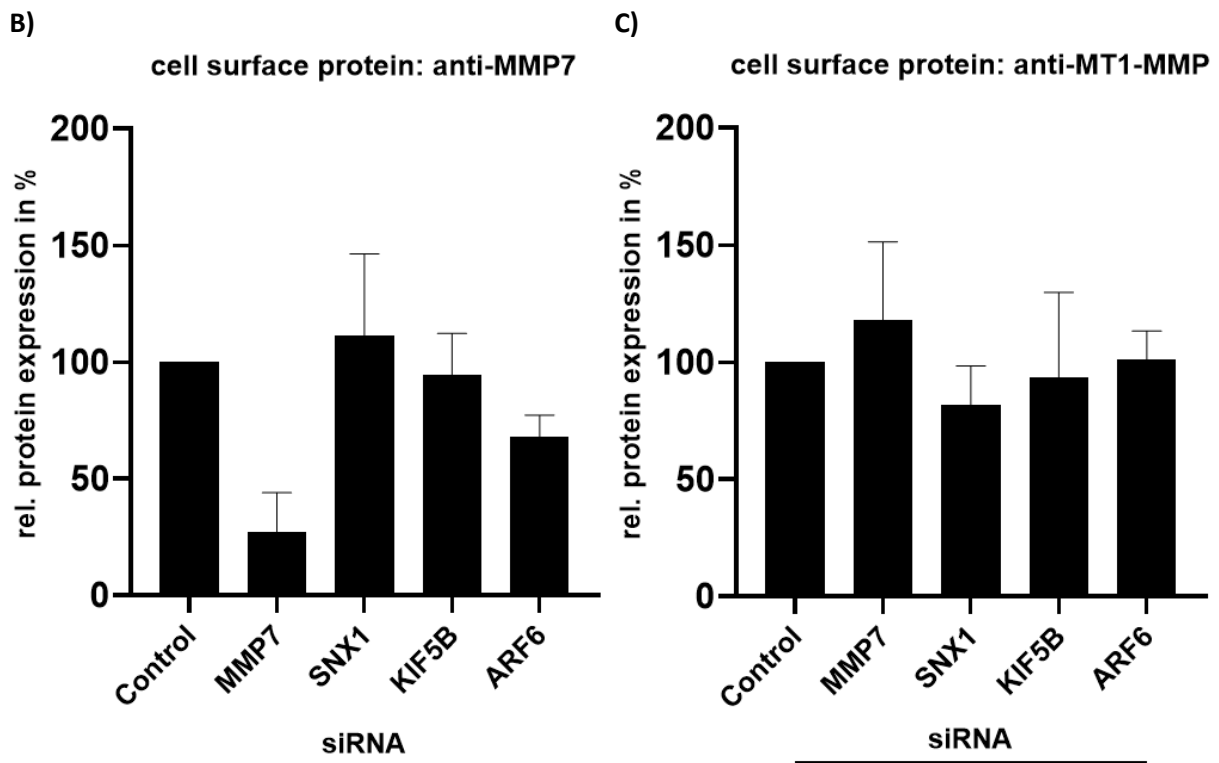


Figure 4.5.2.2: Surface MMP protein levels at knockdown conditions. Western blot from biotinylated fraction of 9-days old macrophages at knockdown-conditions (control-siRNA, MMP7-, SNX1-, KIF5B- and ARF6-targeted siRNA, transfected at day 6 with siRNA) after a surface-biotinylation assay (72 h after transfection with siRNA), n=3. (A) Western blot of biotinylated fractions at the respective conditions stained for GAPDH (house-keeping gene), MT1-MMP and MMP7 and the corresponding graphs for relative protein expression of MMP7 (B) and MT1-MMP (C) - normalized against GAPDH.

Here, the MMP7 surface protein levels were consistently reduced in all 3 donors at ARF6-knockdown conditions to 68%. This might seem counter intuitive compared to the previous observation in the overexpression, since a reduced endocytosis with reduced intracellular levels should lead to an accumulation of surface protein. But the overexpression of the defective ARF6-Q67L-mutant showed the more immediate effect within 6 hours and the knockdown of endogenous ARF6 for 3 days might lead to different results. For MT1-MMP, only a weak impact on the surface-protein levels could be observed by ARF6-knockdown with a mean value of 101%. The effect of KIF5B-knockdown was inconsistent with an increased protein level in one donor and a reduced protein level in the others. For SNX1-knockdown, the impact was more remarkable with 82%.

4.5.2.3 Soluble MMPs in the culture medium at knockdown conditions

The last fraction, which was analysed for its MMP7 protein levels was the culture medium. Therefore, 24h before the surface-biotinylation assay was performed, the culture medium of macrophages was replaced by starving medium without serum. At the third day after transfection, an acetone-

precipitation was performed with this medium. The precipitated protein was applied on a PAA-gel and a western blot was performed (figure 4.5.2.3):

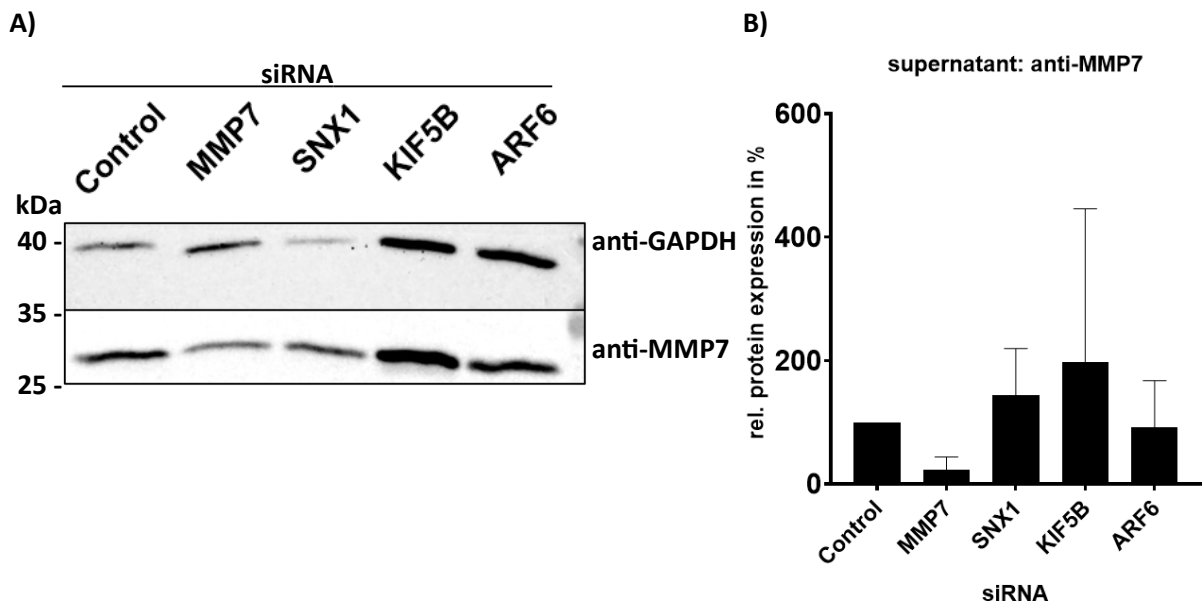


Figure 4.5.2.3: Supernatant MMP protein levels at knockdown conditions. Western blot from acetone-precipitated proteins of 9-days old macrophages at knockdown-conditions (control-siRNA, MMP7-, SNX1-, KIF5B- and ARF6-targeted siRNA, transfected at day 6 with siRNA) after a surface-biotinylation assay (72 h after transfection with siRNA), n=3. (A) Western blot of precipitated proteins at the respective conditions stained for GAPDH (house-keeping gene) and MMP7 and the corresponding bar diagram for relative protein expression of MMP7 - normalized against GAPDH (B).

Unfortunately, only the protein levels of MMP7-knockdown conditions were consistent with a reduced mean value to 29% compared to the control condition. The ARF6-knockdown caused reduced MMP7 protein levels in only 2 of 3 donors. Other knockdown conditions of SNX1 or KIF5B were inconsistent as well. This might be due to the low overall MMP7 protein concentration in this fraction. It is remarkable, that the detection of MMP7 proteins was less difficult in the biotinylated fraction compared to the supernatant. Shedded MT1-MMP could not be detected to compare the possible influence of the respective knockdowns.

Summarized, the intracellular- and surface protein levels of MMP7 and MT1-MMP show differences in ARF6-knockdown conditions as well. The MT1-MMP-protein levels are not significantly altered compared to the control-knockdown. The MMP7-protein levels on the cell surface seem to be less decreased than the intracellular levels, but still remarkable. Thus, not only the intracellular but also the surface protein level of MMP7 seems to be impaired by the ARF6-knockdowns. The protein amount in the culture medium, not associated with the cell surface, has probably a minor importance for the degradative capability of macrophages, since only a low amount of protein could be detected and no consistent effect caused by the ARF6-knockdown. The knockdown of the other endocytic regulators showed other aspects of the intracellular regulation of soluble MMPs. Here, not only MMP7 was affected, but also MMP9 and MMP12. Although, no MMP12 could be detected at the cell

surface, the endocytosis and SNX1 seem to play a role in the regulation of this soluble protease. The importance of ARF6 for MMP7 remains the most prominent, also elucidating its intra- and extracellular localization, the impact on the degradative capability and its regulation by ARF6, SNX1 and KIF5B. This explains the previously described reduction of the degradative capability from macrophages with the impaired endocytic capability of ARF6 on soluble MMPs, but not on MT1-MMP in primary human macrophages. Compared to the overexpression experiments, the knockdown conditions showed a higher impact on the protein levels. This is probably due to the different transfection efficiency with electroporation of primary human macrophages in our hands. For plasmid-transfection, only approx. 30% was usually observed in contrast to a quite high transfection efficiency of 80-90% with siRNA, which are common values, respectively. In contrast to the intracellular and the surface protein levels of MMP7, the supernatant protein level was not impaired by the ARF6-knockdown or at least not in all 3 donors, which seems not to be relevant for the degradative capability of macrophages in the matrix degradation assay. Other endocytic regulators did not show a consistent effect on MMP7.

5 CONCLUSION:

In the present dissertation, different aspects of soluble MMP regulation in primary human macrophages were investigated, especially compared to MT1-MMP:

First, during the differentiation of human blood-derived monocytes into primary macrophages, cultivated *in vitro* for 2 weeks, the expression profile over time of MMP7, MMP9 and -12 was analyzed and compared to the protein expression profile of the surface receptor CD163, which is also a marker for M2-polarized anti-inflammatory macrophages. It was shown that the protein expression of MMP7, MMP9, and MMP12 increased within the first week of differentiation as well as the M2-polarization marker CD163. At the beginning of the second week, MMP7-, and CD163-protein expression decreased over time, statistical analysis revealed a moderate, but significant correlation between both expression profiles, but not between CD163 and MMP9 or CD163 or MMP12. The protein expressions of MMP9 and MMP12 showed the highest correlation compared to the others, suggesting the most similar regulation of these MMPs during the differentiation process. The correlation of both expression profiles to MMP7 expression was lower, but also remarkable. This leads to the question if the protein expression profiles of MT1-MMP, other soluble MMPs, and other polarization markers correlate or not during this differentiation process and needs to be evaluated in further experiments.

Second, the intracellular localization of endogenous MMP7, MMP9, and MMP12 was compared with each other, and also with endogenous MT1-MMP, in differentiated primary human macrophages to investigate the intracellular trafficking of soluble MMPs. Also here, soluble MMPs showed different results. MMP7-positive vesicles colocalized to a high degree with MMP9-stained vesicles in contrast to MT1-MMP, which colocalized only weakly with MMP9. This suggests an intracellular transport of soluble MMPs, represented by MMP7 and MMP9, which is distinguishable from MT1-MMP trafficking. Both, MMP7 and MT1-MMP showed a low colocalization to MMP12, which might represent a third, independent vesicle population. Then, the intracellular localization of soluble MMPs was compared with the localization of two regulators of early endocytosis – EEA1 and ARF6. MMP7 showed a high colocalization to ARF6, in contrast to MT1-MMP, which is supposed to be regulated by ARF6. MMP12 for its part, showed a high colocalization to EEA1 – in contrast to MMP7. These results underlined the previous observation of differently regulated soluble MMPs - not only compared to MT1-MMP, but also compared to each other. As before, further comparison with other MMPs and regulators is required to complete the picture of the regulatory mechanism.

In the third part, the influence of soluble MMPs – represented by MMP7 - compared to MT1-MMP and the endocytotic regulator ARF6 was investigated in zymography assays with different substrates

and in matrix-degradation assays. The zymography assays with collagen type I, IV and gelatin showed no significant differences at knockdown conditions and need probably a refinement of the experimental conditions. It is also necessary to mention, that only whole-cell lysates were used for this assay and no distinction between intracellular and extracellular protein levels was performed. This results were contrasted by the matrix degradation assay with rhodamin-labeled gelatin. Here, a high impact of MMP7-knockdown on the degradative capability of macrophages could be observed, comparable to the decrease of degradation in MT1-MMP-knockdown cells. The loss of degradation was even higher in ARF6-knockdown cells. This suggests a regulatory influence of ARF6, not only limited to one (soluble) MMP. Fourth, the spatial distribution of vesicles at the plasma membrane in relation to podosomes (the main adhesive and degradative structures of macrophages) was compared to MT1-MMP. It is known that MT1-MMP islets are associated with podosomes, but it was unclear, if soluble MMPs are either released at podosomes or surface-associated in foci, comparable to MT1-MMP. The results show no close spatial proximity of MMP7 to podosomes, suggesting an independent regulation of release and surface exposure of soluble MMPs. In the last part, the relationship of ARF6 to soluble MMPs was further examined. In contrast to the previous zymography assays, intracellular and surface-associated protein fractions were distinguished and compared. At first, the effects on MMP-protein levels of ARF6-wt and ARF6-Q67L overexpression were compared with each other. MMP7 and MMP12 showed reduced intracellular protein levels, whereas surface-exposed MMP7 protein levels were increased, when ARF6-Q67L was overexpressed. MMP9 showed no significantly altered protein levels in both fractions. In knockdown-conditions, soluble MMP-protein expression was also compared with MT1-MMP-protein expression, but also different endocytosis regulators and their influence on MMP-protein levels were compared with each other. Surprisingly, both intra- and extracellular protein levels of MT1-MMP were not significantly altered by ARF6-knockdown, whereas MMP7 protein levels were highly reduced in both cases. MMP9- and MMP12-protein levels showed no comparable alteration in both fractions. Besides, both the other endocytotic regulator SNX1, and the exocytotic regulator KIF5B showed an opposite effect on intracellular, but not extracellular MMP7-protein levels. This suggests a regulation of MMP7-endo- and exocytosis on different levels, but a predominant role of ARF6 for surface exposure in macrophages. In the supernatant, only MMP7 protein levels were analyzed, but the high variation between the respective donors was too high and less conclusive. Intracellular MMP9 protein levels were also highly increased in KIF5B-knockdown cells, suggesting a predominant role of this exocytosis regulator, even more than for MT1-MMP. Other soluble MMP-protein levels need to be evaluated as well and potentially shedded MT1-MMP. Altogether, soluble MMPs offer a vast field of investigation and potential therapeutic targeting.

6 DISCUSSION:

In this dissertation, different aspects of soluble MMP-regulation and their variation were investigated in primary human macrophages, exemplified by MMP7, -9 and -12 and compared to MT1-MMP.

6.1 Expression profiles of MMPs

In initial experiments, the expression profiles of MMP7, -9, -12 and of the polarization marker CD163 in blood-derived monocytes during their differentiation to primary macrophages *in vitro* were evaluated. It could be observed, that the singular expression of MMP7, -9 and -12 increased within the first week of cultivation. After that, the first differences could be noticed: The expression profile of MMP7 decreased over time, in contrast to the expression of MMP9 and -12, which remained rather constant. Both, MMP9 and MMP12 showed a high correlation between their expression profiles, but also a significant one to MMP7. Possible explanations for this observation might be a more common regulation of expression between MMP9 and MMP12 in combination with a common intra- and/or extracellular transport. Although it is not possible to distinguish between the localization of the harvested proteins at the time point of classical cell-lysis (without previous protein labeling) in the retrospective, a correlation in protein levels must be caused by some factors such as either transcription or intracellular transport and localization. For example, the overall protein level of a cell is not only defined by their intracellular-, but also by its surface-exposed population. The localization of MMPs at the cell surface or in intracellular compartments such as lysosomes, the Golgi-network, the nucleus or recycling endosomes as well as intracellular stores for initial exocytosis, require a distinct regulation.

MMP7 for its part, might share only one of these aspects with MMP9 and MMP12. It is remarkable, that that the expression of all 3 MMPs increases during differentiation of monocytes into macrophages, gaining the characteristic degradative capability. Also, the observation of a decreasing protein expression of MMP7 in the second week, which correlated to the M2-polarized marker CD163. The observed decrease in the second week, might be due to a polarization-dependent further alteration of the expression profiles, which occurred during the cultivation *in vitro*. In further experiments, it will be necessary to compare the already investigated expression profiles with other soluble MMPs and MT1-MMP as well. In a second step, these expression profiles need to be compared with their functional importance for the degradative capability, after inducing different polarization states during the differentiation process.

The expression of the M2-polarization marker CD163, which decreased as well in the second week, correlated with the expression of MMP7 and thus confirming the already reported correlation to the polarization. Surprisingly, MMP9 and -12 showed no significant correlation in expression to CD163, where at least MMP12 expression should be polarization-dependent, too [29]. This might be an additional hint for differently regulated soluble MMPs, not only referring to MT1-MMP, which is reported to be equally expressed in both polarization states [29], but also between soluble MMPs themselves. M2-polarized macrophages are known to express an anti-inflammatory activity. Due to that, MMP7 seems to be expressed in a polarization-dependent manner as already reported. Nevertheless, these results in context to other soluble MMPs need to be confirmed with other polarization markers (e.g. CD80, CD86 or TLR2, TLR4). For MT1-MMP, no dependence on the polarization state of the macrophage was reported [29]. Although, the evaluation of the expression profile of MT1-MMP would be necessary to complete the picture of the regulation of MMPs in macrophages, also in comparison with other potentially correlating (soluble) MMPs or polarization markers.

Summarized, MMP7, MMP9 and MMP12 expression profiles showed different properties in primary human macrophages: MMP7 protein expression seems to be dependent on the polarization state of the macrophages and correlates with the anti-inflammatory M2 polarization marker CD163. MMP9 and MMP12 showed the highest correlation in their expression profiles, suggesting a close common regulation. It is unclear, whether MMP9 and MMP12 expressions do not depend on polarization as suggested by the data, since only one polarization marker was investigated. The evaluation of expression profiles over time and their correlation would remain a valid tool to characterize the macrophage development and polarization.

6.2 Intracellular vesicle populations of MMPs

The investigation of the intracellular localization of MMPs allows the identification of regulatory transporting mechanisms. In the presented colocalization experiments, the vesicle populations of MMP7, MMP9 and MMP12 became distinguishable, compared to MT1-MMP. Here, a remarkable colocalization between endogenous MMP7- and MMP9-stained vesicles of approx. 40 % was observed in contrast to a low colocalization to vesicles, stained for endogenous MT1-MMP with about 20%. But also in this experiments, the soluble MMPs did not show the same results: MMP12-stained vesicles showed a comparable low colocalization to both MMP7- and MT1-MMP-stained vesicles of about 25%. This suggests on one hand the vesicle population of MT1-MMP-transporting vesicles is distinct from soluble MMPs, but also, that at least two vesicle populations of soluble MMPs share spatial overlap: MMP7 and MMP9 on one hand and MMP12 on the other. This is a challenging result,

referring to the previously evaluated expression profiles over time, where a high colocalization between MMP7 and MMP12 could be expected due to their correlating expression profiles, comparable to the colocalization between MMP7 and MMP9 with a similar correlation in their protein expression. One possible explanation for this observation as already mentioned, could be a similar regulation in protein expression of MMP7 and MMP12, but different intracellular transport mechanisms. And here, another problem occurs, regarding the expression profiles: MMP7 protein expression correlated with CD163 protein expression (M2-polarization), but the expression profiles of MMP12 did not as well as the MMP9-expression profile. Considering that, another factor of regulation, beside intracellular trafficking or polarization-dependent transcription must be assumed. For further experiments, additional stainings might be recommended: Since a high correlation between MMP9 and -12 protein expression profiles was observed, a co-staining is necessary to identify a potential colocalization and to clear the nature of their common regulation (transport or expression?). Although, it is unlikely to observe a high colocalization between MMP9 and MMP12 as well, since different results were observed for the colocalization with MMP7 and a difference in the regulation of protein expression is likely.

In a second step, the regulatory mechanism of endocytosis of soluble MMPs was investigated. For that, the vesicle populations with soluble MMP-cargo were compared with each other in their colocalization with two different regulators of early endocytosis: ARF6 and EEA1. Endocytosis is an important regulatory mechanism to control surface-exposed proteins and the surface exposure of MMPs is crucial for the degradative capability of the respective cells. The immunofluorescence stainings of endogenous MMP7 showed a high colocalization of about 60% with endogenous ARF6. The colocalization was even higher than the one to MT1-MMP with 40%, which was already reported to be regulated by ARF6 [58]. In contrast to that, MMP12-stained vesicles highly colocalized to EEA1-stained vesicles, which showed only a low colocalization to MMP7. This underlined again the previous observation of probably distinct transport- and regulation mechanisms of soluble MMPs from MT1-MMP and inbetween. Also here, additional further stainings need to be performed: MMP9 and -12 co-stained with ARF6, MMP9 co-stained with both ARF6 and EEA1, EEA1 co-stained with MMP7. Some combinations were not performed, yet because of the same host-species of antibodies to avoid unspecific co-staining of different targets. Of course, the intracellular transport is not only defined by endocytosis and surface exposure: Recycling is a closely-related and subsequent process to endocytosis. Hence, co-stainings with regulators of recycling back to the cell surface, might reveal interesting results. Putative candidates would be components of the retromer complex such as VPS26 and SNXs as adaptor proteins. This process is relevant for the surface-exposure of MMPs and hence, their degradative capability, too. The exocytosis of soluble MMPs needs to be investigated as well. It is likely, that the differences in localization is also caused by different exocytosis. Nevertheless, MT1-

MMP, which was already extensively investigated, might define some candidates for the regulation of intracellular transport: various Rabs, SNXs, and KIFs. E.g. a colocalization of soluble MMPs with Rab8a is rather unlikely, since a low colocalization between MT1-MMP and the respective soluble MMPs (except for maybe MMP12) was observed. A former candidate of our lab was Rab6a for exocytosis regulation of soluble MMPs, but only a low colocalization with the respective MMPs and no impact on the degradative capability could be observed by silencing Rab6a (data not shown).

Summarized, the colocalization experiments suggest at least three distinct vesicle populations: 1. vesicles, which contain MMP7 and eventually MMP9, which might be (partially) regulated by ARF6. 2. vesicles with MMP12-cargo, regulated by EEA1. Both can be distinguished from MT1-MMP vesicle populations. Here as well, the field of investigated MMPs needs to be extended as well as for the protein expression profile analyses to validate the given results and to specify the role of allegedly exclusive regulators such as ARF6 and responsibilities for degradative and invasive capabilities of macrophages. In relation to the previous observation with the protein expressions over time, a related transcriptional regulation of MMP7 and MMP12 seems to be more likely, since only a moderate colocalization could be observed. In contrast to that, MMP7 shows a remarkable colocalization with MMP9, suggesting that the correlation seems to be caused by at least some common intracellular transporting mechanisms. The subsequently discussed results will narrow the possibilities down.

6.3 Degradation of ECM-components by soluble MMPs

The degradative capability of macrophages is one of their key abilities to migrate through various tissues. Here, it was investigated with siRNA-mediated knockdowns of MMP7 compared to MT1-MMP and ARF6 in zymography- and matrix-degradation assays. For zymography assays with gelatin, collagen type I and type IV, a variation of the assay was established with rhodamine-labeled substrates. This offered the advantage of continuous observation of the degradation over different time points, without aborting the process. Unfortunately, the zymography experiments with different substrates did not show any differences between the harvested whole-cell lysates. This is another surprising result at first glance, considering the further presented results of the matrix degradation assay with remarkable effects on the degradative capability of human macrophages: The knockdown of either MMP7 or MT1-MMP showed a reduced degradation of rhodamin-labeled gelatin coated coverslips up to 50%. The impact of the ARF6-knockdown was even higher and the respective cells showed only 40% of the degradative capability of macrophages, treated with only control-siRNA. This suggests a cumulative impact of ARF6 on more than one of the respective MMPs (or others, which were not investigated). It is unlikely that the whole-cell lysates, harvested for the zymography assay at

MT1-MMP- or MMP7-knockdown conditions, would show no impact, if the same knockdowns show remarkable results in the matrix degradation assay. The most likely explanation are failed knockdowns or wrong time-points for investigating the degradation in the zymography assays. All 3 selected substrates are known to be degraded by the respective MMPs (or at least one of them): gelatin, collagen type I and IV. In total, the zymography assay results show only remarkable variations between the different donors, but not between the respective knockdown conditions and show the most prominent impact of ARF6 knockdown with collagen type IV as substrate with 90% of reference degradation with a high standard deviation. A degradative activity at the area of MMP7 of approx. 28 kDa, which showed a high colocalization to ARF6, could not be detected in all conditions, possibly due to the low concentration or a decreased substrate-concentration at the lower part of the gel. Since MMPs show an overlapping substrate affinity, it is not possible to selectively assign the observed effects to a specific MMP. Three possible candidates are MT1-MMP, MMP2, which is regulated by MT1-MMP and MMP12 for this size. Nevertheless, the conditions of these assays need to be optimized for further conclusions. It is usually recommended in other publications to add heparine for an increased activity of MMP7, what could be an important addendum of future experiments with a focus on MMP7. It is possible that different zymography assays with other MMP-substrates such as laminin or fibronectin would show different results. Besides, only whole-cell lysates were used for the zymography assay. A different result with a fraction of only surface-associated proteins is possible and needs to be investigated in further experiments.

Nevertheless, the matrix degradation assay confirmed the importance of the respective MMPs for the degradative capability. Also here, other substrates need to be investigated such as collagen type I, which is predominantly degraded by MMP7 and part of the basal lamina or others such as the previously mentioned laminin, fibronectin and collagen IV. In this assay, an impact of the respective knockdowns on podosomes, the main degradative structures of macrophages, is not observed, since the podosome density per cell are was not altered and the degraded areas showed gradual degradation and not ruptured area or mechanical dislocation of fluorescent gelatin.

At this point, it was unclear, which MMP-subpopulation (MT1-MMP or MMP7) was predominantly affected by ARF6-knockdown and responsible for the high impairment of the degradative capability, since it was even higher than knockdown of either MMP7 or MT1-MMP. Hence, it is likely that more than one MMP is affected by ARF6-silencing. In future experiments, potential cumulative effects of the respective MMP-knockdowns and ARF6 should be investigated. This would clarify which pathway of MMP-regulation is more affected.

6.4 MMPs and podosomes

For the degradative capability of macrophages, podosomes are an important component as the main degradative and adhesive structure. Of course, the relationship of soluble MMPs to these structures needed to be investigated. No impact of the ARF6-knockdown (or MMP7, or MT1-MMP) on the podosome number per cell area could be observed in human macrophages. But since the degradative capability podosomes on the ECM is also provided by associated enzymes (beside a mechanic dislocation of ECM-components), it needs to be investigated, if soluble MMPs contribute to that. Similar to the previous colocalization experiments with fixed cells, the spatial distribution of vesicles was compared with the positions of podosomes in live-cell imaging experiments. MMP7-mCherry was overexpressed and the F-actin cytoskeleton was stained with fluorescent SirActin. In combination with TIRF-microscopy, a focus on structures close to the cell-surface could be made. An additional advantage of live-cell imaging is the possibility to take the movement and the spatio-temporal localization of vesicles and podosomes into account. In this case – since no direct colocalization could be observed – the spatial proximity was measured and compared to the positions of MT1-MMP islets, which were already reported to be found at close proximity to podosomes. And again, a different observation could be made in overexpression experiments in live-cell imaging: MMP7-vesicle populations showed only a random distribution in relation to podosomes with a distance of about 1 μm to the closest podosome, unlike MT1-MMP-islets, which show an average minimum distance of about 0.4 μm . The measurement of the average minimum distance is an additional way to recognize structural dependencies and to investigate the structures, required for exocytosis of soluble MMPs or to identify accumulating structures such as islets for MT1-MMP. In our lab, it could be observed, that some vesicles with overexpressed soluble MMPs arrested at the plasma membrane for some seconds, and could be a first indication for an exocytosis event, intracellular stores or accumulations outside of the plasma membrane, but this quite rare event could not be quantified, so far (data not shown). Nevertheless, this “resting accumulations” of soluble MMPs did not show any spatio-temporal proximity to podosomes.

6.5 Regulation of intra- and extracellular MMP protein levels

So far, the role of surface-associated soluble MMPs for the degradative capability of macrophages was indicated in the previous experiments. The lysates for the protein expressions over time did not distinguish between distinct cellular compartments, the zymography assays performed with whole-cell lysates did not show any significantly altered degradation in contrast to the matrix degradation assay, which relies on secreted and probably surface-exposed MMPs. Therefore, the surface-biotinylation assay was performed with one week old macrophages, overexpressing wild type ARF6

and the defective mutant Q67L, where a continuous switch between the active and the inactive state is impaired and hence, the endocytic activity of ARF6. In a second step, cells with ARF6-knockdowns in comparison with knockdowns of other regulators as well in different experiments. The surface-biotinylation assay offered the opportunity to distinguish between surface-associated and intracellular proteins. For knockdown cells, even the extracellular, not surface-associated MMP7 protein level was investigated by acetone-precipitation in combination with the surface-biotinylation assay. The further experiments focused mainly on MMP7 protein level, since the highest colocalization was observed between MMP7 and ARF6.

This assay is a reliable method to detect surface protein levels of a high amount of cells, compared to microscopical techniques. First, the overexpression of ARF6-wild type and ARF6-Q67L was performed and the whole-cell lysate was investigated. It was shown, that MMP7 and MMP12 accumulated intracellularly at ARF6-wild type overexpression to 120% and 129% respectively, in contrast to the overexpression of ARF6 Q67L, where a reduced protein level for MMP7 to 70% and even 40% for MMP12 could be observed. MMP9 showed also a reduced intracellular protein level of about 76%. This suggests an impaired endocytosis by the Q67L mutant. The overexpression of the wild-type ARF6 caused an enhanced endocytosis. Both results support the previous results and the hypothesis of the role of ARF6 for soluble MMPs. The biotinylated fraction of surface-associated proteins of the same samples, showed the converse effect for MMP7 and - to a lesser extent - MMP9: The surface-associated protein level of MMP7 were increased to 123%, MMP9 to 110%, when ARF6-Q67L was overexpressed. For wildtype-ARF6 overexpression, reduced levels of surface-associated proteins to approx. 60% for MMP7 and at least 93% for MMP9. An increased endocytosis leads at constant protein expression to reduced protein levels at the cell surface. It must be mentioned, that the surface-exposure of soluble MMPs in general and its importance for the degradative capability of the respective cell, is an underrepresented aspect and usually not investigated. Here, the colocalization between ARF6 and soluble MMP7 and the impact on the degradative capability in the matrix degradation assay supported the regulatory role of ARF6 for soluble MMPs by the functional activity of ARF6 and the extra- and intracellular protein levels of MMP7. The overexpression of other defective ARF6 mutants (e.g. constitutively inactive ARF6-T44N) would complete the presented observations. If the regulatory function of ARF6 is responsible for the altered intra- and extracellular protein levels and hence, the switch between active and inactive state of ARF6, the constitutively inactive mutant ARF6-T44N would show the same results as the constitutively active mutant ARF6-Q67L.

In a further step, the effect of ARF6-knockdown in human macrophages on soluble MMP7, MMP9, MMP12, and MT1-MMP was compared with other regulators such as SNX1 and KIF5B. When ARF6 was silenced, the intracellular MMP7 protein level were remarkably reduced to 55% of the reference sample. This effect could not be observed for the intracellular MT1-MMP level, which were not

affected. The previously reported reduced surface-protein level of MT1-MMP in some publications, which will be discussed later, could not be confirmed. The protein level at the cell-surface reflected these results and showed reduced MMP7 surface exposure and no effect on the MT1-MMP protein level. More interestingly, the intracellular MMP12 protein level were not affected, as well. The MMP9 protein level showed an inconsistent picture between the respective donors and showed even two-times increased protein levels, but with a high standard deviation. The knockdown of the other regulators SNX1 and KIF5B showed the opposite effect on MMP7: Both, KIF5B and SNX1 knockdowns increased the intracellular protein levels significantly, suggesting an accumulation of internalized soluble MMP7 and probably other soluble MMPs. MMP12 was not significantly affected, MMP9 showed increased average protein level, but with a high standard deviation for KIF5B and SNX1. One plausible explanation for this observations at SNX1-knockdown condition is an impaired recycling process of the retromer complex after internalization and thus an impaired exocytosis. Members of the SNX-family are known to moderate as adaptor proteins the interaction between the retromer complex and endocytosed vesicles during a recycling process, back to the cell surface. The KIF5B-knockdown impaired directly the exocytosis and caused hereby an intracellular accumulation of soluble MMPs as well. This would not directly impair the surface-associated protein levels immediately, in contrast to an impaired endocytosis. Further colocalization experiments with KIF5B and SNX1 and matrix degradation assays at SNX1-, and KIF5B-knockdown conditions would elucidate the role of these regulators.

The surface protein levels were in a further step only compared between MMP7 as a representative for soluble MMPs and MT1-MMP, which was already reported to be regulated by ARF6 [58], [59], [61]. The cell surface-associated MMP7 protein level was reduced to 68%, the MT1-MMP protein level showed no reduction in ARF6-knockdown conditions. This confirms the previous findings and suggests that ARF6 is predominantly the endocytic regulator of soluble MMPs such as MMP7. Other soluble MMPs cannot be excluded, although the results for MMP9 and MMP12 were ambiguous. Nevertheless, MT1-MMP seems not to be affected by ARF6. The knockdowns of SNX1 and KIF5B showed no significant effects on levels of surface-exposed protein, as expected.

The additional acetone-precipitated proteins in the medium, which was kept before the surface-biotinylation assay, showed unfortunately no consistent picture of MMP7 protein levels between the respective donors. In 2 of 3 donors, the ARF6-knockdown caused a reduced average MMP7 protein level. Further donors might elucidate the impact on extracellular, not surface-associated MMP7. Although, it is likely, that the predominant impact on the degradative capability of MMP7 is caused by the surface-associated protein as well as for MT1-MMP.

It is remarkable, that the impact on the MMP7 protein level is more severe in knockdown conditions than in the previously presented overexpression experiments. This is due to the common different transfection effectivities of about 90% for siRNA and approx. 30% for plasmids. Besides, there are alleged contradictions between the results of surface-biotinylation assays performed with ARF6-overexpressing and ARF6-silenced cells. There are some explanations for the different results on the MMP7 protein level: The first possibility would be a negative feedback mechanism for the protein expression of MMP7 itself, transduced by a sensor. The second option might be an impaired recycling of MMP7 by the retromer complex and hence a decreased protein level in both fractions, the intracellular- and the surface-associated one. An increased lysosomal degradation of endocytosed MMP7 would lead to reduced intra- and extracellular protein levels as well.

Summarized, the presented experiments elucidated various aspects of soluble MMP regulation, especially of MMP7 and to a lesser extent of MMP9 and MMP12. Although, in these experiments, the strongest causal relationship seems to be identified between ARF6 and MMP7, the impact of ARF6 is probably not exclusive on MMP7, since the matrix-degradation assay showed different impacts between ARF6- and MMP7-knockdowns, suggesting other affected (soluble) MMPs, not identified, yet. The outstanding role of ARF6 for the degradative capability of macrophages is one more time confirmed, but with a differently explained causal link, compared to the subsequently discussed published data by others.

6.6 ARF6 and MMPs in previous publications

The presented data can be valued by comparison to the existing literature, referring to this topic. To date, there are some publications [58], [61], [59], which postulate a regulatory mechanism between ARF6 and MMPs in general, and most of them address MT1-MMP in particular. These publications contradict to some extent to the present data in this dissertation, which suggests a regulation of soluble MMPs on protein surface levels, but not MT1-MMP.

In 2015, Philippe Chavrier et al. postulated an ARF6-JIP3/4 dependent regulation of MT1-MMP exocytosis in triple negative breast cancer (TNBC) cells [58]. The initial observation was that silencing of either ARF6 or JIP3/4 caused a reduced invasiveness and degradative capability of the respective tumour cells, overexpression of ARF6 showed the opposite effect. Tumour cells expressed their degradative capability through invadopodia, where degradative enzymes such as MT1-MMP accumulate to degrade the extracellular matrix. The degradative enzymes need to be transported on microtubules to the invadopodial plasma membrane. This plus-ended transporting process on microtubuli is regulated by kinesin-1, the opposite directed transport is regulated by dynactin-dynein, named minus-ended transport. The adaptor protein JNK-interacting protein 3 and 4 (JIP3 and 4)

switches between kinesin-1 and dynactin and regulates hereby the directory of the transport. The hypothesis was, that activated ARF6 binds to JIP3/4, and supports by that the exocytosis of plus-ended transport of MT1-MMP to the plasma membrane and thus the degradative capability of the respective tumour cells.

In the respective publication, a FITC-gelatin degradation experiment with ARF6-knockdown cells showed reduced degradation, suggesting a downstream regulation of degradative enzymes. Similar results were obtained with JIP3/4- and MT1-MMP-knockdowns. Nevertheless, the protein expression of MT1-MMP was not affected by ARF6- or JIP3/4-knockdown experiments, the expression of other MMPs was not compared. Endogenous JIP4 and overexpressed MT1-MMP showed colocalization in microscopy pictures, suggesting a regulative interaction. A co-staining of endogenous proteins was not shown or colocalization data between ARF6 and MT1-MMP or other MMPs in comparison. The key-experiment was an ARF6-knockdown in MT1-MMP-pHluorin expressing cells. The pH-value dependent fluorescence of overexpressed MT1-MMP-pHluorin is measured at the cell surface. Hence, the fluorescent MT1-MMP-pHluorin should represent the surface-exposed population of MT1-MMP. In ARF6-knockdown cells, reduced fluorescent flashes were measured in the respective tumour cell lines by live-cell imaging microscopy. Comparing experiments with pHluorin-tagged soluble MMPs were not performed. Summarized, the impact of ARF6-silencing was explained by a reduced MT1-MMP protein level without a comparison to other MMPs.

Although the referring experiments were performed in tumour cell lines and the conclusions made in this dissertation were exclusively performed in human macrophages, the results can be methodically compared. In the present dissertation, both the intra- and extracellular protein expression of MT1-MMP was measured and also compared to other, soluble MMPs. Moreover, it could be confirmed that the intracellular MT1-MMP expression was not altered, but also no changed surface protein levels were measured in contrast to the mentioned publication. It must be mentioned though, that a different method was used to investigate the surface protein levels: The surface-biotinylation assay. Besides, other MMPs, which are not regulated by MT1-MMP, showed an altered protein level, especially MMP7. Also, colocalization experiments with co-stained endogenous proteins, showed that MMP7 colocalized to an even higher level with ARF6 than MT1-MMP in comparing experiments. The respective knockdown experiments were also flanked by overexpression of wild-type ARF6 and its defective mutant Q67L. Of course, both, the respective publication and this dissertation, observe a remarkably reduced degradative capability in ARF6-knockdown cells in comparable experiments, but the explanations of these results are remarkably distinct.

The second paper, which need to be discussed, is published in 2017 by Waheed et al. [59] and illuminates the relationship between MT1-MMP and ARF6 in endometrial cancer. They presented the synergistic effect of calcitriol and progesterone, which leads to apoptosis and a break-off in ovarian-

and endometrial cancer and identify the causal impact on MT1-MMP, NEDD9 and ARF6, which show enhanced protein expressions in advanced-stage endometrial tumors. As shown before, the knockdown of MT1-MMP, ARF6, and NEDD9 reduced the invasive capability of the respective cancer cells. A similar effect was observed at a combined calcitriol-progesterone exposure, suggesting a causal link, additionally on the solubles MMP2 and MMP9. Again, the presented hypothesis suggests an impact of ARF6 on the endocytosis of MT1-MMP and hence, to its surface exposure at the plasma membrane, which is required for ECM degradation and the invasiveness of the respective cells. At first, the correlation between increased expression of ARF6, MT1-MMP, and NEDD9 and tumour progression was examined. Then, the protein expression of the respective targets in 3 different tumour models was presented. In further experiments, the impact of silencing ARF6, NEDD9, or MT1-MMP on the invasiveness of Ishikawa- and HEC-1B cells, the chosen tumour model cell lines, was shown. The expression was also compared with endometrial cancer cells to prove the comparability of their model with the respective cells. Next, the effect of progesterone and calcitriol each separately and combined, was presented in immunofluorescence experiments. It was concluded, that a reduced overall fluorescence intensity of stained endogenous MT1-MMP at exposure of the respective chemicals, is confirming a reduced surface exposure at the plasma membrane. Other MMPs were not stained and measured. The quantification method was also different, compared to the present dissertation, and was not an object-based approach of vesicle structures, but measuring in total the fluorescence intensity of the whole cell. Another experiment was the performed activity assay. Here, the turnover of fluorescent substrates was measured with an assay kit. The results were a remarkably and significant reduction in their cell line models of MT1-MMP, but also of MMP2 and MMP9. Other (soluble) MMPs were not compared, neither as a positive, nor as a negative control.

In summary, the correlation between increased protein expressions of MT1-MMP and ARF6 is a frequent observation, but here again without comparing other MMPs or other ECM-degrading enzymes, which are responsible for the invasiveness of the tumour cells. Other soluble MMPs might be responsible for the degradative capability of macrophages and possibly tumour cells. The object-based approach, performed in this dissertation, is more advantageous, since an exclusion of non-vesicular structures (fluorescent filaments or compartments such as the Golgi) can be excluded from the evaluation. The discussed publication above is also not contradicting to the results, shown in this dissertation. Nevertheless, performing the described activity assay kit in a comparable manner with soluble MMPs, might validate the presented results in future experiments. It is also an interesting hypothesis, that progesterone in combination with calcitriol, might impact the endocytosis activity of ARF6, impairing the surface exposure of MT1-MMP and other soluble, but surface-associated MMPs.

In 2020, Lu et al. [61] supported the hypothesis of ARF6 regulating MT1-MMP activity by mediating the recycling process, initiated through apurinic/aprimidinic endonuclease (APE1). APE1 has two

functions: First, it is able to regulate the activity of transcription factors such as STAT3, p53 and NF- κ B in a redox-dependent manner. Second, APE1 is part of the base excision repair (BER) pathway. At first, silencing of APE1 was reducing the protein level of MT1-MMP and also the invasive capability of the esophageal adenocarcinoma (EAC) cell-line models. With selective inhibitors, targeting either the redox-function with E3330 or interacting in the BER-pathway with APE1-i3, the mechanism was identified to regulate MT1-MMP. The rescue by overexpressing APE1 was successful, but not with the redox-defective C65A mutant. Nevertheless, the mechanistic connection between MT1-MMP and APE1 was identified through precipitation of different endocytic regulators, *inter alia* ARF6. By that, the novel interaction between APE1, and ARF6 was identified. In consequence, ARF6 was also inhibited, and the increasing protein level of MT1-MMP by APE1 overexpression was abolished. By using the broad spectrum-inhibitor of MMPs, GM6001 to compensate the overexpression of APE1, previous results should be confirmed. The conclusion was, that APE1 regulated MT1-MMP protein level through ARF6. It was mentioned, that the possibility was conceded of other additional MMPs being affected by APE1/ARF6-regulation and thus the invasive capability of EAC cells.

In general - as mentioned in the discussion of this paper - other MMPs might be affected as well and thus, comparing screening of their protein levels would be necessary. It would be an interesting additional experiment to perform a co-staining of APE1, ARF6 and MT1-MMP in these cells, also in comparison with other MMPs. The used broad spectrum inhibitor GM6001 could not show an exclusive importance of MT1-MMP for the invasiveness of the cells. In the present dissertation, more specific methods such as knockdowns were performed for MT1-MMP and other MMPs such as MMP7.

The published data offers some further perspectives for subsequent experiments. The role of APE1 and its two functions in human macrophages for soluble MMPs needs to be investigated. The present data can only offer an initial insight into the various regulatory mechanisms of soluble MMPs. As for MT1-MMP, it might be appropriate to focus on one aspect of regulation or only one soluble MMPs as performed in the present dissertation for MMP7 and its endocytosis. The interplay between different soluble MMPs, which represent at least one distinct vesicle population selectively regulated by ARF6, requires further investigation.

Beside of the publications discussed above, the present dissertation might complement some findings in other publications: The described mechanism of ARF6-mediated endocytosis of MMP7 and probably other soluble MMPs is an important mechanism of differentiated primary human macrophages. But not only these cells produce MMPs. For example, MMP9 can be induced already in monocytes by electronegative LDL by activating CD14/TLR4 pathways, responsible for inflammation [63]. Also, endocytosis is not solely regulated by ARF6 or EEA1. WDFY2 is an important regulator for

the endocytosis of MT1-MMP. In early endosomes, WDFY2 colocalizes with EEA1 and plays a role as an antagonist to VAMP3, which is responsible for recycling [64].

There are only a few reported mechanisms for intracellular transport of MMP7. One of it, was published in 2019 by Liu et al., which described the GP73 (Golgi phosphoprotein 73)-mediated trafficking and secretion of MMP7, contributing to metastasis of hepatocellular carcinoma cells [65]. MMPs are transported as zymogens from the ER to the Golgi-apparatus. The Calcium-dependent trafficking of MMP2 and MT1-MMP in the Golgi-apparatus is promoted by the cis-Golgi protein nucleobindin 1 (NUCB1). From there, the MMPs are transported in TGN-derived vesicles to the plasma membrane [66]. The intracellular trafficking of MMPs continues along microtubules and microfilaments in anterograde and retrograde transport. This transport is regulated by myosin Va in both anterograde and retrograde direction. Hence, myosin Va interacts with kinesins and dynein/dynactin. In some cells, such as neurons during their developing or adult neuroplasticity, MMPs are partially secreted in vesicles. MMP2 is secreted in both active and inactive forms in exosomal vesicles [67]. MT1-MMP and MMP2 are also partially secreted together in vesicles in active and inactive form as well, produced by melanoma cells. During the transport, which is mediated by VAMP3 to nascent microvesicles or by VAMP7 to degradative structures such as invadopodia, MMP2 can be activated by MT1-MMP. These extracellular vesicles are involved in ECM-degradation as well and contribute to pathophysiological conditions [49]. Soluble MMPs are also known to be stored in intracellular, membrane-bound compartments for fast release, e.g. in neutrophils [68]. A model of the regulatory mechanisms of soluble MMPs should take this various aspects and publications into account. Although, stringently similar mechanisms in both physiological and pathological cells or different cells such as tumour cells, macrophages and neurons are unlikely.

6.7 Model of soluble MMP regulation

The presented data allows to describe a concept of the putative regulatory mechanism of the intracellular transport of (some) soluble MMPs. In this model, MMP7 and MMP12, possibly also MMP9, are surface-exposed at the plasma membrane and probably MMP9 as well. Surface-associated MMP7 is endocytosed by an ARF6-mediated mechanism, MMP12 is endocytosed by an EEA1-mediated one. Intracellularly, MMP7 and MMP9 are transported mainly in the same vesicle population, distinct to MT1-MMP. MMP12 represents a third vesicle population. Although MMP9 and MMP7 share some common intracellular trafficking, the polarization-independent expression of MMP9 and MMP12 is likely regulated by a common mechanism, distinct from MMP7, which is M2-polarization dependent. A schematic model of intracellular soluble MMP trafficking, is displayed in figure 6.7 to visualize the hypothesis, based on the presented data:

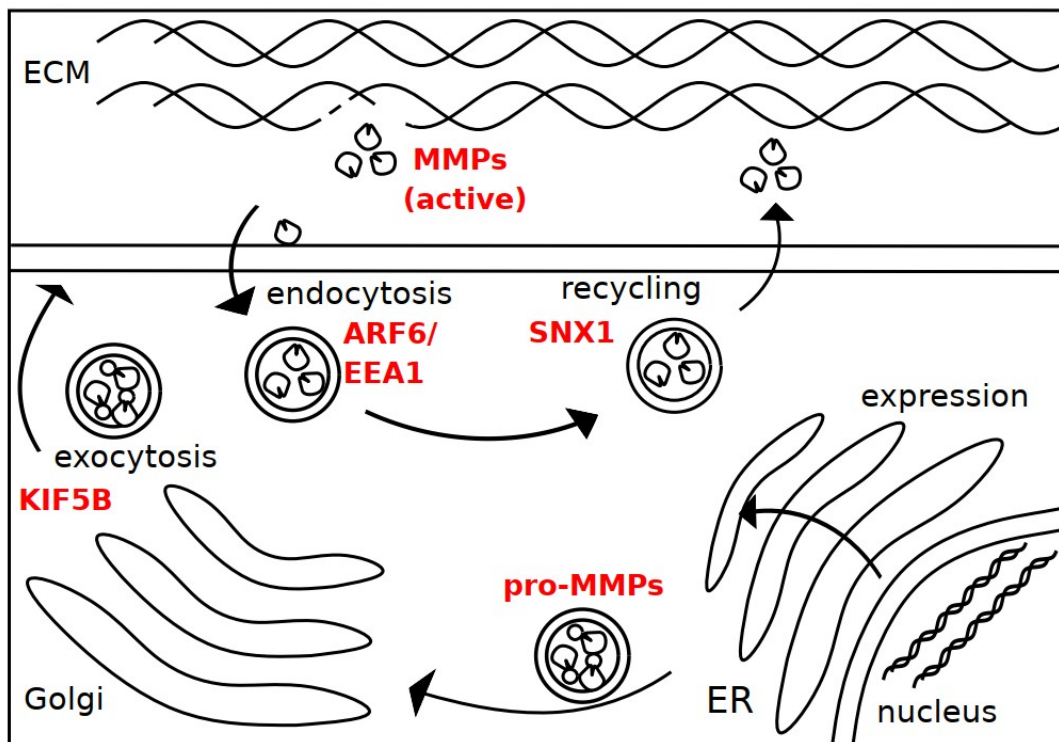


Figure 6.7 Model of trafficking pathways of soluble MMPs. Soluble MMPs are expressed as inactive pro-MMPs in the ER and trafficked into the Golgi-apparatus for posttranslational modification. After that, pro-MMPs are exocytosed by KIF5B to the plasma membrane and are either secreted or surface-associated. The activation might occur during exocytosis or at the plasma membrane. The endocytosis of surface-associated soluble MMPs is regulated by ARF6. Endocytosed MMPs are either degraded in lysosomes or recycled by the retromer-complex, moderated by the adaptor protein SNX1, back to the cell surface.

It will be a task for future experiments to complete this picture. Hereafter, some hypotheses are described: As described before, various surface-associations are possible: Either in association with LRP1 or LRP2, in association with HSPGs or bound to TIMPs and LRP1 or 2, oligomerized with other MMPs, as reported before [69]. The surface exposure of at least MMP7 (and probably other, not yet identified soluble MMPs), which seems to be required for the degradative capability of primary human macrophages, is regulated by endocytosis through ARF6. MMP12 for its part, is putatively endocytosed by EEA1. If only exocytosis would be sufficient for the degradative activity of soluble MMPs, the impact of an impaired endocytosis would be less severe. This suggests an important role of surface exposure and possibly recycling after endocytosis for the activity of soluble MMPs. It would be part of further investigations, if proteins such as WDFY2 or VAMP3 or VAMP7 are subsequent interactors, directing the internalized MMPs either into lysosomal degradation or recycling back to the cell surface. The internalized MMPs can be either degraded in the lysosome or recycled back to the cell surface by the retromer complex, where the adaptor protein SNX1 mediates the association of the vesicles to the retromer components such as VPS26. Also, it would be an interesting goal to investigate the polarization of macrophages and the role of transcription factors such as PPARs.

The relevance of soluble MMPs is not only defined by a comparable importance for the degradative capability of primary human macrophages, but also by the dependence on the polarization state, which distinguishes soluble MMPs from MT1-MMP. Hence, a more selective targeting for therapeutic approaches in the functionality of anti-inflammatory M2-polarized macrophages such as TAMs is possible, without impairing M1-polarized macrophages, which are required to access the hot spot of inflammation either caused by pathogens or tumour cells.

REFERENCES:

- [1] **A. Mantovani et al.**; Macrophages as tools and targets in cancer therapy; *Nature Reviews*; 2022.
- [2] **T. Wynn et al.**; Origins and Hallmarks of Macrophages: Development, Homeostasis, and Disease; *Nature*; 2013.
- [3] **R. van Furth et al.**; The mononuclear phagocyte system: a new classification of macrophages, monocytes, and their precursor cells; *Memoranda*; 1968.
- [4] **R. Dandekar et al.**; Role of macrophages in malignancy; *Annals of Maxillofacial Surgery*; 2011.
- [5] **H. Cohen et al.**; Cardiac Macrophages: How to Mend a Broken Heart; *Cell Press*; 2013.
- [6] **R. van Furth et al.**; The Origin and Kinetics of mononuclear Phagocytes; *The Rockefeller University*; 1968.
- [7] **E. van Goethem et al.**; Matrix Architecture Dictates Three-Dimensional Migration Modes of Human Macrophages: Differential Involvement of Proteases and Podosome-Like Structures; *The Journal of Immunology*; 2010.
- [8] **C. Wiesner et al.**; Podosomes in space - Macrophage migration and matrix degradation in 2D and 3D settings; *Landes Bioscience*; 2014.
- [9] **R. Guet et al.**; Macrophage Mesenchymal Migration Requires Podosome Stabilization by Filamin A; *The Journal of Biological Chemistry*; 2012.
- [10] **A. Fantin et al.**; Tissue macrophages act as cellular chaperones for vascular anastomosis downstream of VEGF-mediated endothelial tip cell induction; *Blood*; 2010.
- [11] **L. Zhu et al.**; Cellular Metabolism and Macrophage Functional Polarization; *International Reviews of Immunology*; 2014.
- [12] **D. Laskin et al.**; Macrophages and Tissue Injury: Agents of Defense or Destruction?; *Annu Rev Pharmacol Toxicol*; 2011.
- [13] **S. Hey et al.**; There and back again: Intracellular trafficking, release and recycling of matrix metalloproteinases; *BBA - Molecular Cell Research*; 2021.
- [14] **C. Tallant et al.**; Matrix metalloproteinases: Fold and function of their catalytic domains; *Biochimica et Biophysica Acta*; 2010.
- [15] **N. Cui et al.**; Biochemical and Biological Attributes of Matrix Metalloproteinases; *Progress in Molecular Biology and Translational Science, Volume 147*; 2017.
- [16] **S. R. van Doren et al.**; Peripheral Membrane Associations of Matrix Metalloproteinases; *Biochimica et Biophysica Acta*; 2017.
- [17] **Z. Chen et al.**; MMP7 interacts with ARF in nucleus to potentiate tumor microenvironments for prostate cancer progression in vivo; *Oncotarget*; 2016.

- [18] **H. Nagase et al.**; Structure and function of matrix metalloproteinases and TIMPs; *Cardiovasc. Res.*; 2006.
- [19] **B. Cauwe et al.**; The biochemical, biological, and pathological kaleidoscope of cell surface substrates processed by matrix metalloproteinases; *Crit. Rev. Biochem. Mol. Biol.*; 2007.
- [20] **E. Ohuchi et al.**; Membrane type 1 matrix metalloproteinase digests interstitial collagens and other extracellular matrix macromolecules; *J. Biol. Chem.*; 1997.
- [21] **K. Holmbeck et al.**; MT1-MMP-deficient mice develop dwarfism, osteopenia, arthritis, and connective tissue disease due to inadequate collagen turnover; *Cell*; 1999.
- [22] **R. Visse et al.**; Matrix metalloproteinases and tissue inhibitors of metalloproteinases: structure, function, and biochemistry; *Circ. Res.*; 2003.
- [23] **W. Bode et al.**; Insights into MMP-TIMP interactions; *Ann. N. Y. Acad. Sci.*; 1999.
- [24] **W. Bode et al.**; Astacins, serralytins, snake venom and matrix metalloproteinases exhibit identical zinc-binding environments (HEXXHXXGXXH and Met-turn) and topologies and should be grouped into a common family, the 'metzincins'; *FEBS Lett.*; 1993.
- [25] **P. Chavrier et al.**; Matrix invasion by tumour cells: a focus on MT1-MMP trafficking to invadopodia; *Journal of Cell Science*; 2009.
- [26] **D. Bau et al.**; Contribution of Matrix Metalloproteinase-7 Genotypes to the Risk of Non-solid Tumor, Childhood Leukemia; *Anticancer Research*; 2017.
- [27] **C. M. Overall et al.**; C-terminal truncation of IFN- γ inhibits proinflammatory macrophage responses and is deficient in autoimmune disease; *Nature Communications*; 2018.
- [28] **M. F. Chan et al.**; MMP12 Inhibits Corneal Neovascularization and Inflammation through Regulation of CCL2; *Scientific Reports*; 2019.
- [29] **C. Bernabeu et al.**; MMP-12, Secreted by Pro-Inflammatory Macrophages, Targets Endoglin in Human Macrophages and Endothelial Cells; *Int. J. Mol. Sci.*; 2019.
- [30] **J. Redondo-Muñoz et al.**; $\alpha 4\beta 1$ integrin and 190-kDa CD44v constitute a cell surface docking complex for gelatinase B/MMP-9 in chronic leukemic but not in normal B cells; *Blood*; 2008.
- [31] **G. Goldberg et al.**; Human 72-kilodalton type IV collagenase forms a complex with a tissue inhibitor of metalloproteases designated TIMP-2; *Proc. Natl. Acad. Sci. USA*; 1989.
- [32] **S. L. Schwartz et al.**; Rab GTPases at a glance; *Journal of Cell Science*; 2007.
- [33] **H. Colognato et al.**; Distinct Requirements for Extracellular and Intracellular MMP12 in the Development of the Adult V-SVZ Neural Stem Cell Niche; *Stem Cell Reports*; 2018.
- [34] **Y. Xi et al.**; Long Non-Coding RNA BCAR4 Promotes Growth, Invasion and Tumorigenicity by Targeting miR-2276 to Upregulate MMP7 Expression in Glioma, *OncoTargets and Therapy*; 2019.

- [35] **C. Fan et al.**; Hes3 Enhances the Malignant Phenotype of Lung Cancer through Upregulating Cyclin D1, Cyclin D3 and MMP7 Expression; *International Journal of Medical Sciences*; 2019.
- [36] **D. Fang et al.**; DKK1 inhibits breast cancer cell migration and invasion through suppression of β -catenin/MMP7 signaling pathway; *Cancer Cell International*; 2019.
- [37] **G. Blanck et al.**; MMP7 sensitivity of mutant ECM proteins: An indicator of melanoma survival rates and T-cell infiltration; *Clinical Biochemistry*; 2019.
- [38] **J. Lu et al.**; Role of Matrix Metalloproteinase 12 in the Development of Hepatocellular Carcinoma; *Journal of Investigative Surgery*; 2019.
- [39] **C. Wu et al.**; High expression of MMP19 is associated with poor prognosis in patients with colorectal cancer; *BMC Cancer*; 2019.
- [40] **R. Sedlacek et al.**; The matrix metalloproteinase RASI-1 is expressed in synovial blood vessels of a rheumatoid arthritis patient; *Immunology Letters*; 1997.
- [41] **N. R. Mahapatra et al.**; A Common Tag Nucleotide Variant in MMP7 Promoter Increases Risk for Hypertension via Enhanced Interactions with CREB (Cyclic AMP Response Element-Binding Protein) Transcription Factor; *Hypertension*; 2019.
- [42] **R. K. Assoian et al.**; Cardiovascular protection in females linked to estrogen-dependent inhibition of arterial stiffening and macrophage MMP12; *JCI insight*; 2019.
- [43] **X. Jia et al.**; Long noncoding RNA ZEB1-AS1 affects paclitaxel and cisplatin resistance by regulating MMP19 in epithelial ovarian cancer cells; *Archives of Gynecology and Obstetrics*; 2020.
- [44] **J. Roman et al.**; On the “TRAIL” of a Killer: MMP12 in Lung Cancer; *American Journal of Respiratory and Critical Care Medicine*; 2017.
- [45] **V. B. Abdul-Salam et al.**; CLIC4/Arf6 Pathway A New Lead in BMPRII Inhibition in Pulmonary Hypertension; *Circulation Research*; 2019.
- [46] **G. Scita et al.**; Secretory and endo/exocytic trafficking in invadopodia formation: The MT1-MMP paradigm; *European Journal of Cell Biology*; 2010.
- [47] **P. Chavrier et al.**; ATAT1/MEC-17 acetyltransferase and HDAC6 deacetylase control a balance of acetylation of alpha-tubulin and cortactin and regulate MT1-MMP trafficking and breast tumor cell invasion; *European Journal of Cell Biology*; 2012.
- [48] **P. Chavrier et al.**; MT1-MMP-Dependent Invasion is Regulated by TI-VAMP/VAMP7; *Current Biology*; 2009.
- [49] **P. Sharma et al.**; SNX27–retromer assembly recycles MT1-MMP to invadopodia and promotes breast cancer metastasis; *J. Cell Biol.*; 2019.
- [50] **J. Bezerra et al.**; Large-scale proteomics identifies MMP-7 as a sentinel of epithelial injury and of biliary atresia; *Sci Transl Med.*; 2017.

References

- [51] **J. Bezerra et al.**; Diagnostic Accuracy of Serum Matrix Metalloproteinase-7 for Biliary Atresia; Hepatology; 2018.
- [52] **Q. Tang et al.**; The expression of MMP19 and its clinical significance in glioma; Int J Clin Exp Pathol; 2018.
- [53] **E. Fiola-Masson et al.**; Activation of the GTPase ARF6 regulates invasion of human vascular smooth muscle cells by stimulating MMP14 activity; Nature - Scientific Reports; 2022.
- [54] **H. G. Svensson et al.**; A role for ARF6 in dendritic cell podosome formation and migration; Eur. J. Immunol.; 2008.
- [55] **N. Naslavsky et al.**; Convergence of Non-clathrin- and Clathrin-derived Endosomes Involves Arf6 Inactivation and Changes in Phosphoinositides; Molecular Biology of the Cell; 2003.
- [56] **W. Hsu et al.**; MicroRNA-145 suppresses cell migration and invasion in upper tract urothelial carcinoma by targeting ARF6; The FASEB Journal; 2020.
- [57] **Y. Xiao et al.**; Roles of Arf6 in cancer cell invasion, metastasis and proliferation; Life Sciences; 2017.
- [58] **P. Chavrier et al.**; ARF6–JIP3/4 regulate endosomal tubules for MT1-MMP exocytosis in cancer invasion; J. Cell Biol.; 2015.
- [59] **S. Waheed et al.**; Progesterone and calcitriol reduce invasive potential of endometrial cancer cells by targeting ARF6, NEDD9 and MT1-MMP; Oncotarget; 2017.
- [60] **J. A. Schmid et al.**; Fluorescence colocalization microscopy analysis can be improved by combining object-recognition with pixel-intensity-correlation; Biotechnology Journal; 2016.
- [61] **H. Lu et al.**; APE1 upregulates MMP-14 via redox-sensitive ARF6-mediated recycling to promote cell invasion of esophageal adenocarcinoma; Cancer Res.; 2020.
- [62] **S. Linder et al.**; Metalloproteinase MT1-MMP islets act as memory devices for podosome reemergence; J. Cell. Biol.; 2016.
- [63] **D. Ligi et al.**; Electronegative LDL induces MMP-9 and TIMP-1 release in monocytes through CD14 activation: Inhibitory effect of glycosaminoglycan sulodexide; BBA – molecular Basis of Disease; 2018.
- [64] **M. Sneeggen et al.**; Tumor suppression by control of matrix metalloproteinase recycling; Molecular and Cellular Oncology; 2019.
- [65] **Y. Liu et al.**; c-Myc transactivates GP73 and promotes metastasis of hepatocellular carcinoma cells through GP73-mediated MMP-7 trafficking in a mildly hypoxic microenvironment; Oncogenesis; 2019.
- [66] **J. von Blume et al.**; Nucleobindin-1 regulates ECM degradation by promoting intra-Golgi trafficking of MMPs; J. Cell Biol.; 2020

References

- [67] O. Sbai et al.;** Vesicular trafficking and secretion of matrix metalloproteinases-2, -9 and tissue inhibitor of metalloproteinases-1 in neuronal cells; *Molecular and Cellular Neuroscience*; 2008.
- [68] L. Dan-Dong et al.;** The rapid lipopolysaccharide-induced release of matrix metalloproteinases 9 is suppressed by simvastatin; *Cell Biology International*; 2015.
- [69] P. Henriet et al.;** Cellular uptake of proMMP-2: TIMP-2 complexes by the endocytic receptor megalin/LRP-2; *Scientific Reports*; 2017.

ABBREVIATIONS:

A	Adenine
AAM	alternatively activated macrophage
ADAM	a disintegrin and metalloproteinase
AM	activated macrophage
ARF	alternative reading frame (protein)
Arp2/3	Actin Related Protein 2/3
C	Cytosine
CCL	CC-chemokine ligand
CD	cluster of differentiation
CSF	colony stimulating factor
ECM	extracellular matrix
EE	early endosome
ER	endoplasmic reticulum
EV	extracellular vesicle
EZM	extrazelluläre Matrix
F-actin	filamentous actin
FL	fetal liver
G	Guanine
GPI	glycosylphosphatidylinositol
GRASP55	Golgi reassembly-stacking protein of 55 kDa
GTP	guanosine-5'-triphosphate
HCS-2/8	human chondrosarcoma 2/8
HOPS	homotypic fusion and vacuole protein sorting (complex)
HPX	hemopexin
HSC	hematopoietic stem cell
HSPG	heparan sulfate proteoglycan
IF	Immunofluorescence
IFN	interferon
IFNGR	interferon-gamma receptor
IL	interleukin
JAK	janus kinase
KIF	kinesin superfamily (protein)
LE	late endosome
LRP	low density lipoprotein receptor-related protein

MBP	myelin basic protein
MCF-7	Michigan Cancer Foundation 7
MDCK	Madin-Darby Canine Kidney (cell)
MMP	Matrix metalloproteinase
mRNA	messenger-RNA
MS	multiple sclerosis
MT-MMP	Membrane-type matrix metalloproteinase
NPF	nucleation promoting factor
NUCB1	nucleobindin-1
N-WASP	neuronal Wiskott-Aldrich syndrome protein
PAA	Polyacrylamide gel
RAB	RAS-related in brain
RE	recycling endosome
SEC	subunit of the exocyst complex
siRNA	small interfering RNA
SNAP	SNARE protein
SNARE	soluble N-ethylmaleimide-sensitive-factor attachment receptor
SNX	sorting nexin
STAT	signal transducers and activators of transcription
T	Thymine
TAM	tumour-associated macrophages
TGN	trans Golgi network
TIMP	tissue inhibitor of metalloproteinases
TM	transmembrane
TME	tumour microenvironment
TRM	tissue-resident macrophage
t-SNARE	target synaptosome-associated protein receptor
U	Uracil
VAMP	vesicle-associated membrane protein
VEGF	vascular endothelial growth factor
VPS	vacuolar protein sorting (complex)
v-SNARE	vesicle synaptosome-associated protein receptor
YS	yolk sac

LIST OF FIGURES

Figure	Page number
1.1.2: Macrophage lineages redefined in mice	12
1.1.3: 2- and 3- dimensional migration modes of macrophages	13
1.1.4: General podosome structure of macrophages in 2D and 3D	14
1.1.5: Tumour-associated macrophages in tumour-supporting activities	15
1.2.1: Overview of schematic MMP-domain structures	18
1.2.3: MMP expressions in M1- or M2-polarized macrophages	20
1.2.4: Trafficking pathways of MMPs	21
4.1.1.1: Software based analysis of Western blots	42
4.1.1.2: MMP expression over time in primary human macrophages	43
4.1.2: Correlations between average protein expressions over time	45
4.2.1: Intracellular IF-stainings for endogenous MMPs	49
4.2.2: IF-stained endogenous MMPs, co-stained with ARF6, and EEA1	52
4.3.1: Zymography-assays at knockdown-conditions	55
4.3.2.1: Evaluation method of the degradation assay	57
4.3.2.2: Matrix degradation assay with primary human macrophages	59
4.4.1: Schematic picture of the nearest neighbour approach	61
4.4.2: Trackmate-based analysis of podosomes and MT1-MMP islets	62
4.4.3: Trackmate-based analysis of MMP7 and podosome positions	64
4.5.1.1: Intracellular MMP protein levels	66
4.5.1.2: Surface MMP protein levels	67
4.5.2.1: Intracellular MMP protein levels at knockdown conditions	69
4.5.2.2: Surface MMP protein levels at knockdown conditions	71
4.5.2.3: Supernatant MMP protein levels at knockdown conditions	72
6.7 Model of trafficking pathways of soluble MMPs	89

LIST OF TABLES

Table	Page number
2.1: Chemicals	27
2.2: Chemicals for cell culture	28
2.3: Buffers	28
2.4: Antibodies for IF and WB stainings	29
2.5: siRNA and sequences for knockdowns	30
2.6: Oligonucleotides for cloning	30
2.7: Purchased plasmids	30
2.8: Kits	30
2.9: Consumables	30
2.10: Inventory	31
2.11: Microscopes	32
2.12: Software	32
List of Figures	98
List of Tables	99

Publications and conferences

Publications:

Sven Hey, Artur Ratt, Stefan Linder; **(2021)** There and back again: Intracellular trafficking, release and recycling of matrix metalloproteinases; *BBA - Molecular Cell Research*.

Kinga M. Wrona, Julia Krause, Jutta Starbatty, Artur Ratt, Stefan Linder, Friederike Cuello, Thomas Eschenhagen, Marc N. Hirt; **(2021)** Characterization of multi-cell-type engineered heart tissues containing human iPSC-derived cardiomyocytes, endothelial cells, fibroblasts, smooth muscle cells and macrophages; *AHA Journals*.

Conferences:

Artur Ratt, Stefan Linder; **(2019)** Regulation of matrix metalloproteases 7, 12 and 19 during proteolytic invasion of human primary macrophages (Poster, awarded with a poster price); Gordon Research Conference; „*Fibronectin, Integrins and Related Molecules; Extracellular Matrix and Integrins: Regulation of Cell and Tissue Function*“ on May. 5-10 in Lucca (Barga), Italy.

„*Degradomics - Protease Web in Health and Disease*“ on Sept. 16–20, (2019) CRC 877 in Kiel at the Baltic Sea, Germany.

„*Protease World in Health & Disease*“ on Sept. 11-14, (2022) CRC877 in Kiel at the Baltic Sea, Germany.

Membership:

member of the Integrated Research Training Group ‘*Proteases and Pathophysiology*’ in the Collaborative Research Center 877 from 15 July, 2018 to 31 December, 2022.

representative of IRTG doctoral researchers from July 2021 to December, 2022.

DANKSAGUNG

In diesem Abschnitt möchte ich den Menschen danken, die mich bei der Erstellung dieser Doktorarbeit unterstützt haben. Zuallererst danke ich meiner Familie für ihre Geduld, ihre aufmunternde Überzeugung in mich und dass diese Arbeit irgendwann fertig gestellt sein wird und ich damit auch zufrieden sein werde.

Herrn Prof. Dr. Stefan Linder danke ich für seinen lehrreichen, geduldigen und freundlichen Umgang, sowie die Freiheit, die er mir eingeräumt hat, mich selbst und meine eigenen Ideen auszuprobieren. Seiner Arbeitsgruppe danke ich allgemein für die fachliche Unterstützung, die interessanten philosophischen, politischen und unterhaltsamen Gespräche, Filmabende und gemeinsamen Restaurantbesuche. Pasquale Cervero danke ich insbesondere nicht nur für seine präzise fachliche Beratung, seine experimentellen Protokolle und seine kritischen Fragen, sondern auch für die Zeit, die er sich genommen hat, um über persönliche charakterliche Entwicklung, Geduld und Empathie zu sprechen und dass er seine sehr weise und geduldige Perspektive in vielen Angelegenheiten mit mir geteilt hat. Lars Wiltfang danke ich für sein Vertrauen in meine fachliche Kompetenz, wenn er Fragen bezüglich der korrekten Durchführung eines bestimmten Experimentes hatte und seine sehr freundliche Art, meinem eigenen gelegentlichen Missmut mit einem Lächeln zu begegnen. Sven Hey danke ich für seinen inspirierenden Idealismus und den Anspruch etwas zu verändern, wenn man selbst unzufrieden ist, anstatt sich mit distanzierter Kritik zu begnügen. Robert Herzog danke ich für die sehr hilfreichen und zeitsparenden Macros, sowie die flachen Witze, um auch ernste Situationen erträglicher zu machen. Marie Vollmost danke ich für die Erkenntnis, dass es lehrreich sein kann, jemandem selbst etwas beizubringen. Bryan Barcelona danke ich dafür, dass er einem den Spiegel vorhält, wir uns beide ohne Ablehnung tolerant unterhalten und persönliche Sympathie empfinden können. Andrea Mordhorst danke ich für ihren offensiven Einsatz, wenn es um die Belange der Arbeitsgruppe ging, ungeachtet der Widerstände. Kathrin Weber danke ich für ihre professionelle Höflichkeit, ihr offenes Ohr, ihre Aufrichtigkeit und ihr organisatorisches Geschick. Karim El-Azzouzi danke ich für die Erkenntnis wie wichtig und hilfreich die Dokumentation von Daten und Protokollen ist. Prof. Dr. Stefan Rose-John danke ich für die Möglichkeit die naturwissenschaftliche Gemeinschaft in Kiel und die Stadt selbst etwas kennengelernt zu haben.